



JIMMA UNIVERSITY
INSTITUTE OF TECHNOLOGY
SCHOOL OF CHEMICAL ENGINEERING

**Application and Optimization of hexavalent chromium (Cr(VI))
removal from aqueous solution using synthesized local termite mound
with chicken eggshell adsorbent**

By

Mebratu Ergete Mengistu




A Thesis Submitted to the School of Chemical Engineering, Jimma Institute of Technology, Jimma University in Partial Fulfilment of the Requirements for the Degree of Master of Science in Process Engineering.

December 2021
Jimma, Ethiopia

JIMMA UNIVERSITY
INSTITUTE OF TECHNOLOGY
SCHOOL OF CHEMICAL ENGINEERING

This is to certify that the thesis prepared by Mebratu Ergete Mengistu entitled ‘**Application and Optimization of hexavalent chromium (Cr(VI)) removal from aqueous solution using synthesized local termite mound with chicken eggshell adsorbent**’ and submitted as a partial fulfillment for the award of the Degree of Master of Science in Chemical Engineering (Process engineering) complies with the regulations of the university and meets the accepted standards with respect to originality and quality.

Approved by examining board:

<u>Abdisa Jabesa (PhD)</u> External Examiner	 Signature	<u>29/12/2021</u> date
<u>Ermias Girma (Assistant Professor)</u> Internal Examiner	 Signature	<u>29/12/2021</u> date
<u>Dereje Tadesse (Assistant Professor)</u> Advisor	_____ Signature	_____ date
<u>Ketema Beyecha (Lecturer)</u> chairman, process Eng.	_____ Signature	_____ date
<u>Ermias Girma (Assistant Professor)</u> School Dean	 Signature	<u>29/12/2021</u> date

December 2021
Jimma, Ethiopia

DECLARATION

I, **Mebratu Ergete** the undersigned, declare that for an award of Master of Science Degree at Jimma University with a thesis entitled “**Application and Optimization of hexavalent chromium (Cr(VI)) removal from aqueous solution using synthesized local termite mound with chicken eggshell adsorbent**” is my original work, and has not been presented for an award of MSc degree in the any other University of Ethiopia, and that all resources of materials used have been duly acknowledged with citation. And I have done this thesis under the supervision of Dereje Tadesse (Assistant Professor) and Yasin Ahmed (Lecturer) at Jimma University School of Chemical Engineering

Mebratu Ergete Mengistu

Msc.Candidate

Signature

date

Dereje Tadesse (Assistant Professor)

Advisor

Signature

date

Yasin Ahmed (Lecturer)

Co-Advisor

Signature

date

ACKNOWLEDGMENT

First and foremost, I would like to praise the Almighty GOD for giving me patience, strength, endurance, wisdom, and health to accomplish this thesis work successfully. Next, I wish to express my deepest gratitude to my advisor Dereje Tadesse for his excellent scientific and invaluable comments, guidance, kindness, constructive criticisms, encouragement, and sharing of his knowledge and skill for each process throughout the entire of this thesis. And also, I would like to thank my co-advisor Yasin Ahmed for his kindly insightful suggestions, and constructive ideas throughout doing this thesis. Here, also I am forced to acknowledge Mr. Dafar G, Mr. Firomsa B, Mr. Worku S, Mr.Tsegaye M, and Mr. Endrias A, for their kindly technical support on laboratory work during my study; plus to these, I extend my grateful to my class mates and my friends. Next, I would like to express my heartfelt appreciation and gratitude to all School of Chemical Engineering staffs for their fine-tuning up to the successful completion of this thesis within time.

Finally, I wish to express my deepest gratitude to my parents and members of my families for all their patiently encouragement and support in every requirement for the success of my work. Last, but not least, I am sincerely like to acknowledge Jimma University, Institute of Technology that providing me with financial support besides giving me an opportunity to do this MSc thesis.

ABSTRACT

Water is a precious resource over the world and a universal solvent for most dissolved particles. On the other hand, the persistence of uncontrollable hexavalent chromium (Cr(VI)) hazards adversely affects life in the world in future generations due to it accounts for several disorders in plants and animals. Such trace ions are taken into consideration as a contaminant whilst their concentrations increase beyond their limit level that causing critical danger to the world. So, in order to avoid these heavy metal effluents from industrial wastewater adsorption is the best, versatile and efficient alternative. Also, it was observed that most of the adsorbents do have not sufficient usability as a result of they have low adsorption capacities with a long contact time, and inability to work at the natural pH of water. Therefore, it was imperatively developed to maximum removal efficiency of Cr(VI) found to be 99.79% at pH, adsorbents dosage, initial Cr(VI) concentration, and contact time were valued to 7pH, 6g/L, 40mg/L, and 75minutes respectively. This was done after the dried and size reduced termite mound-eggshell powder 1:1 mass ratio mixture was thermally transformed at 850°C by using a muffle furnace and the experimental data generated using adsorbent of adsorption with the help of UV-vis spectrophotometry. Extensively, the samples were characterized like its proximate analysis, particle size, surface charge, functional groups, and adsorption isotherm and kinetics models and optimized by using design expert software besides investigating competitiveness of other heavy metals that fit the active site of termite mound-eggshell adsorbent. Based on these Freundlich isotherm as well as pseudo-second-order kinetic models provided a good description of adsorption that fitted well to concerning R^2 value of correlation data. The ANOVA was performed using CCD of quadratic model and its regression coefficient becomes 0.9986 which is favorable as closer to one. The optimum model predictions of 98.96% were in good agreement with a conducted experimental data generated 95.15% output. Extensively, during the study of regeneration adsorbent, desorption was successfully achieved with greater than 85% Cr(VI) ions removal efficiency by using 1.0MNaOH treatment. So, these results show that a mixture of synthesized adsorbents is a better promising for Cr(VI) ions adsorption.

Keywords: *Heavy metals, chromium, adsorption, isotherm and kinetics model*

TABLE OF CONTENTS

DECLARATION	ii
ACKNOWLEDGMENT	iii
ABSTRACT.....	iv
LIST OF TABLES	viii
LIST OF FIGURES	ix
ABBREVIATIONS	x
NOMENCLATURES	xii
1. INTRODUCTION	1
1.1. Background	1
1.2. Statement of the problem	4
1.3. Objectives	6
1.3.1. General objective	6
1.3.2. Specific objectives	6
1.4. Scope of the study	6
1.5. Significance of the study	6
2. LITERATURE REVIEW	7
2.1. Occurrence and methods of removal hexavalent chromium.....	7
2.2. Physical properties of chromium	9
2.3. The oxidation state of chromium metals	9
2.4. Effects of Chromium on human beings	11
2.5. Termite mound nest pedological view and its composition.....	13
2.6. Chicken eggshell fitness as bio sorbent	14
2.7. Conventional technologies for waste water treatment with their drawbacks	15
2.7.1. Sand filtration.....	16
2.7.2. Ion exchange	16
2.7.3. Electrodialysis.....	17
2.7.4. Membrane process	17
2.7.5. Reduction of hexavalent chromium to trivalent chromium ion	20
2.7.6. Coagulation and flocculation	20

2.7.7.	Solvent extraction	21
2.7.8.	Phytoremediation	21
2.8.	Adsorption process technology	22
2.9.	Physisorption and chemisorption processes.....	23
2.9.1.	Physisorption process.....	23
2.9.2.	Chemisorption process.....	24
2.10.	Some types of previous studies adsorbents for chromium removal.....	24
2.11.	Future perspective of adsorption based on literatures.....	33
3.	MATERIALS AND METHODS.....	34
3.1.	Preparation and activation of termite mound-eggshell adsorbent.....	34
3.2.	Determination of experimental batch adsorption parameters.....	36
3.2.1.	Preparation of stock solution for hexavalent chromium	37
3.3.	Characterization Techniques of synthesized adsorbent	37
3.3.1.	Proximate analysis of TMESP adsorbent.....	37
3.3.2.	Fourier Transform Infrared of synthesized TMESP adsorbent.....	40
3.3.3.	UV- visible Spectrophotometer analysis of TMESP-adsorbent.....	41
3.3.4.	X-Ray Diffraction analysis of synthesized TMESP adsorbent	41
3.3.5.	Thermogravimetric analysis.....	42
3.4.	Determination and optimization of chromium adsorption factors	42
3.4.1.	Chromium concentration analysis using UV-visible Spectrophotometer	42
3.4.2.	Optimization of chromium adsorption factors	43
3.5.	Adsorption isotherm studies of synthesized TMESP adsorbent	45
3.6.	Adsorption kinetic model for synthesized TMESP adsorbent	48
3.7.	Determination of point of zero charges using solid addition technique.....	49
3.8.	Specific surface area investigation.....	50
3.9.	Desorption and regeneration of synthesized TMESP-adsorbents	51
3.10.	Investigation of competitiveness heavy metals to synthesized TMESP adsorbent.	52
4.	RESULTS AND DISCUSSIONS.....	54
4.1.	Proximate analysis of TMESP adsorbent.....	54
4.2.	Evaluation of synthesizing termite mound-eggshell mixture.....	57

4.2.1.	Determination of TMESP mixture ratio and calcination parameters for synthesizing	57
4.3.	Characterization of synthesized termite mound-eggshell adsorbent.....	58
4.3.1.	UV-Visible spectrophotometer analysis of TMESP-adsorbent	58
4.3.2.	Fourier Transform Infrared Spectroscopy.....	59
4.3.3.	X-Ray Diffraction analysis of particle size	62
4.3.4.	Thermogravimetric analysis.....	65
4.3.5.	Experimental design and statistical analysis of UV-Visible adsorption results.....	66
4.3.6.	Optimization of efficient removal of hexavalent chromium ions	75
4.4.	Regeneration and reusability study for synthesized TMESP- adsorbents.....	77
4.5.	Studies of removal efficiency based on pre-determined factors	78
4.5.	Determination of point of zero charge	82
4.6.	Adsorption isotherm studies.....	84
4.7.	Adsorption kinetics studies	87
4.8.	Investigation of competitiveness of heavy metals to synthesized TMESP adsorbent	90
5.	CONCLUSIONS AND RECOMMENDATION.....	92
5.1.	Conclusion	92
5.2.	Recommendation	93
	REFERENCES	94
	APPENDIXES	106
	Appendix A: Laboratory experimental setup.....	106
	Appendix B: Laboratory experimental generated data	108
	Appendix C: Characterization of adsorption models.....	111
	Appendix D: Pre-determined parameters output for Cr(VI) removal	114

LIST OF TABLES

Table 2. 1: Characteristics of Palmyra palm fruit seed carbon and commercial activated carbon	27
Table 2. 2: Summary of some previous adsorbent parameters that used for Cr(VI) ions removal	32
Table 3. 1: Parameters of adsorption with respect to its' experimental level.....	44
Table 3. 2: Heavy metals selected to study their competition for TMESP adsorbent	53
Table 4. 1: Proximate characteristics comparison of various bio-adsorbents with current study.	57
Table 4. 2: Experimental result and predicted values for percentage removal of Cr(VI) ions	67
Table 4. 3: Fit summary of sequential model for TMESP adsorbent experimental result.....	68
Table 4. 4: Fit Statistics of Cr(VI) removal efficiency using synthesized TMESP adsorbent	68
Table 4. 5: Analysis of variance (ANOVA) response for Cr(VI) removal efficiency.....	69
Table 4. 6: Optimization solution after criteria is justified	76
Table 4. 7: Optimum conditions and model validation.....	76
Table 4. 8: The point of zero charges of PH (PH _{pzc}) for TMESP adsorbent.....	83
Table 4. 9: Langmuir, Freundlich and Temkin model parameters for the removal of Cr(VI).....	84
Table 4. 10: Data generated from the kinetics of adsorption TMESP-adsorbent models.....	87
Table 4. 11: Competitiveness of heavy metals to synthesized TMESP active site of adsorbent..	90
Table B 1: standard concentration for UV-vis spectrophotometer calibration graph.....	108
Table B 2: Evaluation of point of zero charge (PH _{pzc}) for TMESP-adsorbent surface.....	108
Table B 3: Effect of initial concentration on Cr(VI) removal	109
Table B 4: Effect of pH on Cr(VI) removal using TMESP-adsorbent	109
Table B 5: Effect of adsorbent dose on Cr(VI) removal.....	110
Table B 6: Effect of contact time on Cr(VI) removal	110
Table C 1: Parameters values for Langmuir and Freundlich isotherm models.....	111
Table C 2: Parameters values for pseudo-first-order & pseudo-second-order kinetics model ...	111
Table C 3: TMESP mixture ratio using design expert software synthesizing adsorbent.....	112
Table C 4: Crystalline size derived from XRD data analysis of the TMESP adsorbent	112
Table C 5: Regeneration removal efficiency recorded and calculated from UV-vis output	112
Table C 6: Calcination temperature and time determination for TMESP-adsorbent.....	113
Table C 7: Functional groups analysis on the surface of TMESP-adsorbent	113

LIST OF FIGURES

Figure 4. 1: Absorption spectra of synthesized TMESP adsorbent from UV– visible.....	59
Figure 4. 2: Comparative FTIR image of TMESP adsorbent from raw to its synthesized.....	60
Figure 4. 3: FTIR result for TMESP-adsorbent before and after chromium adsorption	61
Figure 4. 4: Comparison of crystallinity peaks for TMESP adsorbent.....	63
Figure 4. 5: Justification XRD crystallinity peaks for TMESP-adsorbent	64
Figure 4. 6: TGA analysis for synthesized TMESP- adsorbent.....	66
Figure 4. 7: Normal % probability versus residuals and predicted diagnostic plot analysis	71
Figure 4. 8: Contour plot for the combined effect of parameters	72
Figure 4. 9: Combined effect for a 3D plot on Cr(VI) adsorption.	74
Figure 4. 10: Desirability ramp for the optimization of the parameters	77
Figure 4. 11: Graphical expression of desorption versus adsorption efficiency comparative	78
Figure 4. 12: Effects of PH on Cr(VI) removal efficiency for TMESP-adsorbent.....	79
Figure 4. 13: Effects of adsorbent dose on chromium removal at optimum condition.....	80
Figure 4. 14: Effect of Cr(VI) concentration at the optimum point of parameters.....	81
Figure 4. 15: Effects of contact time for Cr(VI) adsorption	82
Figure 4. 16: Point of zero charges of PH for synthesized TMESP adsorbent.....	83
Figure 4. 17: Langmuir isotherm model at optimum parameters	85
Figure 4. 18: Freundlich isotherm model at constant parameters used.....	85
Figure 4. 19: Temkin isotherm model at constant parameters.....	86
Figure 4. 20: Statistical analysis of pseudo-first-order kinetics model kinetic	88
Figure 4. 21: Statistical analysis of pseudo-second-order kinetics model	88
Figure 4. 22: Statistical analysis intraparticle diffusion kinetics model	89
Figure 4. 23: Graphical demonstration of competitiveness heavy metals to TMESP-adsorbent .	91
Figure A 1: Raw material collection and synthesizing of TMESP adsorbent.....	106
Figure A 2: Proximate analysis of ash for TM-ES raw materials before and after mixing	106
Figure A 3: Particle density for TMESP adsorbent using a pycnometer	107
Figure A 4: Batch adsorption process for removal of Cr(VI) ions	107
Figure A 5: Point zero charge of (PH _{pzc}) determination	108
Figure D 1: Proportionality of parameters as one factor effect for Cr(V) adsorption.....	115
Figure D 2: Contour plot for the combined effect of adsorption parameters	116
Figure D 3: Combined effect for a 3D plot for Cr(VI), adsorbent dosage, PH, & contact time.	117
Figure D 4: Proportionality of parameters as all factors effect for Cr(V) adsorption.....	118
Figure D 5: Residual versus TMESP- adsorbent and run experiment.....	119
Figure D 6: Cubic interaction of parameters for Chromium removal efficiency	119
Figure D 7: standard concentration for UV-vis spectrophotometer calibration graph	120
Figure D 8: Regeneration efficiency recorded and calculated using UV-vis generated data	120

ABBREVIATIONS

AAS	Atomic Adsorption Spectrophotometer
AC	Activated Carbon
ACRS	Activated Carbon of Rice Straw
ANOVA	Analysis of Variance
ASTM	American Society for Testing and Materials
BPP	Banana Peel Powder
CAC	Commercial Activated Carbon
CCD	Central Composite Design
CS	Chitosan
Cr(VI)	Hexavalent Chromium
DDI	Daily Dietary Intake
DOE	Design of Experiment
EPA	Environmental Protection Agency
GBPs	Grafted Banana Peels
GG/nZnO	Guar Gum–nano Zinc Oxide
LDL	Low-Density Lipoprotein Cholesterol
MKAC	Mango Kernel Activated Carbon
MSSP	Moringa Stenopetala Seed Powder
nANB	nanoporous Adsorbent Neem Bark
NTU	Neclophely Turbidity Unit
PFOKM	Pseudo-First-Order Kinetic Model
PPFSC	Palmyra Palm Fruit Seed Carbon
PSOKM	Pseudo-Second-Order Kinetic Model

RO	Reverse Osmosis
RSM	Response Surface Methodology
SEM	Scanning Electron Microscopy
TMESP	Termite Mound Eggshell Powder
UF	Ultra-Filtration
UV	Ultra Violet
WHO	World Health Organization
XRD	X-Ray Diffraction

NOMENCLATURES

A_1	Absorbance one
A_2	Absorbance two
A_v	Average absorbance
abs	unit of absorbance
a.u	arbitrary unit
b	Temkin Constant
C_e	equilibrium concentration Cr(VI) in solution
C_f	initial Cr(VI) concentration
C_i	Cr(VI) concentration at time t
D	mean crystalline size [nm]
hr	hour
K	Shape factor
K_L	Langmuir constant (L/mg)
K_1	Lagergren rate constant (min^{-1})
K_2	pseudo-second-order rate constant (mg/g/min)
n	Freundlich constants, intensity of adsorption
q_e	amount adsorb per gram of the adsorbent at equilibrium
q_{\max}	maximum adsorption capacity (mg/g)
q_t	amount (mg) adsorbate per gram of adsorbent
t	time (min)
T	Temperature ($^{\circ}\text{C}$)
θ	Bragg angle
λ	Wavelength [nm]
Δ	Change sign
ρ	Density

1. INTRODUCTION

1.1. Background

Access to pure and reliable sufficient amount of potable water is being crucial to keeping secure health and well done for the metabolism of life's; hence, by the United Nations convention considered as a universal human right; but, this vision remains a dream for numerous developing countries in Asia, South America, and Africa (Kasozi *et al.*, 2019). Also, according to Bain *et al.*(2018) reports, globally the water target had been declared met in 2010; however, the sanitation aim had been missed by over 700 million people. On the other hand, the word "heavy metals" has been increasingly used in several publications and legislation incorporation relevant to the most notable environmental concerns over the last few decades (Tanhaei *et al.*, 2020). Also, metals and semimetals or metalloids that have been linked to pollution and are extremely environmentally poisonous or ecotoxicity that have detrimental effects on humans and animals are often referred to as heavy metals. Such trace ions are considered as non-biodegradable that allows them to accumulate in the soil, atmosphere, and living tissues in addition to these many are soluble in aqueous media, making them readily accessible to living organisms within aqueous (Alghamdi *et al.*,2019; Ali *et al.*, 2019; Ali *et al.*, 2016). These types of metals are highly environmentally toxic; even if there, such as Cu(II) is an essential element for plant growth utilizing as antiseptics, feed additives, and organic fertilizers (Liu *et al.*, 2016; Abbas *et al.*, 2018). When, the concentrations of such metals rise above their limit point that they endanger living organisms such as plants, livestock, and humans, so they are considered contaminants. In the study of Uwizeyimana *et al.* (2017) states, transition metals are naturally present in soils, sedimentary rocks, and water bodies, so they have their common background concentration. Even though as Alam *et al.* (2020) explain, water is considered as earth's blood; Various industrial processing are the main sources of water pollution, and it may vary extensively with the nature of the industry in terms of urbanization and industrialization. Chromium (Cr), iron (Fe), cadmium (Cd), nickel (Ni), cobalt (Co), zinc (Zn), copper (Cu), manganese (Mn), tin (Sn), mercury (Hg), silver (Ag), lead (Pb), and arsenic (As) are among the heavy metals that are primarily discharged from factories (Alghamdi *et al.*, 2019; Ghorbani *et al.*,2016). Among these according to Raouf M. & Raheim A. (2016) report the most toxic heavy metals are lead, mercury, and chromium which becomes a critical problem worldwide.

Mining, metallurgical, paints, pigments, inks, fungicides, photography, metal finishing, wood preservation, leather tanning, refractories, aerospace, electroplating, cloth printing, and dyeing are the main anthropogenic sources for those heavy metal (Bahador *et al.*, 2021; Islam *et al.*, 2019; Ali *et al.*, 2019). Also, these industrial effluents are highly undesirable in nature and are responsible for a number of diseases in plants and animals, as they can pose toxicity and global environmental issue in both higher and lower species, such as humans and animals, which require a small amount of these metals to live (Aigbe & Osibote, 2020; Reta *et al.*, 2021). As Ouyang *et al.* (2019) investigation explains, only one-third of the world's population can get pure water, and trace metal ions are one of the main pollutants that distort this natural water content. Because it causes DNA damage, disruption of enzyme activities, reduced individual survival, productivity, and growth rate, changes in individual behavior such as feeding rate, and extends to decrease in the total earthworm population biomass and density could all result from the combined contamination caused by pesticides and metal ions. For instance, organophosphates have been classified as the most toxic pesticides (Uwizeyimana *et al.*, 2017). Among these toxic metals ions, chromium is a very common metal in our environment that is found richly on earth that can be inhaled, touched, drunk, and eaten by humans in different circumstances of life (Ali *et al.*, 2020). As Bhaumik *et al.* (2012) explain water is the major medium of chromium intake by humans.

Hexavalent chromium is known as one of the most toxicity and environmental hazardous for human health among other its oxidative states, and it is used in a variety of industries; thus, its level of in wastewaters must be reduced to a permissible limit before discharging into the nearby natural water bodies (Abraha , 2009). According to Abbas *et al.* (2018), studied the mischievous of industrial pollution with Cr(VI), the rate of this perilous materials increase in man`s body who is smoking tobacco. Generally, Chromium (VI) found as stable oxoanions in a water solution such as chromate (CrO_4^{2-}), hydrogen chromate (HCrO_4^-), dichromate ($\text{Cr}_2\text{O}_7^{2-}$), and hydrogen dichromate (HCr_2O_7^-) (Tanhaei *et al.*, 2020). So, to avoid this different physio-chemical processes have been developed for the purification of various trace metal ion contaminants. To do these there are different conventional treatment technology for the removal of these heavy metal ions including; chemical precipitation, ion exchange, chemical oxidation, coagulation-

flocculation, solvent extraction, filtration, UF, RO, electrodialysis, and photodegradation are the most available methods (Linlin *et al.*, 2020; Hossain *et al.*, 2019; Raouf M. & Raheim A. 2016). Among these, chemical precipitation is commonly used for the removal with the help of chemical precipitators like sodium hydroxide, magnesium oxide, calcium hydroxide, calcium magnesium carbonate (Alam *et al.*, 2020). However, they have their own inherent constraints such as produce a large amount of sludge, less efficiency, sensitive operating conditions, and costly disposal. So, in this aspect adsorption type of technology is favorable and technically easy for removing trace metal ions at low concentrations emerging as a potential alternative for industrial wastewater (Raouf M. & Raheim A., 2016). Adsorption is the process by which one material adheres or bound to the surface of another material through physical or chemical attraction; means it works on the principle of adhesion.

Some of the most well-known used adsorbents for Cr(VI) removal include AC, biological materials, chitosan, fly ash, and others (Padmavathy *et al.*, 2016). Beyond these adsorbents also used for the analysis of aromatic volatile organic compounds (VOCs) such as toluene, benzene, m-xylene, and styrene (BTXS) in the air, the potential use of AC as a low-cost and efficient alternative sorbent material in thermal desorption is presented and validated (Lee *et al.*, 2019). For this reason, the eggshell that mainly composed of calcium carbonate (94.03%) or calcite, amino acids and has a cellulosic structure; So, it is expected to be good for both bio sorbent water treatment processes and catalysts in biodiesel production (Bhaumik *et al.*, 2012; Makuchowska, 2019). On the other hand, as Chisanga *et al.* (2017) determination, termite mound (TM) soil in the name of anthill samples taken from Nigeria contain Fe_2O_3 , SiO_3 , Al_2O_3 , K_2O , CaO , and Mg that exist in various concentrations of oxides which were due to parent materials in the vegetation around, and fertilizer use. So, based on this elemental content TM can be projected as the best candidate for future promised adsorbent and if use in mixture form of the two above resources is favorable. Because most of the countries have possessed these raw materials including Ethiopia should be actively engaged in finding such a best type of alternative adsorbent. Beatriz *et al.* (2020) explain that the mixture of these types of adsorbents beyond their individual oxide composition advantages their mixture can have synergistic effects in the adsorption of water contaminants.

1.2. Statement of the problem

It is very appropriate to say that water is vital both universal solvent and as well as being a crucial component of the metabolism process within the human body and it should be essentially clean and fresh for the existence of life. However, increased industrial and agricultural activities have resulted in the production of a variety of harmful chemicals, which are the primary pose of a serious threat to global water contamination. Especially, the persistent proliferation of industries enormously releases transitional metal ions into the aquatic environment that acute in threatening health injuries or detrimental effects on both flora and fauna which live either aquatic or terrestrial due to their accumulation of these pollutants in different forms to downstream from the contaminant sources. These types of perilous ions are non-biodegradable and have a vigorous biodegradation resistance and primarily bind to nucleic acids in living organisms. So, continuous flows of untreated or partially treated chromium-containing wastewater from industrial pollution to the nearby streams acute higher health impact on the downstream societies and ecological degradation in water bodies, by causing highly toxic, carcinogenic, mutagenic, and teratogenic properties in living organisms (Yusuff, 2019). For instance according to Kannan A. & Thambidurai S. (2008) explanation during the tanning process for converting rawhides or skins in leather industries and electroplating release chromium (VI) 4520 mg/L and 2500 mg/L concentration respectively. During the transformation of these rawhides or skins into leather and related products accomplishment process by means of tanning agents, it generates toxic metals, colored, highly turbid, and foul-smelling wastewater. The main components of this toxic effluent include chromium, sulfide, volatile organic compounds, large quantities of solid waste, suspended solids like animal hair and trimmings. Also, as Labied *et al.* (2018) state that effluents from tannery industries Cr(VI) concentration 1300–2500mg/L released; while its tolerance limited to 0.05mg/L for potable water. Furtherly, according to Teklay *et al.* (2018) reports, Ethiopia is the most promising leather producing country in Africa; mainly focus on leather industry economic sectors that set 28 tanneries, 16 medium and large scale footwear manufacturers, 15 garments and goods factories, 3 gloves factories, and 368 micro and small scale enterprises; however, simultaneously it discharges significant amount of contaminated waste. For example, as Abraha G. (2009) explains Sheba tannery from the Tigray region of Ethiopia discharge 120m³/day of contaminated waste to the environment.

The carcinogenicity of chromium to humans and other living organisms has prompted extensive research into treatment technologies, with varying degrees of success; in general, the most effective methods are more expensive. Therefore, scrutinizing research that focuses on developing cost-effective, efficient, and environmentally friendly treatment technology is the best alternative. Currently, a series of different adsorbents has been investigated as an urgent solution. Based on these adsorption processes have received significant attention due to chromium ions that cannot be removed efficiently by other techniques (Ali *et al.*, 2016). Still, there was an investigation by Yusuff (2019) that claim the adsorbents such as silica gel, alumina, commercial activated carbon and molecular permeable are efficient in trace metals discarding from polluted water but they are expensive and also most of the sources for AC crops are edible or cattle fodder and seasonally available. For this matter currently, a series of different adsorbents has been investigated and extended to use as alternative methods by using locally available and inexpensive adsorbents which cannot be depleted and environmental friend. To this effect as Dereje *et al.* (2021) explains in Ethiopia, volcanic rocks are also applied to remove hazardous pollutants from tannery wastewater. Because, it is obvious that innovation of new materials emphasis to technological influence on water purification, from desalination membranes to atmospheric water scavenging; however, still the most difficult aspect of technological solutions is the cost of these precious technologies (Haddad *et al.*, 2019). This challenge was tried to be alleviated by different numerous researchers who find that the adsorption by using eggshell adsorbent; but still it has its own limitation according to Yusuff (2019) during the study of Ni^{2+} removal which reveals relatively low capacity than termite mound mixed with eggshell that increases the number of the molecular adsorption sites beside it contains several metal oxides for effective removal from an aqueous solution. Based on these limitations and background adsorbents in this thesis study was focused on utilizing locally available and low-cost resources with justified four influenced parameters of batch process of adsorption by synthesizing termite mound-chicken eggshell mixture adsorbent and characterize the potential of improvement adsorption capacity as an adsorbent to remove Cr(VI) from aqueous solution.

1.3. Objectives

1.3.1. General objective

The main objective of this thesis is to investigate the application and optimization of hexavalent chromium (Cr(VI)) removal from aqueous solution using synthesized local termite mound with chicken eggshell adsorbent.

1.3.2. Specific objectives

The specific objective of the thesis is to:

- Synthesize and characterize of termite mound-chicken eggshell adsorbent.
- Optimize and determine the effects of parameters on the removal of Cr(VI).
- Evaluate the best fitting of adsorption isotherm and adsorption kinetics models.

1.4. Scope of the study

This thesis was covered from harvesting raw materials and synthesizing termite mound- eggshell mixture to characterize and evaluate its effectiveness of adsorption based on the synthesized adsorbent and determined the independent variables concerning its removal efficiency or capacity of hexavalent chromium (Cr(VI)) from aqueous solution. The physicochemical properties of the synthesized TMESP adsorbent were characterized by XRD, FT-IR, TGA, and UV-visible. The removal efficiency of Cr(VI) was investigated by considering different parameters like adsorbent dosage, initial concentration of Cr(VI) ions, pH, and contact time. The effect of adsorption parameters was studied and optimized through a CCD of response surface methodology. The adsorption isotherms and time-dependent kinetic model were investigated.

1.5. Significance of the study

Since the industry become tremendously overwhelmed the world from year to year steadily increased the presence and contamination of heavy metals in our water supplies should be a concern as negative impact on life existence; especially for a human being that actively participates in the factory (Tao *et al.*, 2015). Based on this pre-condition this thesis mainly has great relevance in terms of improvement with a paramount adsorption capacity of toxic heavy metal ions from aqueous solutions by using locally available resources that improve indispensable alternatively economic and environmental advantages for the country and to survive generations besides deservingly waste reduction from industries.

2. LITERATURE REVIEW

2.1. Occurrence and methods of removal hexavalent chromium

Chromium was first found in 1797 by the French chemist Nicolas Louis Vauquelin and it was named chromium (Greek Chroma, “color”) because of the many various colors that exist in its compounds (Aigibe & Osibote, 2020; Alam et al., 2020). In the Ali *et al.* (2016) report, chromium is the earth’s 21st most ubiquitously element and the sixth most abundant transition metal. The principal chromium ore is ferric chromite and less common sources include crocoite, lead chromate, chrome ochre, and chromium oxide (Bisht *et al.*, 2015). Chromium is occurring as a natural element in soil, rocks, and volcanic dust that come from the earth’s crust. As Thallapalli & Prasad (2016) verify, it is enter into the biological cycle through potable water, food, and air of an environment. Industrially contaminated water is mostly identified by considerable transition metal content that needs treatment before disposal to get rid of water pollution. The most important industrial sources of chromium in the atmosphere are those analogous to ferrochrome production and metal plating (Bahador *et al.*, 2021). Also, it occurs in the environment in different forms under various chemical, physical, and morphological conditions. Ore refining, cement-producing plants, chemical and refractory processing, automobile brake lining and catalytic converters for automobiles, leather tanneries, during the manufacturing processes of catalysts and chrome pigments also contribute to the atmospheric burden of chromium (Islam *et al.*, 2019; Nogueira *et al.*, 2019; Khalil *et al.*, 2021). According to the World Health Organization (WHO) standards, its tolerated level in drinking water is 0.05mg/L and its concentration in industrial-contaminated waters is different from 0.5 to 270 mg/L (Rai *et al.*, 2016; Padmavathy *et al.*, 2016; Bahador *et al.*, 2021). But in Azis *et al.* (2021) explanation contaminated streams from electroplating may contain up to 2500mg/L Cr(VI), which should be adjusted to a permissible stage before being released to the environment. Especially, wastewaters released from tanneries are ranked as the biggest polluters of all other industrial contaminated waters. Among the various tanning systems, the most known all over the world are the chrome and vegetable tanning industries. Today, 80–90% of leathers produced factories in the world are Chrome-tanned leather (Nur-E-Alam *et al.*, 2020). Thus, it is a must to purify these chromium bearing contaminated waters in order to mitigate that threat.

Numerous physical and chemical techniques have been innovated to the purification of released chromium to bring their level down to the tolerable effluent levels (Rai *et al.*, 2016). The frequent conventional technologies used for treating heavy metals from aqueous streams include chemical precipitation, membrane filtration, coagulation, ion exchange, adsorption, etc., (Khalifa *et al.*, 2019; Khalil *et al.*, 2021). However, since they have their own drawbacks like incomplete removal, high reagent cost, and energy requirements, the generation of highly toxic sludge that needs careful disposal have made it imperative for an economical treatment technology that is able to remove trace metals from aqueous effluents (Ali *et al.*, 2016). Therefore, this requirement improved for the treatment strategy that is easy, robust, and also addresses local resources and constraints. In the study of Khalil *et al.* (2021), adsorption has emerged as an inexpensive and effective technique for the removal of Cr(VI) from polluted water. Adsorption is also an efficient and versatile technique for removing chromium, particularly when combined with appropriate regeneration procedure (Kannan & Thambidurai, 2008). This idea specifically elaborated by Maheshwari & Gupta (2015) as adsorption has taken as one of the most efficient techniques for the removal of Cr(VI) on an industrial level. Extensively, several types of research have justified that nanomaterials are the efficient sorbents for the treatment of transitional metal ions from contaminated water due to their unique structural properties. Also, as Makuchowska (2019) justifies this effectiveness of water solution purification relay on numerous parameters, among others pH, concentration, sorbent particle size, dose of adsorbent, contact period, and competitive sorption of ions. Nanomaterials-adsorption serves as sorbents for treating transition metal ions from contaminated effluent water, it should fulfill the following criteria: 1) The nano sorbents themselves should be free from toxicity. 2) The sorbent that exists should be enhanced to high sorption capacities and selectivity to the minimum concentration of contaminants. 3) The adsorbed wastes could be easily removed from the surface of the nano-adsorbent. 4) The sorbents could be improved or extended to infinitely recycled (Kassahun *et al.*, 2017). So far, several nanomaterials such as carbon nanotubes, graphene, carbon-based material composites, non-metal or metal oxides, and polymeric sorbents have been investigated in the removal of trace metal ions from aqueous solution, and the outcome indicates that these nano-scale materials reveal as high adsorption capacity (Aigbe & Osibote, 2020).

2.2. Physical properties of chromium

Hexavalent chromium is used in stainless steel, chromium plating, and other alloys factories. For instance, on cars and bicycles, produces a smooth, silver finish that is highly defender to corrosion. This chromium metal has a bcc (body-centered-cubic) crystal structure, and 7.2g/cm^3 density with atomic numbers 24, and 52g/mol the molecular weight at room temperature and boiling point of 2672°C and 1907°C (Ali *et al.*, 2019; Aigibe & Osibote, 2020). According to Ghorbani-Khosrowshahi & Behnajady (2016) explanation, chromium has a broad usage in the industry like electroplating industries among different trace metal ions; due to its strong crystalline structure, corrosion resistance, and yellow color. Also, chromium metal is a lustrous, brittle, hard metal and highly reactive with oxygen in the air, instantaneously it yields a thin oxide layer that is impermeable to oxygen and resists the metal below from corrosion. Its color is silver-gray which can be significantly polished and it does not tarnish in air, when incinerated it burns and forms green chromic oxide. The solubility of chromium composition is different concerned its particular oxidation state. For example, compounds of trivalent chromium, with the exception of acetate, hexahydrate of chloride, and nitrate salts, are totally insoluble in aqueous water. The zinc and lead salts of chromic acid are practically not soluble in freezing water. The alkaline metal salts (e.g., calcium, strontium) of chromic acid are slightly soluble in water. Some hexavalent compounds, such as Cr(VI) oxide (or chromic acid), ammonium, and alkali metal salts (e.g., sodium and potassium) of chromic acid are easily dissolved in aqueous water. However, based on the reactivity arrangement potassium has a higher stage among others. On the other hand to minimize the severity of hexavalent chromium compounds should reduce to the trivalent form in the presence of an oxidizable organic matter agent. but, in natural surface waters where there is a low concentration of reducing materials, hexavalent chromium compounds are more stable than others (McNeill & Mclean, 2012).

2.3. The oxidation state of chromium metals

Chromium is a heavy metal that occurs in various forms of oxidation states ranging from Cr (-II) up to Cr(+VI); among these, the trivalent and hexavalent states are the most common stable ones (Berihun, 2017; Silva *et al.*, 2016). In an aqueous environment, hexavalent (VI) and trivalent (III) chromium have distinct properties (Saravanakumar *et al.*, 2017). As Rajapaksha *et al.*

(2018) explain, Cr(VI) is highly soluble in water and forms mobile oxyanions, which are known to be toxic to biological cells. Conversely, the trivalent of its state is known to form highly stable and insoluble OH precipitates which is regarded as chemically inert for this reason. Indeed, excessive uptake of chromium (III) can cause health impacts as skin rashes, stomach upset and ulcers, respiratory problems, weakened immune systems, kidney and liver damage, alteration of genetic material, lung cancer and cause death (Teklay *et al.*, 2018; Abbas *et al.*, 2018). This trivalent chromium is predominantly known in air emissions in the form of small particles that are termed as aerosols. The maximum permissible concentration of chromium is 0.05 mg/L for in drinking water and 0.1mg/L for discharge to inland surface water according to WHO established regarding health considerations; in addition to this according to United States of Environmental Protection Agency (EPA) guideline recommendation states for potable water should not exceed beyond 100µg/L Cr(VI) (Khan *et al.*, 2017; Khalifa *et al.*, 2019). The study by Rajendran (2011) indicates, that chromium is accounted as an important nutrient for several organisms in trace amounts and an essential element that is required in small quantities for carbohydrate digestion. In terms of chemical and biological reactivity as well as physicochemical properties, toxicity, and nutritional value of chromium is significantly the most controversial transitional element among the various heavy metals ions. While Cr(VI) is very toxic, mutagenic, with a well-known perilous carcinogenic impact on humans, Cr(III) contributes at small amounts as an important nutrient in human and animal health (Silva *et al.*, 2016). All individual needs of Cr(III) are taken by eating which is available in fruit, vegetables, meat, seeds, and yeast which can be useful for human health. Trivalent chromium decreasing cause heart disorders, disorders of metabolism, and diabetes. Chromium (VI) anions are highly mobile and can readily soluble in aquatic solution due to repulsive electrostatic interactions with soil particles that are negatively charged. In aqueous solution, Cr(VI) is considered as the most noxious that found in different forms depending upon the pH, such as chromate ($\text{Cr}_2\text{O}_4^{2-}$), hydrochromate (HCrO_4^-), or dichromate ($\text{Cr}_2\text{O}_7^{2-}$) (Tanhaei *et al.*, 2020; Yosuff, 2019). However, Cr(III) species normally carry positive charges and are less mobile since they can be easily adsorbed on the soil particles. In human blood, the chromium only exists in Cr(III), where it is responsible for the maintenance of blood metabolism. According to Ali *et al.* (2016) reports, the recommended daily dietary intake (DDI) of chromium (III) for a human is 50–200micrograms per day. Chromium (III) is essential to

normal glucose, protein, and fat metabolism and is thus an essential dietary element. According to Abraha *et al.* (2009) states, insufficient dietary intake of chromium(III) leads to increases in risk factors associated with diabetes and cardiovascular disease including elevated circulating insulin, glucose, triglycerides, total cholesterol, and impaired immune function. Also, Cr(III) plays an important role in insulin signaling and glucose metabolism is also involved in the regulation of levels of glucose and low-density lipoprotein cholesterol (LDL) in the blood (Silva *et al.*, 2016; Nogueira *et al.*, 2019). In contrast, the greater toxicity of Cr(VI) is related to its greater solubility in aqueous media and bio-membrane permeability, which facilitates the interaction with proteins and nucleic acids (Silva *et al.*, 2016; Owalude & Tella, 2016).

2.4. Effects of Chromium on human beings

Chromium incorporates many oxidation states with unique toxic properties. For instance, trivalent chromium (Cr(III)) is important for human beings during the carbohydrate metabolism process; in contrast to this, hexavalent chromium (Cr(VI)) is considered notoriously toxic due to its carcinogenic, mutagenic, and teratogenic properties (Rai *et al.*, 2016; Khan *et al.*, 2017). Humans can exposure to chromium through breathing, touching skin, drinking, and eating with its elemental ions and its compounds. On the other hand, Cr (VI) compounds are found to be a hundred times more toxic than Cr(III) compounds since it has a high solubility in water and it behaves in high mobility (Chen *et al.*, 2014). Extensively, as Ali *et al.* (2019) claim in groundwater, chromate (VI) is approximately 1000 times as toxic as chromite (III) and more mobile. These concepts are supported by Alam *et al.* (2020) explanation as Cr (VI) are 500 times more poison than the trivalent one. Therefore, exposure to this Cr(VI) can have a variety of adverse effects on human health, namely allergic reactions, nasal septum injury, asthma, throat inflammation, and lung cancer. Also, strong exposure to Cr(VI) causes encompasses cancer in the digestive tract (Stomach disorders) and may cause gastric pain, nausea, vomiting, severe diarrhea, breathing (lungs), ulcers, dermatitis, weak immune system, impaired fertility, harm to unborn children, kidney, liver, nervous system, gastrointestinal ulcers, eye damage or blindness, hemorrhage and change in genetic material (Khan *et al.*, 2017; Islam *et al.*, 2019; Ali *et al.*, 2020; Tanhaei *et al.*, 2020). As Ali *et al.* (2019) studied, chromium contamination in water deteriorates or damages the health of not only humans but also entire ecosystems.

The disposal of trace metals into wastewater through human and industrial activities has become the main bottleneck for both humans and aquatic life. Chromium is as transition metal ions ranked to the top sixteen toxic contaminants that have detrimental effects on human health (Ali *et al.*, 2019). High volume of chromium dosage has been explained as risk that causes damage to the human kidney and the liver at minimum concentration; it also causes skin irritation and ulceration. As in several kinds of research justified exposure to high amount Cr(VI) concentration also causes cancer in the digestive tract and lungs (Owalude & Tella, 2016; Ali *et al.*, 2016). The toxicological concern for Cr(VI) stems from the fact that it is easily reduced as it able release free radicals that can have carcinogenic and mutagenic effects on cells (Liu *et al.*, 2015). The existence of Cr(VI) as an elemental form in nature is rare; it is usually found in coupled form with other elements in the form of compounds such as iron(II) chromite (FeCr_2O_4). Consequently, chromium is extracted its metal forms from these compounds to be used. Therefore, any pollution form of Cr(VI) in the environment is regarded as an anthropogenic activity (Liu *et al.*, 2015). The study of Rajapaksha *et al.* (2018) at biochar adsorbent justify that Cr(VI) is widely used in different industries such as chrome plating, textiles, leather tanning, brass, electrical and electronic equipment, and catalytic processes release Cr(VI) into surface water bodies, soils, and aquifers. According to Kannan & Thambidurai (2008) reports tanning is a process of converting rawhides or skins into leather release chromium (VI) 4520 mg/L concentration. That utilizes a considerable amount of tanning powder, which in major contain chromium sulfate ($\text{Cr}_2(\text{SO}_4)_3$), that generated by the reduction of Cr(VI) to Cr(III) using sulfur dioxide. According to Nur-E-Alam *et al.* (2020) reports, approximately 30-40% of the used chromium in the reduction process is discharged into the tanning process water. Concerning to this impact the levels of Cr(VI) from such factory effluents must be reduced to a tolerable limit before discharging into the downstream waters being used for domestic purposes by the nearby communities (Abrah *et al.*, 2009). As various researches paper reports the tanning activity is crucial for the calfskin industry and most tanneries within the world approximately 90% utilize chromium salts to deliver leather, since these salts give superior calfskin adaptability, better leather flexibility, superior water resistance and a high shrinkage temperature. Unfortunately, chromium salts are not totally settled by skins and the remaining amount around 30% of the initial one remains within the spent tanning liquor (Abraha G., 2009). The US EPA allows a

maximum of 0.15g/kg of chromium to be released in the leather tanning industry's effluent and approved 0.1mg/L as the maximum permissible concentration of Cr(VI) in drinking water (Maheshwari & Gupta, 2015; Genawi *et al.*, 2020).

2.5. Termite mound nest pedological view and its composition

Termites are social insects that belong to the Kalotermitidae family of fauna and, along with the analogous to wasps and bees, under the order of Isoptera (Garcia *et al.*, 2013). Termites are essential in ecosystem functioning as they not only constitute a main component of the animal biomass in soil but also significantly influence nutrient cycles by bioturbation and stimulation of soil organic matter synthesis action (Kristiansen & Amelung, 2001). According to Kipsanai *et al.* (2017) reports, a termite mound (TM) is a pile (heap) of the soil of the earth, sand or, pine needles, a composite of these and other materials that build up at the entrances of the subterranean dwellings of termite colonies. Most investigations have exposed that TM consists of essentially large concentrations of total nitrogen (N) and exchangeable cations than the surrounding soils. The opportunities of using termite mound soil as an amendment in crop production have been explained by different scholars. For example, Chisanga *et al.* (2017) describe the nutrient status of organic soil amendments from TM sources as other positive value on crops that encompass weeds suppression. Termite hills are called mounds constructed by termites which substantially modify the physicochemical properties of soil and have the ability to transform mineralogy of clay by gathering woody debris for their nests and forage for large quantities of insect prey and honeydew as food for their colonies (Fufa *et al.*, 2014). Active termite mounds are thus enriched with soil organic matter and inorganic nutrient elements, such as Ca, K, Mg, Na, and P, relative to nearby surface soils. The activity of termites' can also transform (i) the physical characteristics of the soil, such as infiltration and porosity (ii) decomposition speed of organic matter (iii) soil microbial community including faunal biomass of ecosystem. It is an omnivore, feeding on invertebrates, applying honeydew, and forming colonies with thousands of individuals. Unlikely that the chemical process forward for deodorization there is a decomposition of organic matter, followed by crystallization of formerly organically complexed to inorganic oxides to have occurred. There is also a suggestion that the degradation of podzolic features within the termite mounds results from other processes, such as

(i) a specification by the termites of less podzolized sites in the woods for their hills, or (ii) a biological disturbance of podzolic features by bioturbation and loosening of soil, the latter favoring water infiltration and further nutrient and metal leaching from the soil (Kristiansen & Amelung, 2001). Since a termite mound is a form of clay which is formed by workers termite insects. It is huge, surrounded by vegetation, and can persist for several years. According to Fufa *et al.* (2014), these TMs resources are abundantly distributed in nature around southern and western parts of Ethiopia, its average TM abundance is estimated to be 12mounds per hectare. Also, in addition to its wide availability the Kipsanai *et al.* (2017) study prove that this termite mound specimen mainly consists of silica (SiO_2), alumina (Al_2O_3), iron oxide (Fe_3O_4), zircon oxide (ZrO_2), and many other metal oxides. This elemental composition of the termite mound is also evidenced by Fufa *et al.* (2014) as it encompasses mainly silicon, aluminum, iron, and titanium oxides which are precious materials for adsorption purposes. Especially, the presence of zirconium oxide nanoparticles serves as an adsorbent without any modification was explained by Dereje *et al.* (2021). In another way, many scholars of literature have used SiO_2 , Al_2O_3 , TiO_2 , and Fe_3O_4 as an adsorbent component for transitional ions removal from aqueous solutions. Also, according to Dereje *et al.* (2021) report, the valuably of these types of oxide compositions within adsorbent during the study of pumice and scoria for removal of phosphate.

2.6. Chicken eggshell fitness as bio sorbent

The chicken egg mainly consists of three major components: the white or albumen, shell, and yolk. This eggshell part of chicken egg incorporates the cuticle, spongy calcareous, crystal layer, layer pores, cores, and mammillary layer. The membranes found on the inner surface of the eggshell exist like a single layer but can be categorized into two identical layers of fibrous material. When one layer bounds the albumen the other is bound to the "tips" of the calcified material of the shell. They are regarded as the inner and outer shell membranes respectively. Chicken eggshell is physically looked at as it contains high crystalline CaCO_3 that comes partly from the chicken bones (Badrealam *et al.*, 2020). In more elaboration, Badrealam *et al.* (2020) explain that the chicken can easily mobilize 10% of her bone for its own purpose. The membranes of chicken eggshells can serve as an adsorbent for the purification of reactive dyes from colored polluted effluents and transitional metal ions from dilute contaminated waters

(Ajala *et al.*, 2018). So, based on the contents of the chicken eggshell serves as a useful adsorbent to remove the trace metal ions from the aqueous solution for the contaminated water treatment (Badrealam *et al.*, 2020). Also, as Ajala *et al.* (2018) justified, the chicken eggshell has been weighed to an average of 1.6% of the total chicken egg with a thickness between 0.33 and 0.35mm. Besides these according to Bhaumik *et al.* (2012) reports, chicken eggshell majorly consists of calcium carbonate (94.03%), amino acids, calcite, and has a cellulosic structure; thus, it is expected to be a good bio sorbent. However, as Sumathi (2017) explanation, commercial nanoparticles of CaO have much attention due to it has high applications such as marble, coral, chalk, cement, and glass as building materials, paints, paper, pulp, and medicine. Thus, preparing such invaluable chemicals composition materials from easily available resources like eggshell need high intension. Also, the calcium content of chicken eggshells is 2300.33 ± 3.80 mg/L while the duck eggshell is 42.3 mg/L and turkey eggshell 50.1mg/L (Ajala *et al.*, 2018). So, based on this experimental ingredient information this thesis was focused to scrutinize the readily available chicken-eggshell adsorptive capacity of adsorption by mixing with flourish termite mound to synthesis an adsorbent that provides a conspicuous role of adsorption.

2.7. Conventional technologies for waste water treatment with their drawbacks

Industrial wastewater is generated from fresh water which is used as integrated part of chemical process industries for various activities starting from raw material stage to product finishing stage. As an outcome, wastewater of different characteristics are generated depending upon the types of industries like petroleum refinery, petrochemical, fertilizers, fine chemicals, pharmaceuticals, etc. This industrial wastewater is adversely affecting human health and its environment as it content toxic heavy metals, suspended solids, and complex organic compounds. However, it should be fulfill the minimum criteria of quality as per the WHO standards. But this requirement is not fulfilling standards due to changes in its characteristics like physical, chemical and even in biological. Hence, it is essential to develop a rapid, simple, effective, and efficient method for the treatment of industrial and municipal wastewater. Apart from these, various wastewater treatment technologies are discussed including ion exchange,

electrodialysis, membrane-based methods, coagulation and flocculation (Gangaraju et al., 2021; Bayuo *et al.*, 2020).

2.7.1. Sand filtration

In rural areas of developing countries and for slow sand filtration, a small-scale installation is believed to be the easiest and high-performance technique of contaminated water purification. However, some background information shows that some operational challenges such as massive algal growth and oxygen depletion may lead to system failure. The former leads to a premature clogging of the filter whereas the latter results in anaerobic conditions in the filter bed due to the production of hydrogen sulfide and other taste and odor-producing substances (Silva *et al.*, 2015). According to Wiesman's (2012) explanation, the modification of sand filter like the stratified sand filter is also based on intermittent sand filter, the difference being its particle size and layering of the filter media of aqueous solution.

2.7.2. Ion exchange

One of the most frequent and successful treatment procedures for liquid radioactive waste is an ion exchange method. It is a well-known technology that has been used in both the nuclear and other manufacturing sectors for several years. Despite its advanced state of development, several countries are studying various elements of ion exchange techniques in order to increase its efficiency and economy in its applications to liquid radioactive waste management. The ion exchange process is extremely efficient at transferring radioactivity from a high volume of liquid to a small volume of solid. The purification and tendency of radioactive used ion exchange materials is a lengthy process that requires careful consideration of the materials' properties as well as their compatibility with various processing, storage, and disposal alternatives. The management of spent ion exchange media should be considered in the context of an incorporated pollution management system for all radioactive contamination; for instance, ion-exchange waste may make up such a small percentage of the total waste stream that modified purification for ion exchange media considered as more expensive. However, the radiochemical properties of spent in ion exchange media may need specialized handling, even though the volumes may represent a small fraction of a facility's waste inventory (Simina & Meghea, 2014).

2.7.3. Electrodialysis

Electrodialysis (ED) is an innovative advanced separation process that becomes known for the purification of potable water from sources of water bodies and treats industrial contaminant water. The ED process is serving as common on a commercial scale. The main purpose of the ED process is to remove salt from the aqueous solution by passing through the aqueous media in terms of an ion-exchange membrane and the cell of this ED is categorized into compartments by placing anion and cation exchange membranes between the two electrodes that act as the cathode and anode. Direct electric power is supplied between the two electrodes. Consider the feed solution containing sodium chloride that passes through the ED system and is concentrated in one compartment. The cations across the cation exchange membrane and the anions are restricted. Anions can only pass through the anion exchange membrane, which limits the passage of cations. The salt concentration in this compartment reduced; however, the salt concentration in the adjacent compartment continues to increase. Therefore, the salt concentration decreases in the replacement compartment and raise in the remaining compartments. Both desalinated water and concentrated brine come from adjacent compartments. The applied potential serves as the driving force for the ED process. When the salt concentration is low and is considered an energy-saving process, ED is the first choice (Habib, 2018).

2.7.4. Membrane process

Membrane filtration is a physical separation of conventional technology that uses a semipermeable membrane to discard suspended solids from an aqueous stream. MF and UF, along with nano-filtration (NF) and reverse osmosis (RO), are all considered as pressure-driven membrane filtration (Li *et al.*, 2012). Comparison with similar processes types of membrane microfiltration is basically the same as other filtration technologies that use pore size distribution to physically separate particles. It is similar to other technologies, such as ultrafiltration/nano-filtration, and reverses osmosis, but the only difference is the size of the retained particles and the osmotic pressure.

Microfiltration (MF): Microfiltration is typically used as a pre-treatment for other purification techniques like ultrafiltration and as a post-treatment for granular media filtration. The typical particle size for microfiltration is between 0.1 and 10micrometers. These membranes can

separate macromolecules with approximate molecular weights of less than 100,000 g/mol. The filters used in the microfiltration process are specifically designed to prevent particles like silt, algae, protozoa, and big bacteria from passing through (Li *et al.*, 2012). Extreme microscopic, atomic, or ionic materials such as water (H₂O), monovalent ions such as Sodium (Na⁺) or Chloride (Cl⁻) ions, small colloids, dissolved or natural organic matter, and viruses still can pass through the filter. With a driving force ranging from low to medium pressures (about 100-400kPa) parallel or tangential to the semi-permeable membrane in a sheet or tubular form, the suspended liquid can also travel through at a high velocity of around 1–3m/s. To allow liquid to travel through the membrane filter, a pump is frequently installed on the processing equipment. There are also two types of configuration pumps: pressure-driven and vacuum-driven. To monitor the pressure drop between the outlet and intake streams, a differential or regular pressure gauge is frequently fitted. Microfiltration membranes are most commonly used in the water, beverage, and bio-processing industries. The procedure for exiting stream after treatment using a micro-filter has a recovery rate that is generally between about 90-98 percent (Brema & Selvarani, 2017).

Ultrafiltration (UF): Ultrafiltration membranes are the best alternative for retaining micro-organisms, yeast, and suspended particles, while salts, proteins, and smaller organic molecules can pass through the membrane. UF modules are used in a wide range of applications, varying from RO pretreatment, potable water production, wastewater treatment, foods and beverage applications. According to Lubello *et al.* (1918) justification, the substantial capacity of microfiltration and ultrafiltration has significant importance in the removal of microorganisms including viruses reducing or eliminating expenses for disinfection. UF treatment provided notably good results for what concerns removal capacity of up to TSS (0.18mg/L) and turbidity (0.18NTU). Also, in Brema & Selvarani's (2017) investigation, UF membranes have pore sizes ranging from 0.01µm to 0.1µm and can retain proteins, endotoxins, viruses, and silica. UF has diverse applications which span from contaminated water purification to pharmaceutical uses.

Nanofiltration (NF): Nano-filtration is a relatively new type of membrane technology with properties that lie in between UF and RO. While RO membranes are the most commonly used in seawater desalination. Nano-filtration membranes are used in several contaminated water

treatment and industrial applications for the selective removal of ions and organic compounds, as well as in a few specialized saltwater desalination applications (Shahmansouri & Bellona, 2015). Also, as Shahmansouri & Bellona (2015) extensively states, NF has been employed for the removal of arsenic, pesticides, inorganic carbon, oxyanions (e.g. bromate, perchlorate, phosphate, sulfate), and various emerging organic contaminants. These types of membrane filtration have pores sized from 0.001 μm to 0.01 μm and filters multivalent ions, synthetic dyes, sugars, and specific salts. As the pore size drops from MF to NF, the osmotic pressure requirement increases. Reverse osmosis is the finest separation membrane process available, pore sizes range from 0.0001 μm to 0.001 μm . RO can retain mostly all molecules except for water and due to the size of the pores, the required osmotic pressure is significantly greater than that for MF. Both reverse osmosis and nano-filtration are fundamentally different since the flow goes against the concentration gradient, because those systems use pressure as a means of forcing water to go from low pressure to high pressure.

Reverse Osmosis (RO): Reverse osmosis is an innovative membrane-type process for purifying water by separating dissolved materials from the feed stream, resulting in permeating and preventing streams for a wide range of domestic and industrial applications (Garud *et al.*, 2011). According to (Garud *et al.*, 2011), dissolved solids, color, organic contaminants, and nitrate are all removed from the feed stream using RO technology. Not only does reverse osmosis allow for the integration of UF (in the event that reverse osmosis alone fails), but it also broadens the spectrum of conceivable applications by incorporating scenarios when RO is utilized in the treatment cycle (Lubello *et al.*, 1998). In the study of Brema & Selvarani (2017) RO is the finest separation membrane process available, pore sizes range from 0.0001 μm to 0.001 μm . RO also has a capacity to uptake mostly all molecules except for water as a result of the size of the pores, and the osmotic pressure required is significantly more effective than that for microfiltration. Because such systems employ pressure to force water to go from low pressure to high pressure; also, reverse osmosis and nano-filtration are basically different as a result of the flow in nano-filtration going against the concentration gradient.

2.7.5. Reduction of hexavalent chromium to trivalent chromium ion

Reduction is a process in which the higher valance state of chromium ion is converted or reduced to the lower valance state using reducing agents. This technique offers several advantages such as the recovery of chromium from contaminated wastewaters; recycling of treated water and short treatment times. Reduction is a treatment method in which reducing chemicals are used to convert the higher valance state of chromium ion to the lower valance state. This method has various advantages, including recovering chromium from contaminated wastewaters, recycling treated water, and reducing treatment timeframes. However, the limitation includes additional chemical requirements and hazardous sludge formation. This method is standard to serve in purifying chromium (VI) ion industry contaminated aqueous by reduction and coagulation techniques, but the decreasing percentage to reduce of chromium (VI) is still not significant and too expensive relatively (Azis *et al.*, 2021).

2.7.6. Coagulation and flocculation

Coagulation is one of process technology to neutralize charges and then to form a gelatinous mass to trap particles in order to increase mass to settle down or be trapped in the filter; on the other hand, flocculation is gentle stirring or agitation to encourage the particles thus form agglomeration large sufficient to settle or be filtered from solution (Engelhardt, 2010). However, conventional coagulants like ferrous sulfate, aluminum sulfate (alum), ferric chloride, and ferric chloro-sulfate are possible links to Alzheimer's disease which becomes an issue in wastewater treatment (Llitan, 2010). Hence, it needs special attention that forwards to shift towards using biodegradable polymer, chitosan in treatment, which are more environmentally friendly. As Engelhardt (2010) investigates particles in aqueous smaller than about 10 microns are hard to discard by simple settling or by filtration. This is especially true for particles smaller than one micron–colloids. Coagulation is, the efficiency generated by the addition of a chemical to a colloidal dispersion resulting in particle disorder by the reduction of the forces tending to keep the particles separate. Electrocoagulation (EC) is a straightforward method that is generally considered unreliable; however, due to improved technology, many pollutants are now eliminated with this method. EC works by supplying low electric current to the wastewater and thereby the electrical charge that keeps the heavy metals together is negatively charged and the

metals are coagulated from the aqueous phase to come together in the mass (called the sludge or floc). The floc developed by EC is more stable, larger, and can be easily taken out by a normal physical filtration system. EC is usually conducted with Al or Fe electrodes (Kunal *et al.*, 2019).

2.7.7. Solvent extraction

Pesticides such as dichlorodiphenyltrichloroethane (DDT) and dicofol can be removed from aqueous contaminants using solvent extraction and adsorption process. In today's culture, pesticide poisoning of surface and groundwater has become a major concern. Even if these pesticides have a number of benefits that can help farmers increase their yields. They can also help to limit the negative health effects that disease-carrying insects have on humans. However, pesticide overuse is hazardous to both the environment and individuals. They are long-lasting organic contaminants that build up in fatty tissues. Industrial effluents must be treated before being discharged into pesticide-containing wastewater. Recovery procedures like solvent extraction are particularly useful in the pesticide manufacturing sector because they may recover one or more components from polluted water. The chemical value recovered can help offset processing expenses and perhaps give a net advantage. There are three primary processes in the solvent extraction process. The first step is extraction, which involves transferring the solute from water to a solvent. The second stage is the solute removal step, which involves separating the solute from the solvent and returning the solvent to the extractor. The solvent recovery stage is the third step, in which the solvent is extracted from the contaminated water raffinate (Sreedharan, 2018).

2.7.8. Phytoremediation

Phytoremediation is a process for extracting or eliminating metal contaminants and inactive metals from polluted wastewater and soils that is both efficient and cost-effective. In general, phytoremediation entails the employment of plants as both "accumulators" and "excluders," or stabilizers, of pollutants. This technology has the potential to be both low-cost and eco-friendly. Various techniques are already in use to purify the environment from contaminants that migrate into non-polluted areas as dust or leachates through the soil, as well as the spread of heavy metals containing sewage sludge, but the majority of them are expensive and lack a systematic approach to their optimal performance. According to (Tangahu *et al.*, 2011) states many plant

species have been successful in absorbing pollutants from soils, including lead, cadmium, chromium, arsenic, and different radionuclides. Plants have highly specialized mechanisms for translocating and accumulating micronutrients by nature. The same mechanisms are involved in the uptake, translocation, and accumulation of hazardous elements, indicating that micronutrient uptake mechanisms are of great interest to heavy metal removal phytoremediation methods. Heavy-metal contaminated soils are typically remedied through excavation or onsite management, and then disposed of in a landfill. This form of disposal just shifts the contamination problem, as well as the harmful effects of moving contaminated soil and contaminant migration from the landfill into the surrounding environment, to another location. Soil washing is an alternative to excavation and landfill disposal for clearing polluted soil. This method is quite expensive, and it produces a heavy metal-rich residue that will require considerable treatment. Furthermore, because these physio-chemical approaches for soil remediation remove all biological processes, land can be used as a medium for plant growth. Exudate from root plants stabilizes, demobilizes, and binds pollutants in the soil matrix, limiting their bioavailability. All of these forms of phytostabilization processes are referred to as phytoremediation. Through phytoextraction mechanisms, certain plant species can absorb and hyper accumulate critical metal contaminants for growth (Fe, Mn, Zn, Cu, Mg, Mo, Ni) and surplus nutrients in harvestable root and shoot tissue from the growth substrate. Rhizo-filtration is the precipitation of pollutants in the solution around the root zone onto plant roots or the sequestration of contaminants in the roots by a created wetland to filter communal polluted water (Tangahu *et al.*, 2011).

2.8. Adsorption process technology

Adsorption is one of the most effective processes in advanced polluted water treatment technologies and is widely used by academic and industrial researchers to remove various pollutants. Activated carbon is one of the most studied adsorbents in the water treatment process. It is one of the best-known conscientious methods used to adsorb harmful compounds that incorporate heavy metal removal from contaminated water. It's a surface-based process in which van der Waals forces keep the adsorbate on the adsorbent's surface. Electrostatic attraction and chemical bonding can also cause it. This method is based on the binding of particles or

molecules in a solution to the surface of adsorbents. It can also be done by collecting gas or liquid materials on the surface or in a porous solid of another substance in the form of molecules, atoms, or ions (Mhemeed, 2018). Adsorption is also used in industries for gas separation and purification because of its less energy-intensive than other traditional separation processes, such as distillation and gas absorption (Zeng, 2016). According to Yousef *et al.* (2020), justification adsorption treatment is the most convincing because it operates at low concentrations with less operation time and at a much lower cost than other treatment technologies. The least expensive treatment allows for reuse in a variety of applications. This type of technology has simple operation methods, produces high-quality treated effluent with great prominence, adsorbents can be desorbed, has a dynamic design, and a high-efficiency regeneration process.

2.9. Physisorption and chemisorption processes

Adsorption is defined as two fundamental concepts: physisorption and chemisorption, which are based on the force of attraction between the adsorbent and the adsorbate. These adsorption processes are an important factor in determining whether adsorption is physical or chemical. Chemical adsorption, also known as chemisorption, is caused by chemical forces, whereas physical adsorption, also known as physisorption, is caused by van der Waals forces. However, which types of adsorption will be prominent in a given environment may be difficult to anticipate. To that aim, the adsorption process is classified into two types based on the sorts of forces that exist between the adsorbent and the adsorbate. Sometimes these kinds of adsorption are able to adsorb in the combination with chemical adsorption as well as physical adsorption and both forces are termed as solvent adsorption (Mhemeed, 2018).

2.9.1. Physisorption process

Physical adsorption of the pure fluid phase is successful when the intermolecular attraction between the adsorbent and the pure fluid (solute) molecules is greater than the attraction between the solute molecules themselves. As a result, physical adsorption is analogous to condensation; an exothermic process is accompanied by a heat dissipation procedure. The entropy changes of the adsorbate 'S' must be negative since the adsorbed state is more ordered than the non-adsorbed state in the case of the adsorbent/adsorbate interaction because at least one degree of freedom is lost. In this type of adsorption process, the Gibbs free energy change ΔG is negative, so the

enthalpy change ΔH that accompanies physical adsorption is always negative (exothermic) which indicates that at all temperatures the adsorption process is spontaneous in nature (Yusuff, 2019). Physical adsorption has behaved both reversible and quick characteristics as Van der Waals electrostatic forces (intermolecular forces and atom interactions) keep molecules on the surface (Mhemeed, 2018). As a result, the absence of contact energy, such as mechanical vibration across the interface, might disrupt the binding between adsorbate and adsorbent. Thus, the most important physical adsorption factors are pore size, pore-volume, pore shape, and surface area. At low temperatures, the activation energy is primarily physical adsorption 5 to 10 kcal/mol (Acharyya *et al.*, 2020).

2.9.2. Chemisorption process

Chemisorption involves the transfer of electrons between the adsorbate and the adsorbent. Because chemical adsorption happens via the chemical connection between the adsorbate and the adsorbent's surface, it usually takes place at a temperature higher than the adsorbate's critical temperature. Chemical adsorption, like other chemical processes, necessitates activation energy. For chemical adsorption, the specific surface area of the phase, the type of active sites, the number of active sites, and the stability of the active sites are all important factors. Chemical adsorption occurs as a result of a chemical reaction between the adsorbate's molecules with atoms and the adsorbent's molecules with atoms. Chemical adsorption is irreversible because of the molecules that have been chemically adsorbed cannot move on the surface of the internal contact. The key benefits are the excellent selectivity of separation and the capacity to manage very low solute concentrations. Chemisorption is also accelerated by elevated temperature, where the activation energy varies between 10-100 Kcal/mol (Acharyya *et al.*, 2020).

2.10. Some types of previous studies adsorbents for chromium removal

There is a natural tendency of phenomenon for components of a liquid or a gas to collect often as a monolayer but sometimes as a multilayer at the surface of solid material is called adsorption. Adsorption is one that assures adsorptive is specifically transferred from the fluid phase to the surface of particles suspended. It is a very significant economical, convenient and easy operation method. Adsorption has advantages over other techniques as the reason of its simple design with a sludge-free environment and can involve low investment in terms of both initial cost and land

required. In this topics, ten articles with different adsorbents namely activated mango kernel, magnetic nanoparticles, activated rice straw, palmyra palm fruit seed, Flayash, neem bark nanoparticle, guar gum–nano zinc oxide, Moringa Stenopetala seed powder, and banana peel powder, chemically modified banana peels, and Moringa Oleifera AC, chitosan, and iron oxide nanoparticles and their adsorption efficiency with respective contact time were reviewed. These section of reviewing parameters that used for removing chromium using different adsorbents was used as a reference frame for this thesis; means for the synthesized termite mound-chicken eggshell adsorbent (Badessa et al., 2020; Kumar et al., 2017; Bahador et al., 2021).

2.10.1. Adsorption chromium (VI) by mango kernel activated carbon

Mango is a seasonal tropical fruit that produced in various countries and this mango kernel (MK) is nearly 5% of the total fresh fruit weight. Since it is primarily lingo-cellulosic in nature, an effort has been made in the work to prepare activated carbon (AC) with the objective to use it as an adsorbent for removing hexavalent chromium. It is seen that the adsorption efficiency has 85 percentages which can be directly linked to the availability of increasing adsorption sites with the increasing amount of adsorbent. At a higher adsorbent dose, there are not enough Cr (VI) in the solution to occupy the active sites and hence the adsorption tends to become constant (Rai *et al.*, 2016). Also during the study of Rai *et al.* (2016) the maximum adsorption capacity of Cr(VI) was found to be 7.8 mg/g at PH_2 for initial Cr (VI) solution concentration 20mg/L, adsorbent dose of 0.25 g/100 mL, 35 °C operating temperature, 150 rpm for fifty minutes equilibrium time. The PH_{pzc} value of the MKAC was existed to be 6.8, which proves that at this pH the net surface charge of the adsorbent is zero, whereas, at $\text{pH} > 6.8$, it is negatively charged and $\text{pH} < 6.8$, the adsorbent surface is positively charged. The equilibrium data were well fitted to the Langmuir adsorption isotherm and a pseudo-second-order kinetics model (PSOKM) relation indicates the adsorption process (Rai *et al.*, 2016).

2.10.2. Adsorption chromium by using magnetite nanoparticles

As (Padmavathy et al., 2016) reports adsorption by magnetite nanoparticles synthesized experimentally was used for the removal of Cr (VI) from synthetically prepared wastewater. The preparation of magnetic nanoparticles was accomplished by the sol-gel method in the laboratory and analyzed using scanning electron microscopy (SEM) supported with energy dispersive X-

Ray spectroscopy. Batch adsorption studies were conducted to study the effect of parameters like pH, time, initial concentration, and adsorbent dosage. As initial concentration was varied from 10 to 60 ppm, pH, time, adsorbent dosage, the temperature was kept constant the efficiency varies from 70 to 66%. As adsorbent dosage increases from 5 to 10 g/L removal efficiency first increases, reaches a maximum, and then decreases; because of at lower adsorbent concentration number of active sites is higher. As the pH was increased from 3 to PH 10, the percent of removal efficiency decreased. The maximum amount adsorbed under these conditions was 72%, at time 120minutes, adsorbent dosage 8g/L, pH3, and at 30°C operating temperature (Padmavathy *et al.*, 2016).

2.10.3. Adsorption chromium (VI) by activated carbon rice straw

As Kumar *et al.* (2017) state that 100g of dried samples were carbonized at 450 and 700°C for two hours in a muffle furnace. The batch adsorption process was used to determine the effect of activated carbon of rice straw for Cr(VI) removal from aqueous solutions. The initial Cr (VI) concentration of 1.5mg/L at 25°C, pH 8, and for one gram of activated carbon rice straw (ACRS) was able to give chromium removal efficiency of 96.72%. It was studied that the total amount of adsorption of Cr (VI) onto ACRS 42% to 90 % with an increase of pH from 3.1 to 8.0. Also, this adsorption reduced from 74.2 to 47.2% by increasing the Cr(VI) concentration from 1.5 to 5.0 mg/L. Also, this removal efficiency was decreased from 80.3 to 72% by increasing the adsorbent particle size from 100 to 200 micrometers. The adsorbed doses of Cr (VI) tend to increase with the increase of pH and attain equilibrium at 100minuntes. It has been found that the lower free concentration of Cr(VI) for smaller ACRS particles is significantly less than that for the larger adsorbent particles(Kumar *et al.*, 2017).

2.10.4. Adsorption chromium (VI) by Palmyra palm fruit seed carbon

The suitability of the carbon derived from Palmyra palm fruit seed carbon (PPFSC) and commercial activated carbon (CAC) was also evaluated for the removal of chromium (VI) in tannery industrial wastewater. Palmyra palm fruit seed was cut into small pieces and air-dried. Then it was treated with concentrated sulfuric acid in a ratio of 2:1 (PPFS: H₂SO₄) and the resulting product was kept in the oven at 200°C for 10 hr. Experiments were conducted with chromium (VI) effluent from the tannery industry at 2.26pH with 100mL of 167mg/L of Cr(VI)

solution with different carbons doses of PPFSC and 9.84 pH for CAC. The percent of Cr(VI) elimination in each instance was established by usual that maximum Cr(VI) removal was 89 % using 3.5 g of PPFSC and only 63 % achieved with 5.75gram of CAC. The percent of removal increases with time and attains equilibrium at 3hour for PPFSC and 5hour for CAC. This indicates that PPFSC is more effective for the treatment of tannery wastewater when compared to CAC based on the contents of the following Table 2.1 values. Langmuir equation was applied for adsorption equilibrium for both carbons based on the assumption that maximum adsorption and Table 2.1 elaborates the impact physical properties on adsorption capacity and efficiency (Kannan A. & Thambidurai*S., 2008).

Table 2. 1: Characteristics of Palmyra palm fruit seed carbon and commercial activated carbon

S. No.	Control test	PPFSC	CAC
1	Bulk density (g/L)	0.67	0.56
2	Moisture %	0.47	0.27
3	Ash %	3.25	1.20
4	Solubility in water %	1.40	3.599
5	Solubility in 0.25 M (HCl) %	2.97	5.41
6	PH	2.26	9.50
7	Decolorizing power (mg/g)	15.00	2.25
8	Phenol number	76.00	88.00
9	Ion exchange capacity (m. Equiv/g)	0.19	Nil
10	Surface area (m ² /g)	184.60	421.00
11	Porosity %	12.16	2.40

2.10.5. Removal of Cr(VI) from contaminated water using Fly ash adsorbent

The fly ash that was served in this investigation was gathered from National Thermal Power Corporation (NTPC), Tanda, and washed with distilled water then dried at 110°C for five hours. The activation of fly ash was performed by treating it with concentrated sulphuric acid (98% w/w) in a 1:1 weight ratio and is kept in an oven maintained at a temperature range of 150°C for 24 hour. Again it is washed with distilled water to remove the free acid. Then a stock solution of

Cr(VI) is prepared by dissolving 2.8287 g of 99.9% potassium dichromate ($K_2Cr_2O_7$) in distilled water and a solution made up to 1000mL. This solution is diluted as required to obtain the standard solutions containing 20-400 mg/L of Cr(VI) . The effect of the contact time and the pH of the solution were studied at 30°C with an initial Cr(VI) concentration of 50mg/L and an adsorbent amount of 10g/L. Removal efficiency is found to decrease with an increase in the initial PH (1-3) and reached 82% at the initial pH value of 1. The percentage removal increases from 77% to 84.9% by increasing the adsorbent amount from 4 to 24g/L respectively. The increase in Cr(VI) removal with an increase in the fly ash amount is due to the increase in surface area and adsorption sites available for adsorption of Cr(VI). However, the decrease in adsorption capacity by increasing the adsorbent amount is fundamentally due to the active sites remaining unsaturated during the adsorption process. The efficiency of removal reduced from 81% to 53% and the adsorption capacity raised from 1.8 to 22 mg/g with an increase in the initial Cr(VI) concentration from 20 to 400 mg/L, respectively. The decrease in the efficiency of purification of Cr(VI) can be explained by the fact that all the adsorbents had a limited number of active sites, which would have become saturated above a certain Cr(VI) concentration. The experimental equilibrium data fits well with the Langmuir-Freundlich model and the adsorption process follows PSOK model. Fly ash shows a higher desorption efficiency by more than 95% for the removal of Cr(VI) at a contact time of 22h for entire batch studies(Suresh & Babu, 2014).

2.10.6. Adsorption chromium (VI) by fresh nanoporous adsorbent neem bark

In a recent study, fresh nanoporous adsorbent neem bark (nANB) was used for the removal of Cr(VI) from an aqueous solution. The crushed neem bark through a roller crusher, jaw crusher, and ball mill sequentially was treated with concentrated sulphuric acid (H_2SO_4 ; 98% w/w) in a 1:1 weight ratio and subjected to a heat treatment in an oven at 70°C for 24 hours. Finally, the particles were repeatedly washed in distilled water for removing free acid and color impurities. Batch experiments were performed with approximately 2.8287 g of 99.9% potassium dichromate ($K_2Cr_2O_7$) is dissolved in distilled water and the solution is made up to 1000 mL for preparing 1000 mg/L stock solution of Cr(VI). The effect was studied by varying the adsorbent amount from 4 to 28g/L, initial Cr(VI) concentration from 60 to 200 mg/L, pH from 2 to 12, contact time at 48 hours and the maximum adsorption capacity of fresh neem bark and nANB was found to be

14.33 and 26.95mg/g, respectively, from equilibrium experiments at 35°C with an adsorbent dosage of 6g/L, initial Cr(VI) concentration 100mg/L, pH 2.70, and contact time at 48 hours. Langmuir model is found to be the best-suited isotherm model giving a maximum adsorption capacity of 26.95 mg/g for the removal of chromium (VI) ions. The adsorption capacity of nANB for Cr(VI) removal was found to be almost two times the adsorption capacity of the fresh neem bark. Therefore, nANB is considered an efficient adsorbent for further experimental studies. In the present work, the nanoporous adsorbent was prepared in granular form, which makes it more applicable for the continuous treatment of industrial effluent streams. The results of this study indicate that the prepared nANB proves to be an efficient and effective adsorbent that can be used for Cr(VI) removal from wastewater. In the saturated nANB, there is a significant reduction in the amount of Cr(VI) present on the surface of the adsorbent which supports the removal of 91.4% of Cr(VI) (Maheshwari & Gupta, 2015).

2.10.7. Removal of Chromium (VI) by using guar gum–nano zinc oxide adsorbent

Guar gum is a polysaccharide composed of galactomannan units. The hydrogel of guar gum has been used to remove Cu(II) in aqueous solution and modified guar gum with multi-walled carbon nanotubes, magnetic iron oxide nanoparticles, methyl-methacrylate, polyacrylamide or silica for the removal of toxic dyes (neutral red and methylene blue), Cr(VI) and Cd(II) from aqueous solution. It was, therefore, considered worthwhile to incorporate nano ZnO particles with guar gum, which may be easily separated after the adsorption process (Khan *et al.*, 2017). As Khan *et al.* (2017) report the adsorption efficiency of guar gum–nano zinc oxide (GG/nZnO) biocomposite, dynamics, and thermodynamics of the uptake of Cr(VI) ions from aqueous solution. Adsorption laboratories were conducted at a fixed agitation speed at ambient temperature (303K) under batch mode technique concentration (10–30mg/L), with varying doses of GG/nZnO biocomposite (0.5–2 g/L), pH range of 2–10, in a thermostatic water bath shaker for time intervals ranging from 10 to 60 minutes. The adsorbent was separated from the solution by centrifugation and the residual concentration of Cr(VI) in the supernatant liquid was determined spectrophotometrically. The maximum amount adsorbed efficiency at pH 7, concentration 15 mg/L, contact time 50minutes, and adsorbent doses 0.75 mg/L conditions was 95.62%.

2.10.8. Removal of chromium (VI) by using chemically modified banana peels

The adsorptive removal of Cr(VI) from waste water solutions was studied by acrylonitrile grafting banana peels (GBPs). These banana peels were treated with 10% HCl, followed by alkaline hydrolysis with 10% NaOH, and washed thoroughly. The bleaching of alkali hydrolyzed peels was accomplished with sodium chlorate (NaClO_3) in the presence of H_2O_2 and glacial acetic acid. The grafting co-polymerization of acrylonitrile onto the bleached pulp was initiated by Fenton's reagent ($\text{Fe}^{+2}/\text{H}_2\text{O}_2$). The optimum conditions for adsorption of Cr(VI) were found to be: at constant temperature of 25°C , pH 3, adsorbent dose of 4g/L, agitation speed 300 rpm, with initial concentration 400 mg/L, and contact time of 120 minutes. The increase in adsorbent amount increases the number of available active sites for the uptake of metal ions. The adsorption efficiency of Cr(VI) onto GBPs was recorded to be 96%. The adsorption data were fully fitted with the Freundlich and Langmuir isotherm model and followed a pseudo-second-order kinetic model (Ali *et al.*, 2016).

2.10.9. Removal of chromium (VI) using moringa stenopetala and banana peel powder

Adsorption by moringa stenopetala seed powders (MSSP) and banana peels powder (BPP) can be used to remove Cr(VI) ions from polluted water. Adsorption experiments were showed maximum removal efficiency for Cr(VI) at 120 minute of contact time, adsorbent dose of 20g/L and pH₂ by MSSP and pH₄ by BPP. The percentage removal of Cr(VI) increased with increasing adsorbent dose from 5 to 20g/L and contact time from 60 to 120 minute. The maximum removal efficiency of chromium by MSSP is 92.17% and by BPP is 90.07% at 30 mg/L. The decrease in percentage removal of the metal ion with increasing initial concentration may be due to the saturation of adsorption sites on the adsorbent surface. The increase in adsorption capacity with increasing initial concentration is because at a fixed adsorbent dose with increasing the metal concentration. Freundlich isotherm model showed a better fit to the equilibrium data than the Langmuir model. The kinetics of adsorption for chromium was well by the pseudo-second-order kinetic model and the calculated equilibrium sorption capacity of the model showed good agreement with the sorption capacity obtained from experimental results (Badessa *et al.*, 2020).

2.10.10. Chromium removal by Moringa Oleifera, chitosan, and iron nanoparticles

As Bahador *et al.* (2021) studied the effect of chitosan (CS) and iron oxide (Fe_3O_4) magnetic nanoparticles on the chromium adsorption property of Moringa Oleifera AC was explored at pH₂

and 50minute, temperature 25°C, initial concentration of chromium 20mg/L, adsorber dose of 1g/L, and mixing speed of 400rpm to study the kinetic behavior. During experimentation materials & solutions CS was purchased and Acetic acid (C₂H₄O₂), potassium dichromate (K₂Cr₂O₇), NaOH, HCl, FeCl₃.6H₂O, and FeCl₂.4H₂O were provided from Merck Company. The working solutions were made using double distilled water (DDW). The maximum single-layer adsorption capacity of AC, CS/AC, AC/Fe₃O₄, and CS/AC/Fe₃O₄ adsorbents was 56.78mg/g, 114.80 mg/g, 121.70 mg/g, and 130.80 mg/g, respectively. The acquired findings revealed that the modification of AC by chitosan and Fe₃O₄ nanoparticles increased the chromium adsorption efficiency. Also, according to this study reports that, the maximum removal efficiencies for chromium (VI) ions using AC, AC/Fe₃O₄, CS/AC, and CS/AC/Fe₃O₄ samples were determined to be 97.55%, 98.34 %, 97.55 %, and 99.36 %, respectively. This yield was obtained at the dose of 2g/L (activated carbon) and 1 g/L (other composites). By increasing the concentration of chromium (VI) from 10 mg/L to 200 mg/L, the removal efficiencies using AC, CS/AC, AC/Fe₃O₄, and CS/AC/Fe₃O₄ were reduced from 98.68 %, 98.24 %, 98.72 %, and 99.75 % to 54.82 %, 57.55 %, 62.52 %, and 67.36 %. Under optimal conditions, the maximum elimination of chromium for AC, CS/AC, AC/Fe₃O₄, and CS/AC/Fe₃O₄ was quantified as 98.68%, 98.24%, 98.72%, and 99.75 %, respectively. This shows that as the material composites or mixed compositions emphasis the adsorption behavior adsorbent. The adsorption isotherm of chromium ions using this composites material was investigated using the Langmuir, Freundlich, and Dubinin-Radushkevich isotherm models. The results indicate that the Freundlich isotherm model has the best potential with R² values >0.96 to describe multilayer adsorption behavior with the best-fitting pseudo-second-order kinetic model (Bahador *et al.*, 2021).

Table 2. 2: Summary of some previous adsorbent parameters that used for Cr(VI) ions removal

S. NO.	adsorbent	PH	concentration (mg/L)	dosage (g/L)	Time (min)	Efficiency (%)	References
1	MKAC	2	20	2.5	150	85	(Rai <i>et al.</i> , 2016).
2	magnetic nanoparticles	3	10	8	120	72	(Padmavathy <i>et al.</i> , 2016)
3	ACRS	8	1.5	1	100	96.72	(Kumar <i>et al.</i> , 2017)
4	PPFSC	2.26	167	3.5	180	89	(Kannan A. & Thambidurai*S., 2008)
5	Flyash	1	50	10	22hrs	95	(Suresh & Babu, 2014).
6	nANB	2.7	100	6	48hrs	91.4	(Maheshwari & Gupta, 2015)
7	GG/nZnO	7	15	0.75	50	95.6	(Khan <i>et al.</i> , 2017)
8	GBPs	3	400	4	120	96	(Ali <i>et al.</i> , 2016)
9	MSSP& BPP	2	30	20	120	92.17	(Badessa <i>et al.</i> , 2020)
10	CS/AC/Fe ₃ O ₄	2	20	1	50	99.75	(Bahador <i>et al.</i> , 2021).

Not only these tabulated ones the removal of chromium from aqueous solution using various materials of agricultural and biological origin, which have been studied as potential chromium bio-sorbent like plant leaves, saw dust, sugar cane bagasse, fungal, algal, bacterial biomass, sugar beet pulp, maize cob, and rice hulls that accomplished either in batch or continuous bioreactors process (Sen & Dastidar, 2010).

2.11. Future perspective of adsorption based on literatures

Based on the summarized Table 2.2 adsorption processes which were collected from some previous listed kinds of literature that the least contact time and small amount dose of adsorbent consumption with high efficiency to remove Cr (VI) from dilute concentration of contaminated solution are the best ones in order to become nearly compatible WHO standards' (Padmavathy *et al.*, 2016; Bahador *et al.*, 2021)'. Also, purification of Cr(VI) may improve in the future by utilizing locally available resource of adsorbents that are relatively inexpensive, environmentally friendly, and have a high significant adsorption efficiency value in a dilute concentration of chromium with nearly neutral PH adjustment that accomplish within a short contact time without use of costly additional chemicals that may have negative side effects on human health. On the other hand, most of the sources of activated carbon from crops which are edible or cattle fodder and seasonally available. For example adsorption by using mango kernel and groundnut hull that seasonally obtained with small quantity. So, it should be replaced by abundant locally available resources which cannot easily deplete. Generally, during adsorption the concentration of Cr(VI) should be overwhelm from aqueous solution in order to improve the sustainability of human beings living in the future generation by focusing global threatening current issue such as kidney suffer concerning as proliferation of industries by increasing the capacity of adsorbents for removal of this toxic metal ions within a short contact time and minimum dose of adsorbent that adsorb low concentration. Also, it is preferable if the type of adsorption has environmental advantage in terms of the reuse of wastes and easily available resources like termite mound-chicken eggshell blend adsorbent to increase efficiency of adsorption because of it incorporate oxides of CaO, SiO₂, ZrO₂, Al₂O₃, and Fe₃O₄ that can make it as favorable for the adsorbent.

3. MATERIALS AND METHODS

3.1. Preparation and activation of termite mound-eggshell adsorbent

During the preparation of the termite mound-eggshell (TMES) blending, the lump of termite mound was harvested from specific places of East Shewa zone, Dugda wereda, and Qorke Adii kebele farmland of Ethiopia, and also the chicken eggshell was collected from the cafeteria and restaurant of Jimma city. This collected eggshell raw material was carefully washed several times with tap water sequentially with distilled water after being soaked for a day to discard the impurity and white membrane from it. Thereafter, it was heated up at 110°C in an oven for 24hours in order to remove the water added during washing the dirty. This dried chicken eggshell was grinded by mechanical grinder using pestle and mortar. According to Yusuff (2017) studies, the desired sieve size were less than 300micrometer for blending proportion with termite mound powder. Analogously, for the lump form of termite mound powder preparation, the lump of termite mound size reduction was performed by crushing and sieved with the same size as an eggshell respectively after dried at 105°C for 6hours to remove its moisture content. Finally, it was kept in a covered polyethylene plastic that used as airtight container. The 100g eggshell powder taken at one to one mass ratios in respect to the termite mound powder was dissolved in 500mL of distilled water and stirred by a magnetic stirrer that attached to a hot plate at room temperature for 2 hours with 600rpm to form a homogenized slurry (Yusuff, 2019). Then it was been put in an oven for 12hours at 130°C to assure the removal of excess moisture within the slurry using oven equipment. Then the blended raw material powder of TMESP was thermally activated at 850°C calcination temperature using muffle furnace equipment for 4hour with a heating rate of 10°C per minute, and then cooled synthesized TMESP put in a desiccator to safe from environmental disturbance. After calcined adsorbent preparation achieved the proximate analysis like moisture content, ash value, fixed carbon content, densities, and porosity analysis was performed. In the end, by using equipment like FT-IR, XRD, TGA, and UV-vis were determined the adsorbent surface character and adsorption efficiency besides evaluating adsorption isotherm and kinetics respectively. To attain the required result care was taken to avoid sample contamination during collection, preparation, and analysis. The overall procedure was summarized in Figure 3.1 using Wondershare EdrawMax 11.5.0 software.

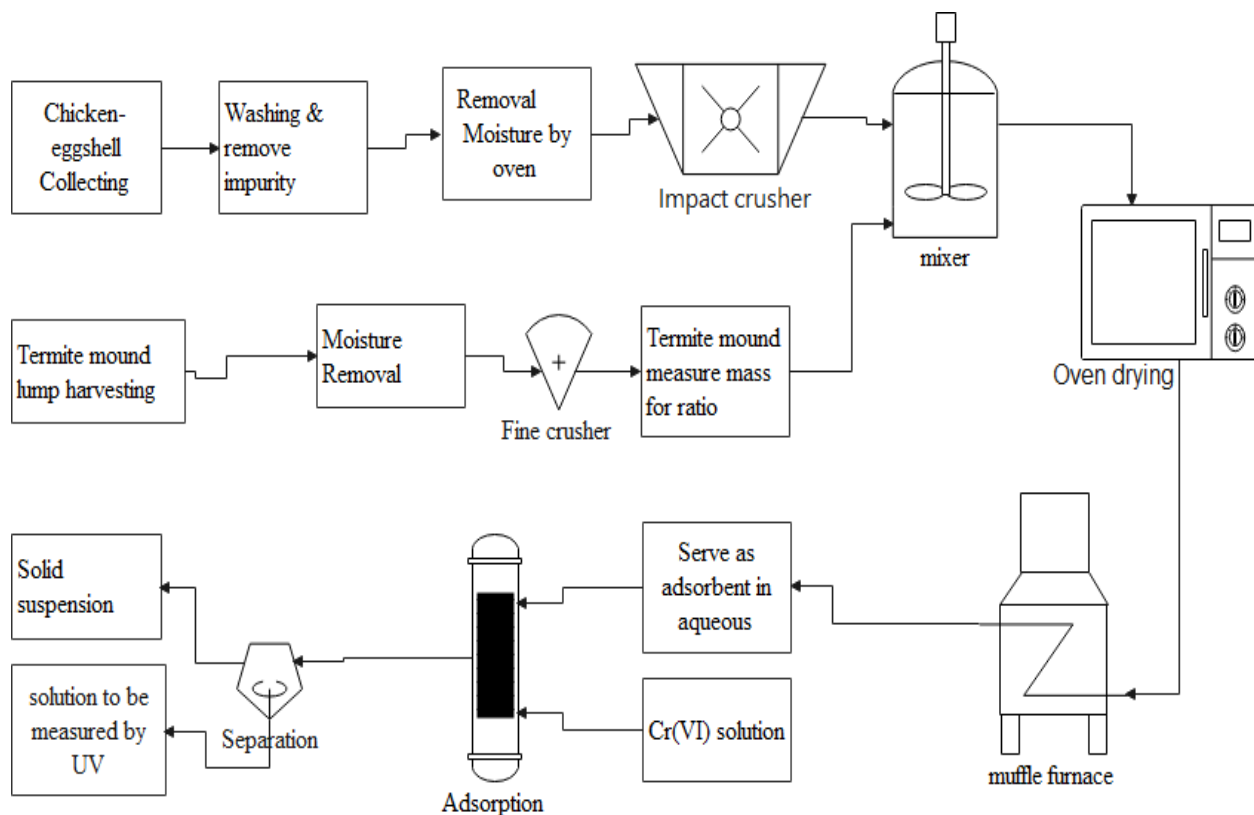


Figure 3. 1: Flow diagram and setup for synthesis of termite mound-eggshell mixture adsorbent



Figure 3.2: physical demonstration of adsorbent preparation: (A&B) Raw Materials of TM-ES, (C&D) powder of TM-ES, (E&F) calcination process, and (G&H) synthesized of TMESPs.

3.2. Determination of experimental batch adsorption parameters

Batch adsorption experiments were conducted to investigate the effect of contact time, pH, adsorbent dose, and initial concentration of adsorbate on removal efficiency and capacity from the prepared stock solution. Based on Rotimi & Okeoghene's (2014) justification, that the sorption process is mainly dependent on pH, contact time, initial metal ion concentration, and sorbent dosage. The adsorption during this laboratory experiment from a stock solution of Cr(VI) was prepared at constant temperature $25\pm 2^{\circ}\text{C}$ from 99.9% of pure dipotassium dichromate ($\text{K}_2\text{Cr}_2\text{O}_7$) which is red-orange crystalline solid, odorless physical properties, and the working condition of Cr(VI) solutions was directly diluted from the stock solution by pouring distilled water into beaker through the funnel. Based on the principles the adsorption process of Cr(VI) onto the TMESP adsorbent carbonaceous porous material was had conducted in conventional Leaching/Jar Test (JLT6) apparatus, accommodating a series of six beakers together with six-spindle steel paddles under different time ranges of from 30 to 90 minutes of intervals between batch during the experimental adsorption accomplishment. To do this a mass of measured adsorbent was added into a series of flasks which contain different initial concentrations of Cr(VI) solutions were prepared using 20 to 100 mg/L ranges and stirred at room temperature that adjusted to the speed of 150 rpm for a pre-determined contact time until equilibrium of adsorption attained by following Table D1 scattered allocated time. The pH ranged between 1 to 9 values of the solution were titrated with the help of a magnetic stirrer during the adsorption process using 0.1M NaOH and 0.1M HCl prepared solution and the dose of adsorbent ranged from 3 to 15g/L concerning several researchers parameters used including Billah *et al.* (2021). After the contact times determined for adsorption were achieved the adsorbate and adsorbent mixture within the solution was separated by using 55mm diameter what man filter paper with $11\mu\text{m}$ pore size supported by vacuum filtration. The concentration of chromium that remains in the solution was determined by using the UV-visible spectrophotometer apparatus technique. The amount of chromium adsorbed onto the surface of incinerated porous materials and residue Cr(VI) within the water were calculated based on the mass balance formula as stated in Equation (3.11). Here, in this thesis the experimental phenomena of data analysis was performed by using stat-ease design expert 11.1.2.0 x64 and origin lab 2018b software accordingly.

3.2.1. Preparation of stock solution for hexavalent chromium

To prepare the stock solution of dipotassium dichromate ($K_2Cr_2O_7$), 2.82g analytical grade was added to 1L deionized water to obtain 1000ppm Cr(VI). From the standard of stock solution, 1.0, 2.5, 4.0, 5.5, 7.0, 8.5, and 10.0mL Cr(VI) dilution of solutions were accompanied by pipetting from the $K_2Cr_2O_7$ stock solution into different 100mL volumetric flasks that considered the concentration of heavy metals as contaminated water. Because the efficiency of removal is more dependent on pH, adsorbate concentration, contact time, and adsorbent dosages factor as investigated by different scholars (Rotimi & Okeoghene, 2014). To control PH two volumetric flasks, that contain 0.4gram of 0.1MNaOH and 0.87mL of 0.1MHCl acid solution were prepared and diluted to 100 mL of distilled or de-ionized water. During the preparation of 1ppm solution, 1mL of the stock solution was poured and mixed with 99 mL of deionized water. Likewise, the other stock solution was added into mL of deionized water for preparation of ppm solution. Finally, the adsorbent 0.3, 0.6, 0.9, 1.2and 1.5g was added and PH was adjusted to 1 to 9 accordingly in prepared solution with respective time allotted from 10 to 90minutes that contribute a key role. When the sample of solid dipotassium dichromate is added to water, the compound dissolves and dissociates to yield potassium ions and dichromate ions uniformly distributed throughout the mixture as the following Equation (3.1):



3.3. Characterization Techniques of synthesized adsorbent

3.3.1. Proximate analysis of TMESP adsorbent

In this part of the study, the analysis was involved the determination of moisture contents, ash value, Volatile matter, fixed carbon content, and porosity of termite mound-chicken eggshell powder of adsorbent were investigated based on standard test methods known as the American Society for Testing and Materials (ASTM) by following standard procedures and each value collected from experimentally generated data.

3.3.1.1. Moisture content determination

For moisture content can be performed after the size of the powder of TM-ES was determined by sieve of proper mesh size analysis is carried out based on ASTM D2867-99 at 105°C in an oven. Based on this analysis the higher removal percentage of moisture content from the sample

refers to enhance adsorption capacity. In this thesis 10gram of identical TMESP samples in a separate petri dish keep in an oven at 105°C temperature for 24hours.

$$\% \text{ Moisture content} = \frac{w_i - w_f}{w_s} \times 100\% \quad (3.2)$$

Where W_i = weight of the sample and petri dish before drying and W_f = weight sample and petri dish after drying for both raw materials, and W_s =weight sample alone before drying.

3.3.1.2. Determination of Ash Content of TMESP adsorbent

The method was used for ash content determination based on ASTM D2866-94 standards at 750°C temperature. Clean dried crucibles were weighed using electronic mass balance and 20.08gram of each sample was weighed into the crucibles. They were dried using a moisture removal oven until constant mass were observed. Then, the samples were transferred into a muffle furnace using pair of tongs and ashes at 750°C temperature for 4 hours until white ash was obtained. The samples were removed and cooled in a desiccator and reweighed. The percentage of ash was obtained and an average was taken (Evbuomwan & Sodje, 2020). In this observation, the lower the ash contents the better material for adsorption behavior.

$$\% \text{ Incombustible matter} = \frac{w_f - w_i}{w_s} \times 100\% \quad (3.3)$$

$$\% \text{ Ash content} = 100 - \% \text{ incombustible matter}$$

Where, the weight of the sample before igniting (W_s), the weight of empty crucible (W_i), and weight sample and crucible after igniting (W_f) by muffle furnace for TMESP mixture.

3.3.1.3. Determination of Volatile Matter of TMESP adsorbent

Determination of Volatile Matter Content concerning ASTM D5832-98 by taking 15g of sample TM-ES mixture of moisture-free activated carbon was heated in a furnace at 550°C for 10 minutes without air (Evbuomwan & Sodje, 2020). The ratio of change of weight to original weight in percentage gives the volatile matter content and is given by:

$$\% \text{ Volatile} = \frac{w_2}{w_1} \times 100\% \quad (3.4)$$

Where: W_2 = weight loss (initial weight – final weight)
 W_1 = original weight

3.3.1.4. Determination of Fixed Carbon Content of TMESP adsorbent

This is the residue left after the moisture, volatile, and ash value was given up. It is deduced by subtracting from 100, the percentage of moisture, volatile matter, and ash content (Evbuomwan & Sodje, 2020). The fixed carbon content (FC) is given as Equation (3.5):

$$FC = 100 - (\%moisture + \%volatile\ matter + \%ash) \quad (3.5)$$

3.3.1.5. Determination of adsorbent porosity techniques for TMESP adsorbent

Porosity is the fraction of the total powder volume that is taken up by the pore of adsorbent. The porosity of the TMESP was determined based on the particle density and bulk density of the powder using Equation (3.8) and (3.7) respectively. The porosity of TMES powder and their synthesized powder was obtained from bulk and particle density using the Equation (3.6):

$$\text{Porosity} = \frac{\text{Particle density} - \text{Bulk density}}{\text{Particle density}} * 100\% \quad (3.6)$$

i. Bulk density

The bulk density was determined according to ASTM D2854-96 standard testing procedure. A measured mass calcined TM-ES powder was placed into 100mL graduated cylinder and record the volume occupied by the solid sample then take its mass to the volume ratio (Ektepe *et al.*, 2017). The value was calculated as follows using Equation (3.7):

$$\text{Bulk density (g/mL)} = \frac{\text{Mass of calcined sample (g)}}{\text{Cylindrical volume of sample (mL)}} \quad (3.7)$$

ii. Particle density

Particle density (true densities) was measured in a pycnometer that predict the adsorbent to determine how the total storage capacity can be obtained from the adsorption process (Kunowsky *et al.*, 2013). This physical property of adsorbent termed as particle density for both fine raw material of TM-ES powder and their calcined powder was determined using a Pycnometer instrument. As using the following procedure:

- a. Mass of the dry Pycnometer was measured
- b. Mass of Pycnometer plus distill water were measured

- c. The density of distilled water at room temperature=0.99753g/L
- d. Mass of Pycnometer plus some extent of calcined TMESP sample was measured
- e. The remained space was filled with distilled water and their mass was measured
- f. Mass of sample and distilled water separately
- g. The volume of distilled water alone
- h. Volume of Pycnometer
- i. The volume of the sample alone

$$\text{Particle density (g/mL)} = \frac{\text{Mass of calcinated sample within Pycnometer (g)}}{\text{Volume of sample within Pycnometer (mL)}} \quad (3.8)$$

3.3.2. Fourier Transform Infrared of synthesized TMESP adsorbent

Fourier Transform Infrared (FTIR) spectroscopy has been developed as a tool for the simultaneous determination of organic components, including chemical bonds, as well as organic content. The objective of this investigation was to demonstrate how to read and assess the chemical bond and structure of organic matter within a specific material using FTIR, in which the qualitative analysis results were then compared with the kinds of literature. The vibrational molecule of the spectrum is aware to be a unique physical property and is characteristic of the molecule. In short, the IR spectrum is divided into three wavenumber regions: far-IR spectrum ($<400\text{cm}^{-1}$), mid-IR spectrum ($400\text{-}4000\text{cm}^{-1}$), and near-IR spectrum ($4000\text{-}13000\text{ cm}^{-1}$) (Khalifa *et al.*, 2019; Khalil *et al.*, 2021). The mid-IR spectrum is the most widely used in the sample analysis, but the far- and near-IR spectrum also contributes to providing information about the samples analyzed. Based on the study of Wang *et al.* (2021) and Liu *et al.* (2015) the TMESP-adsorbent investigation was accomplished as the following procedure the sample was prepared in the form of a tablet by homogenizing with KBr (Potassium bromide) powder and synthesized adsorbent in proper ratios to form pellet using California Bearing Ratio (CBR) tester instrument. The analysis of synthesized TMESP adsorbent was performed using 1mg TMESP to 100mg KBr ratio of pelletized sample in spectrum of FTIR spectroscopy (Perkins Elmer L1600300) before and after the adsorption experiments that have wavenumber range of $4000\text{-}400\text{cm}^{-1}$ spectra that distinguish the location of group function within the materials. In this investigation mid-IR spectrum ($400\text{-}4000\text{cm}^{-1}$) is used because of its popularity and availability.

3.3.3. UV- visible Spectrophotometer analysis of TMESP-adsorbent

Ultra Violet (UV)-visible spectroscopy or ultraviolet-visible spectrophotometry uses light in the visible region that refers to absorption or reflectance spectroscopy in the UV-visible spectral region (Sumathi, 2017). This types of absorptions are commonly had electronical behavior in nature and are associated with resonating structures in the molecule. It is an important tool for qualitative and quantitative justification of single components of the isolated extract. Based on these assumptions the surface of the synthesized TMESP adsorbent was analyzed by using a spectral UV-visible spectrophotometer instrument. Accordingly, the characteristic of absorption peak for the synthesized TMESP adsorbent was determined using UV-visible absorption spectrophotometer in the wavelength range of 200 to 700 nm.

3.3.4. X-Ray Diffraction analysis of synthesized TMESP adsorbent

X-Ray Powder Diffraction (XRD) is the most widely used to study the phase and crystal structure of substances. Each chemical molecule or phase has a unique diffraction pattern when the material is analyzed by XRD. Consequently, the composition, crystal form, intramolecular bonding way molecular configuration, and conformation, etc., were determining the unique diffraction pattern of the material. According to Saravanakumar *et al.* (2017) justification, the diffraction patterns were proved against a wide range of libraries of patterns from well-defined materials to identify and quantify the phases that exist in the sample. The XRD analysis has the advantages of no damage to the sample, any pollution, quickness, and high measurement accuracy, and it can offer a large amount of information about crystal integrity (Liu et al., 2015). In Saravanakumar *et al.* (2017) and Sumathi (2017) study XRD analysis was determined by using Debye-Scherrer's expression with Cu-K α radiation with a wavelength of 1.54178Å unit and examined the adsorbent crystallite size as follows (3.9).

$$D = \left(\frac{K\lambda}{\beta \cos \theta} \right) \quad (3.9)$$

Where D is the crystallite size of the active phase, λ is the X-ray wavelength, K is a constant, called shape factor; its value can vary from 0.89 to 1.39 depending on the crystallite shape. Since the sample of crystallites is considered as spherical geometry the value of K can be used as 0.94,

θ is the angle of diffraction (Bragg angle), while β is the full width at the peak half maximum (FWHM) in radians (Ramli *et al.*, 2019; Yusuff, 2019).

3.3.5. Thermogravimetric analysis

Thermogravimetric analysis (TGA) is determining weight changes in a material as a function of temperature (or time) under a specified atmospheric environment. Its principle uses incorporate measurement of a material's thermal stability, filler and plasticizer content of polymers, oxidative stability, low molecular weight monomers within polymers, moisture and solvent content, and the percent composition of components in a compound. In the study of Slopiecka *et al.* (2012) TGA is the best commonly known method used for kinetic analysis of devolatilization process different materials such as plastic, rubber-derivative, water evaporation, natural fibers, various types of biomass during thermal degradation. TGA analysis was carried out by gradually raising the temperature of a TMESP in a calcination furnace as its weight is quantified on an analytical mass balance that remains outside of the furnace. Also, according to Reta *et al.* (2021) explanation TGA analysis involves the percent of mass loss that is measured if thermal conditions determine the losses of a volatile composition and component of decomposition. This analysis reveals the chemical reactions, such as combustion, including mass losses; however, the physical changes, such as melting, do not incorporate in this analysis. Therefore, the weight of the sample is plotted against temperature or time to illustrate thermal transitions for the specified material of TMESP-adsorbent.

3.4. Determination and optimization of chromium adsorption factors

3.4.1. Chromium concentration analysis using UV-visible Spectrophotometer

The UV-visible Spectrophotometer quantitative chromium concentration determination was, generally performed in solution, by using PerkinElmer Lambda 25 equipment which has a wavenumber range 320-1100nm or is justified based on the Beer-Lambert law ($A=\epsilon bCe$) equation. The Beer-Lambert law indicates that the absorbance of the solution of a molecule at its maximum wavelength is proportional to the length of the fixed light path of a cell that is termed as a cuvette and the concentration of the solution. However, this investigation was accomplished by using the former one which is not sophisticated and more accurate. The residual supernatants Cr(VI) ion concentration was determined by measuring at 540 nm wavelength from the filtered

aqueous solution using UV-visible Spectrophotometer after calibration curve was drawn using Cr(VI) concentration range (Rai *et al.*, 2016; Rajapaksha *et al.*, 2018; Linlin *et al.*, 2020). Based on the value of this wavelength the Cr(VI) concentration remains within a solution, adsorption efficiency and capacity of the adsorbent to uptake can be calculated by using the following formulas Equation (3.10) and (3.11) respectively.

$$\% \text{ Adsorption} = \frac{C_i - C_f}{C_i} * 100 \quad (3.10)$$

Where C_i and C_f are the initial and final concentrations of the metal ions were in the solution (ppm). The amount of adsorbed Cr (VI) per gram of adsorbent was calculated using:

$$q_e (\text{mg/g}) = \frac{(C_i - C_f)V}{W} \quad (3.11)$$

where C_i (mg/L) and C_f (mg/L) are the initial and equilibrium concentration of Cr (VI) respectively, V(L) is the volume of dilution in solution it is taken as a constant 100mL, W (g) is the mass of TMESP-adsorbent, q_e (mg/g) is the metal uptake capacity of adsorbent (Kuang *et al.*, 2020; Nogueira *et al.*, 2019; Bahador *et al.*, 2021)

3.4.2. Optimization of chromium adsorption factors

For optimizing hexavalent chromium uptake from stock solution based on the factors and response parameters using Response Surface Methodology (RSM) and Central Composite Design (CCD) of regression procedure of statistical analysis system by using stat-ease design of expert (DOE) 11.1.2.0 x64 software analysis was performed. Under this methodology, there are many classes of response surface designs that are occasionally useful in practice, such as CCD, Hybrid design, Box-Behnken design, and Three-level Factorial design (Moradi *et al.*, 2016). Correlation among independent variables and responses were obtained by fitting them into a second-order polynomial equation in terms of ANOVA analysis. The experimental design is used to optimize the process parameters of the adsorption and at the same time to generate a mathematical model by considering the individual and interactive effects of the process parameters. In this study, optimization was considered to determine optimum conditions that can give the best removal efficiency from the performed experiments using CCD. To determine the optimum conditions of the adsorption experiments, four independent process parameters such as pH, initial Cr(VI) concentration, adsorbent dosage, and contact time were investigated on the

percentage removal of Cr(VI) ions. The percentage removal of Cr(VI) ion was considered as the response variable. The CCD contains 2^k factorial runs, C_o center runs, and $2k$ axial runs in which the total experimental runs (N) could be conducted as:

$$N=2^k+ 2k+ C_o \quad (3.12)$$

Where k is the number of independent parameters and C_o is the number of center points. A total of 30 experimental runs incorporating the six center points were designed using CCD of RSM for the analysis of the adsorption of Cr(VI) ions from aqueous solutions. The process parameters such as initial Cr(VI) ion concentration, pH of the solution, contact of time, and dosage of the adsorbent were optimized by CCD allocating decision of optimization criteria. This CCD term is a type of response surface design that can fit a full quadratic model with respectively for sequential and factorial experimentation. Its drawback is, has higher design points and expensive than Box-Behnken design methods to run with the same number of factors. For the design of experiments, the lowest (-1), central (0), and the highest (+1) levels are specified in Table 3.1 below. In this study, the adsorption parameters were designated based on the study of previous researchers' investigations.

Table 3. 1: Parameters of adsorption with respect to its' experimental level.

Pre-determined independent factors			Levels of factors				
Name	Units	Coded	$-\alpha(-\infty)$	-1	0	+1	$+\alpha(+\infty)$
Adsorbent	g/L	A	3	6	9	12	15
Cr (VI) Concentration	mg/L	B	20	40	60	80	100
Contact time	min	C	30	45	60	75	90
PH	PH	D	1	3	5	7	9

Each above table numeric factor which set to five levels which include plus and minus alpha (axial points) as well as plus and minus factorial points including their center point. The categorical factors are added, the central composite design is to duplicate for every combination of the categorical factor levels. And an empirical second-order polynomial model that fits the percentage removal of Cr(VI) to the adsorption independent factors was developed and expressed as following Equation (Reta *et al.*, 2021; Yosuff A., 2017).

$$Z = \beta_o + \sum_{i=1}^4 \beta_i x_i + \sum_{i=1}^4 \beta_{ii} x_i^2 + \sum_{i=1}^4 \sum_{j=i+1}^4 \beta_{ij} x_i x_j \quad (3.13)$$

Where, Z is the removal efficiency of Cr(VI) predicted response by the model, β_o is the offset term (constant-coefficient), x_i (i=1-4) and x_j are the studied independent adsorption factors, β_i , β_{ii} , and β_{ij} are the linear, quadratic, and interaction regression coefficients among factors respectively.

3.5. Adsorption isotherm studies of synthesized TMESP adsorbent

For the solid-liquid adsorption system, the adsorption behavior and preparation of the termite mound-eggshell mixture were described by the adsorption isotherm model. This model can indicate the distribution of adsorbate molecules between the solid phase and the liquid phase at equilibrium. The equilibrium of adsorption is established when the concentration of adsorbate in bulk solution is in dynamic balance with that on the liquid adsorbate interface. The relationship between the amount of substance adsorbed per unit mass of adsorbent at constant temperature and it is significant to understand the adsorption behavior in order to describe the adsorption process using the appropriate adsorption isotherm model. Therefore, the distribution of Cr (VI) ions between the adsorbent and solution were determined by adsorption isotherm models such as Langmuir, Freundlich, and Temkin models were used to generate compatible experimental data. It also helps to find out the best fitting isotherm model to evaluate the efficiency of the prepared termite mound-chicken eggshell adsorbent in a batch adsorber experiment (Owalude & Tella, 2016). These models equation examined the fitted one to the experimental data using origin software graphical analysis.

3.5.1. Langmuir adsorption isotherm

The equilibrium adsorption data for the concentrations of Cr (VI) ions were solved using the non-linear and linear form of Langmuir's isotherm Equations (3.14) and (3.15) respectively to determine the distribution of Cr (VI) ions between the adsorbent and adsorbate of the solution. Also according to Matouq *et al.* (2015) justification, the Langmuir isotherm assumes monolayer adsorption on a uniform surface with a finite number of adsorption sites. So, this type of isotherm model demonstrates the formation of monolayer adsorption of the adsorbate on the surface of the adsorbent (Dereje *et al.*, 2021). Extensively, the assumptions of the Langmuir equation include the following: a) maximum absorption occurs when the adsorbent surface is covered by a single layer of soluble material; b) The absorption energy or heat of adsorption is identical at all the points; c) The adsorbed material cannot move on the adsorbent surface; d) The adsorption consists entirely of a monolayer at the surface; e) There is no interaction between molecules on different sites and each site can hold only one adsorbed molecule.

$$q_e = \frac{K_L q_{\max} C_e}{1 + K_L C_e} \quad (3.14)$$

Where C_e is the equilibrium concentration of the chromium ions in solution (mg/L), q_e is the equilibrium concentration of Cr(VI) ions on the adsorbent (mg/g), q_{\max} and K_L is Langmuir constants related to sorption capacity and the rate of adsorption respectively.

Equation (3.14) is transformed mathematically into linearical form expression as equation (3.15)

$$\frac{C_e}{q_e} = \frac{1}{K_L * q_{\max}} + \frac{C_e}{q_{\max}} \quad (3.15)$$

Maximum adsorption capacity (q_{\max}) is the monolayer capacity of the adsorbent (mg/g) and an essential feature of the Langmuir isotherm can be expressed in terms of separation factor (R_L) which is a dimensionless constant also referred to as equilibrium parameter. R_L can be calculated by using Equation (3.16) (Matouq *et al.*, 2015; Yosuff, 2019):

$$R_L = \left(\frac{1}{1 + K_L C_0} \right) \quad (3.16)$$

Where C_0 is the initial adsorbate concentration (mg/L), K_L can be obtained from the Langmuir plot of C_e/q_e versus C_e . The separation factor R_L indicates the isotherm shape as:

$R_L > 1$ Unfavorable, $R_L = 1$ Linear, $0 < R_L < 1$ Favorable and $R_L = 0$, it is irreversible.

3.5.2. Freundlich adsorption isotherm

Freundlich isotherm model describes the relationship between non-ideal and reversible adsorption and the presence of multi-layer adsorption or heterogeneous adsorption which can be demonstrated by Equation (3.17) and (3.18) represents the non-linear and linear form of the adsorption model respectively (Matouq et al., 2015; Dereje *et al.*, 2021).

$$q_e = K_F C_e^{1/n} \quad (3.17)$$

Where q_e is the amount of Cr(VI) ions that was adsorbed at equilibrium per unit gram of the adsorbent (mg/g), C_e is the residual equilibrium concentration of the Cr(VI) ions in the solution (mg/L), and K_F and n : (heterogeneity factor) are the Freundlich adsorption model constants related to the adsorption capacity and adsorption intensity respectively.

$$\log_e q_e = \log_e K_F + \frac{1}{n} \log_e C_e \quad (3.18)$$

If $n = 1$ then the partition between the two phases is independent of the concentration. The slope ($1/n$) linear graph ranges between 0 and 1 that measures the adsorption intensity or surface of heterogeneity and as it approaches zero, exaggerate more heterogeneous of the process. As Matouq *et al.* (2015) state, if the value of $1/n$ is below one it indicates chemisorption's process (adsorption is the chemical process). On the other hand, $1/n$ being above one indicates cooperative adsorption (adsorption is a physical process) (Kale, 2017). Using Equation (3.18), linear graph $\log_e(q_e)$ was plotted against $\log_e C_e$ and a straight line gave the intercept of $\log K_F$ and the slope of $1/n$. The numerical value of $1/n$ is less than 1 and also positive for the two adsorbents indicating a favorable adsorption process (Owalude & Tella, 2016).

3.5.3. Temkin adsorption isotherm

The Temkin model considers the interaction between adsorbent and contaminant as a chemical adsorption process. The Temkin isotherm expressed equation is as shown in Equations (3.19).

$$q_e = \frac{RT}{b} \ln(AC_e) \quad (3.19)$$

The Linearized form of Temkin equations (3.20) and (3.21) as following:

$$q_e = \frac{RT}{b} \ln A + \frac{RT}{b} \ln C_e \quad (3.20)$$

$$q_e = B \ln A + B \ln C_e \quad (3.21)$$

Where $B=RT/b$, R is the universal ideal gas constant (8.314 J/mol/K), T is the temperature (K) or 298K, q_e is the amount of Cr(VI) adsorbed at equilibrium, C_e equilibrium concentration in mg/L, b is the heat of sorption constant (J/mol) in Temkin isotherm, A (L/g) is the Temkin isotherm equilibrium adsorption constant and B is the constant related to the heat of adsorption (J/mol) (Kuang *et al.*, 2020).

3.6. Adsorption kinetic model for synthesized TMESP adsorbent

The reaction pathways and adsorption mechanisms give extremely useful information in the adsorption process in terms of adsorption kinetics analysis (Dereje *et al.*, 2021). The influence of contact time on the removal efficiency or capacity of hexavalent chromium ions was studied using sorbent concentration (adsorbents) in the time range by using pseudo-first-order, pseudo-second-order, and Weber and Morris intra-particle diffusion models of adsorption kinetics.

3.6.1. Pseudo-first order adsorption kinetics

To explore the kinetics of the chromium ion elimination process using Lagergren's Pseudo-first-order adsorption kinetics (PFOKM) absorber was modeled to determine as below applying the boundary conditions $q_t = 0$ to $q_t = q_e$ for $t = 0$ to $t = t$ that conducted at room temperature. This pseudo-first-order model justifies the adsorption process of liquid-solid phase systems concerning the adsorption capacity that is attributed to more physical adsorption interactions than chemisorption (Stephen *et al.*, 2017).

$$\frac{dq_t}{dt} = k_1(q_e - q_t) \quad (3.22)$$

$$\ln(q_e - q_t) = \ln q_e - \frac{k_1}{2.303} t \quad (3.23)$$

Where q_e and q_t (mg/g) are the weight of chromium(VI) adsorbed at equilibrium and time (min) adsorbed per gram of adsorbents respectively, k_1 (1/minute) is the Lagergren's rate constant for PFOKM (Badessa *et al.*, 2020; Bahador *et al.*, 2021). The values of K_1 (or $k_1/2.303$) and q_e can be obtained from the slope and the intercept of a linear straight-line plot of $\ln(q_e - q_t)$ versus t (Dereje *et al.*, 2021).

3.6.2. Pseudo-second order adsorption kinetics

The pseudo-second-order rate expression is based on the adsorption capacity of the solid phases, which has been applied for analyzing chemisorption kinetics rate (Matouq *et al.*, 2015; Singha & Das, 2011). The linear relationship of pseudo-second-order adsorption kinetics (PSOKM) is as follows using boundary conditions $q_t = 0$ and $q_t = q_e$ for $t=0$ and $t = t$, respectively.

$$\frac{dq_t}{dt} = k_2 (q_e - q_t)^2 \quad (3.24)$$

$$\frac{t}{q_t} = \frac{1}{k_2 q_e^2} + \frac{t}{q_e} \quad (3.25)$$

Where k_2 is the second-order-rate constant ($\text{g.mg}^{-1}.\text{min}^{-1}$) that can be determined for different adsorbate concentrations according to the linear plots of t/q_t versus t for PSOKM (Kuang *et al.*, 2020; Badessa *et al.*, 2020). The values of K_2 and q_e can be obtained, from the intercept and slope of the linear respectively.

3.6.3. Intra particle-particle diffusion

Intra particle-particle diffusion is one of the models used for identifying the rate adsorption step in adsorption processes. According to this model, if the plot of q_e versus $t^{0.5}$ gives a straight line, then the adsorption process is controlled by intra-particle diffusion, while if the data exhibit multilinear plots, then two or more steps influence the adsorption process (Yusuff, 2017).

$$q_t = K_i t^{0.5} + I \quad (3.26)$$

Where q_t (mg/g) is the amount of hexavalent chromium removed at a time (min), K_i is the intra-particle diffusion coefficient obtained from the slope of a curve, and 'I' is the intercept.

3.7. Determination of point of zero charges using solid addition technique

The point of zero charges of the adsorbent is an important characteristic parameter that determines the net surface charge of the ion in a given solution by the solid addition method. According to Xiao & Thomas (2004) explanation, several factors affect the adsorption of aqueous metal ion species on thermally modified materials; these include the surface charge and the speciation of metal ions in solution that leads to dependence of the amount adsorbed on the point of zero charges (pHpzc), isoelectric point, and experimental conditions, such as ionic strength,

pH, and concentrations of species in solution. Here, the pHzpc purpose is to specify the electrical neutrality of the adsorbent at a particular pH value. Thus, the charge on the surface of a specific adsorbent becomes zero. So, the pHzpc of adsorbent materials ion was measured using evidence obtained from Dereje *et al.* (2021) that solid addition technique. Based on this information and Bhaumik *et al.* (2012) investigation, this study was performed by taking 10g of 1.0MNaCl dissolved in 50mL solution and distributed into ten a series of 100mL conical flasks. The initial pH (pH₀) values of the solution were adjusted from 3.0 to 12.0 by adding either 0.1MHCl or 0.1MNaOH. Then 1.5g of calcined TM-ES powder was added to each conical flask which was securely tight (capped) with parafilm immediately. Then, the flasks were placed into a constant room temperature shaker for 48 hours with 270rpm. The final pH values of the suspension liquid for each sample were filtered and measured again according to a procedure written by (Kavitha & Thambavani, 2014). The difference between the initial and final pH (Δ pH) values in the y-axis was plotted against the initial pH₀ (x-axis). The point of intersection of the resulting curve with the x-axis gave the PHpzc. The pH of the aqueous solution has an influence on the surface charge of the adsorbents as well as the degree of the ionization and speciation of unique pollutants. Change in the pH impacts the adsorptive technique via dissociation of useful functional groups as the active sites on the surface of the adsorbent. This is because of it leads to a shift in the reaction kinetics and the equilibrium characteristics of the adsorption process. Adsorption of the range of cationic and anionic species on such adsorbents can be explained on the foundation of the aggressive adsorption of H⁺ and OH⁻ ions with the adsorbate. It is a common observation that the surface adsorbs anions favorably at decreased pH due to the existence of H⁺ ions, whereas the floor is lively for the uptake of cations at extreme pH due to deposition of OH⁻ ions (Singha & Das, 2011). Thus, the surface charges of TMESP-adsorbent furnish an essential position in adsorption processes and decide the conduction of materials in the adsorption mechanism.

3.8. Specific surface area investigation

The calcined termite mound eggshell powder of specific surface area was determined using the technique explained by Kavitha & Thambavani (2014) during the study of clay minerals which has nearly the same composition as TMES powder the high specific surface area, chemical, and

mechanical stability, layered structure, high cation exchange capacity (CEC), Brönsted and Lewis acidity, have made excellent materials for adsorption. Based on these principles one gram of adsorbent and 1.5g of NaCl was mixed in 100 mL of distilled water to form a solution. The mixture was shaken manually for a few minutes. Its final pH was adjusted to 4 with 0.1MHCl. It was then titrated against 0.1M NaOH to raise the pH from four to nine and the volume (mL) of 0.1MNaOH used was measured in replicate and the average value was taken for the surface area of calculation by sears method as follows in Equation (3.27) (Kavitha & Thambavani, 2014) :

$$S = 32 * V - 25 \quad (3.27)$$

Where S is the surface area of bio adsorbent per gram (m^2/g), V is the volume of 0.1MNaOH in mL needed to increase the pH of the sample from 4 to 9 within solution. The constants numbers 32 and 25 coefficients of physical parameters.

3.9. Desorption and regeneration of synthesized TMESP-adsorbents

Regeneration of adsorbent is as explained by Kulkarni & Kaware (2014) very crucial aspect of recovery of the solute during the adsorption procedure and subsequent recycling of adsorbent are significant attributes of adsorption process observed from cost as well as an environmental point of view. This process can be accomplished using various methods like solvent washing, chemical and electrochemical and thermal methods were used effectively for regeneration of an adsorbent (Kassahun *et al.*, 2017). Similarly, in this thesis regeneration and reusability of the vacuum filtrated used cake remained on 55mmØ diameter and 11µm pore size what man filter paper of TMESP adsorbents were collected and treated with 50mL of 1.0MNaOH solution that diluted using distilled water solution to exaggerate the desorption purposes to give awareness the recycling efficiency and reusability of the adsorbent powder (Singha & Das, 2011; Billah *et al.*, 2021; Rotimi & Okeoghene, 2014). Regeneration and reusability of termite mound-chicken eggshell adsorbents studying were performed using 100mL of aqueous solutions that incorporate 6g/L of adsorbent with 0.3mm synthesized TMESP-adsorbent particle size immersed into Erlenmeyer flasks containing 40mg/L Cr(VI) metal ion that agitated with 150rpm and withdraw the result after equilibrium is attained within 45minute. Finally, the used TMESP adsorbent was regenerated by washing multiple times using deionized water with the help of a centrifuge that runs at 3000rpm until the value of pH becomes nearly neutral (Fufa *et al.*, 2014). This

regenerated powder of adsorbent was dried using an oven at 105°C for two hours to remove the water added in the metal ion removal situation of adsorbate from the adsorbent. To evaluate the reusability of the adsorbent, the adsorption and regeneration processes were repeated five times using the same regenerated sequence. The procedure of desorption adsorbent cycles was performed at optimum conditions and the desorption percentage of Cr(VI) ions was calculated according to the following equation (Singha & Das, 2011; Bayuo *et al.*, 2020) (3.28).

$$D_e \% = \frac{C_{de}}{C_{ad}} * 100\% \quad (3.28)$$

Where D_e is the desorption percentage of heavy metal ions, C_{ad} is the value of chromium ions adsorbed (mg/L) and C_{de} is the concentration of chromium ions desorbed, (mg/L).

3.10. Investigation of competitiveness heavy metals to synthesized TMESP adsorbent.

This subtopic investigation mainly ventures on the propensity of heavy metals to fit the active site of the prepared TMESP adsorbent. Among various contaminated water treatment technologies explained in the introduction parts of this paper, adsorption techniques have been used for the treatment of transitional metal ions contaminants that are considered as a highly effective, economical, eco-friendly, and not sophisticate for operational method and it has great significance for exploring the appropriate adsorbents because of the severity of trace metal pollution and high processing costs are increasing (Ouyang *et al.*, 2019). Since the trace toxic metals ions exist in wastewater and industrial discharged effluents are a major environmental concern; their competitive for adsorption is also the usual challenge situation in real applications, and it is critically necessary for determining the overall performance of an adsorbent beside most popularly known parameters like initial concentration, PH, adsorbent dose and contact time (Xiao & Thomas, 2004). Also, as Makuchowska (2019) justifies the effectiveness of water solution purification depends on the competitive sorption of ions; in addition to those common parameters like pH, concentration, contact period, sorbent particle size, and dose of adsorbent. Extensively, as Dereje *et al.* (2021) prove in phosphate adsorption from the aqueous solution the presence of competitive ions significantly affects the removal efficiency of the targeted ion adsorption process from dissolved aqueous. In more detail, according to Liu *et al.* (2016)

explanation, the adsorption of Cr(VI) on modified kaolin was hindered by the presence of phosphate due to competitive adsorption. Based on this assumption the competitiveness of heavy metals like copper (Cu), silver (Ag), lead (Pb), nickel(Ni), zinc (Zn), cobalt (Co), were studied by dissolving with Cr(VI) from stock solutions in separated beakers to perform batch adsorption processes. However, most of the papers focus on a single atom of adsorption that should be extended to scrutinized their competitiveness to fixed adsorbent because of this metals ions may be use in the current wide spread industries simultaneously. Also, according to Kunal *et al.* (2019) reports freshwater in lake and pond are often found to be polluted by heavy metals such as As, Zn, or Pb which are toxic in nature and non-biodegradable. For this thesis the parameter of adsorption for competition of determined transition metals fixed to optimum condition; but as Liu *et al.* (2016) reveal that removal of chromium in the existence of Cupper ion onto kaolin was investigated under different pH of adsorption and as pH of solution increased due to protonation significantly reduced the removal effectiveness of Cr(VI) on mesoporous silica and its capacity become vary. The method of efficiency and capacity calculation is the same using Equation (3.10) and (3.11) respectively.

Table 3. 2: Heavy metals selected to study their competition for TMESP adsorbent

The chemical formula of heavy metals compound	Heavy metals ions	The atomic weight of heavy metals (g)	Mass of sample (g) to 1ppm
CuCl ₂	Cu(II)	63.546	2,12
CuO	Cu(II)	63.546	1.25
Ag(NO ₃)	Ag(I)	107.87	1.57
PbCl ₂	Pb (II)	207.2	1.34
Pb(NO ₃)	Pb (II)	207.2	1.6
NiF ₂	Ni (II)	58.7	1.65
Ni(NO ₃) ₂	Ni (II)	58.7	3.11
ZnSO ₄	Zn (II)	65.38	2.47
Co(NO ₃) ₂	Co (II)	58.93	3.10
CoCl ₂	Co (II)	58.93	2.2
K ₂ Cr ₂ O ₇	Cr (VI)	52	2.82

4. RESULTS AND DISCUSSIONS

The adsorption efficiency of synthesized termite mound-chicken eggshell adsorbent to remove Cr(VI) heavy metal ion adsorbate from the synthetic water with regards to the results of experimental data generated or evaluated was discussed as following concerning to the methodology section for synthesizing as well as for batch adsorption process.

4.1. Proximate analysis of TMESP adsorbent

In this section of investigation, the analysis has involved the evaluation of moisture contents, porosity, ash content, and fixed carbon content of termite mound-chicken eggshell mixture based on standard test methods known as the American Society for Testing and Materials (ASTM).

4.1.1. Moisture content determination

Moisture content can be performed after the size of the powder of chicken eggshell and termite mound were determined by sieve of proper mesh size analysis is carried out based on ASTM D2867-99 at 105°C in an oven. Based on this analysis the higher removal percentage of moisture content from the sample refers to the enhancement of adsorption capacity. So, in this experiment, moisture content for termite mound sample was 10.31%, for chicken eggshell sample 4.3%, and their average 7.31% was accomplished within identical time and ambient temperature of experimental room using 10gram of specimen. However, the result shows as there is some deviation from the value 1.17% that investigated for eggshell by Bhaumik *et al.* (2012) and 0.98% from Reta *et al.* (2021) experimental reports. On this point as Ajala *et al.* (2018) states the high moisture content tends to promote microbial contamination and chemical degradation in many substances. Thus, this criterion proves as TMESP adsorbent has a higher resistance to microbial contamination and chemical degradation.

4.1.2. Determination of Ash Content

The result was obtained in this experimental determination, the lower the ash contents the better material for adsorption behavior. Based on this principle percentage of incombustible matter residue value was recorded for termite mound raw material alone, chicken eggshell raw material alone and their mixture (termite mound- chicken eggshell) after 20.08gram of TMESP sample igniting at 750°C by muffle furnace was 81.15%, 76.71%, and 92.22% respectively. These

percentages were nearly agreed with Reta *et al.* (2021) report 78.2% for hen eggshell during lead removal from aqueous solution investigation.

4.1.3. Determination of Volatile Matter

Volatile matter investigation was performed for termite mound-chicken eggshell mixture which resulted in mixture 2.39%, Eggshell alone 2.54% and Termite mound alone 2.91% is obtained from 15gram of the sample of identical powder after heated in a furnace at 550°C for 10 minutes without air. This value of volatile matter is indicated the residual organic compounds within synthesized adsorbent and it is almost the same as 2.7% that was investigated for hen eggshell (Reta *et al.*, 2021). These magnitudes show that, since it is very low it has no significant influence for synthesizing termite mound-chicken eggshell mixture adsorbent.

4.1.4. Determination of Fixed Carbon Content

The fixed-carbon content or the residue of termite mound-chicken eggshell was determined by subtracting from 100 the percentages of moisture, volatile matter, and ash from a sample and it has resulted in 82.53%. Higher percentage of fixed carbon content means that improve good surface of adsorbent for adsorption purpose to attract the adsorbate.

4.1.5. Determination of Porosity of adsorbent

i. Bulk density

Bulk densities of grounded raw material average for both and synthesized termite mound-chicken eggshell were 0.696g/mL which is less than 0.8024g/mL that obtained from Bhaumik *et al.* (2012) investigation and this density extremely reduced to 0.41 g/mL after calcined by muffle furnace. This physical property technique demonstrates that the bulk density of synthesized adsorbent was less than the fresh ground termite mound-chicken eggshell powder as a result of its existence inside void space. The smaller bulk density the higher porosity of adsorbent was obtained (Singha & Das, 2011).

ii. Particle density

In this study, the particle density (true density) of experimental result for both termite mound-eggshell powder raw material and its calcined was raised from 1.21g/mL to 2.22g/mL respectively and similar to 2.01 g/mL particle density of eggshell alone studied by (Reta *et al.*, 2021). From that overview, the bulk density TMESP decreased from the raw material to the

modified samples whereas the particle density increases from the raw to the synthesized termite mound-chicken eggshell powder and this indicates the porosity is increased with a high value of particle density and low with high value of bulk density and vice versa of expression.

iii. Porosity

The porosity parameters and chemical compositions of the materials can be well-tuned by changing the activating agents (steam and carbon dioxide) and reaction temperature. In the current study, the average powdered TMESP porosity obtained 42.48% which is greater than 25.4% for eggshell studied by Bhaumik *et al.* (2012) and their synthesized product was raised to 81.53% of porosity. The result obtained was also nearly similar to 81.34 percentage as reported by Reta *et al.* (2021) during studying lead (II) removal using synthesized hen eggshell adsorbent. An increase in porosity means the adsorbent has a relatively large potential of adsorbing the adsorbate because of the large contact surface (Kassahun *et al.*, 2017; Haddad *et al.*, 2019; Singha & Das, 2011). Therefore, the synthesized (thermal modification) of termite mound-eggshell exhibits the existence of a high porosity structure.

4.1.6. Specific surface area determination

According to Bhaumik *et al.* (2012) explanation during the study for adsorption of fluoride using chicken eggshell the heterogeneous pores and cavities provided a larger exposed surface area that improve the adsorption behavior of materials. Based on this statement the surface area of TMESP adsorbent was calculated using Equation (3.27) under the portion of materials and methodology. This was done by dropping 0.1MNaOH required to adjust the pH of the solution from allocated 4 to 9 PH the cumulative titration drop average for raw materials of termite mound-chicken eggshell was 1.6mL and for synthesized of TM-ES powder the volume was increased to 2.6mL respectively. After calculation, the average of TM-ES powders obtained from the experimental result of specific surface area was 26.2m²/g which is greater than from Bhaumik *et al.* (2012) report for eggshell that was 21m²/g obtained using Brunauer-Emmit-Teller (BET) surface area measurement technology. Similarly, according to Reta *et al.* (2021) report during studying of hen eggshell for removal of lead (II) specific surface area of calcium oxide nano-particle was 77.4m²/g. However, the specific surface area for calcined TMESP adsorbent was calculated to 58.2m²/g. This increment result of surface area from raw powder to thermally

modification of TMES powder proves the adsorption tendency of the specimen in addition to the above proximate analysis justification.

Table 4. 1: Proximate characteristics comparison of various bio-adsorbents with current study (Singha & Das, 2011)

Adsorbents	Bulk density (g/cm ³)	Dry matter (%)	Moisture content (%)	Point of zero charge	Ash content (%)
Rice straw	0.36	92.74	7.26	6.85	9.40
Rice bran	0.42	89.32	10.68	6.10	11.72
Rice husk	0.54	90.98	9.02	6.05	11.80
Hyacinth roots	0.48	88.75	11.25	6.59	10.74
Neem leaves	0.71	91.67	8.33	6.94	13.58
Coconut shell	0.82	93.84	6.16	6.62	9.23
TMESP	0.41	92.695	7.31	7.6	7.78

4.2. Evaluation of synthesizing termite mound-eggshell mixture

4.2.1. Determination of TMESP mixture ratio and calcination parameters for synthesizing

To prepare termite mound and chicken eggshell powder it was dissolved in 100mL of distilled water that homogenized by magnetic stirrer with 600rpm at various proportion ratios as illustrated in the following Table C 3 that displayed by design expert 11soft ware output almost yields the same efficiency. Also, according to Yusuff' (2017) explanation; the mixing ratio of TMESP adsorbent has no significant effect on adsorption capacity and morphological properties of the mixture of adsorbent and was optimized to 1:1.86 using three variables of batch adsorption processes. Actually, all output of termite mound-chicken eggshell powder adsorbent was checked by using UV-visible spectrophotometer of absorptions equipment. Analogously, the calcination temperature and time were determined based on Yusuff' (2019) explanation and the principle of calcium carbonate decomposition to calcium oxide that ranges from 700 to 1000 temperature and 1 to 4 hours residence time and it was optimized to 850.17°C. Concerning this, the batch

adsorption of the full experiment was accomplished using the maximum value of these pre-examined conditions which was 850°C temperature within four hours residence time as tabulated in Table C 6 using design expert software randomly scattered. The batch process of adsorption for justification results was obtained using 1.0g of TMESP mixture adsorbent, at neutral pH, for 1hour contact time, 60mg/L initial Cr(VI)concentration with ambient room temperature.

4.3. Characterization of synthesized termite mound-eggshell adsorbent

4.3.1. UV-Visible spectrophotometer analysis of TMESP-adsorbent

In this subtopic study, the determination of the Ultraviolet-visible spectrum of the synthesized TMESP adsorbent was demonstrated as shown in the following Figure 4.1 maximum peak occurs at 377.8nm; which is the same to Sumathi (2017) reports 380 nm indicating the formation of nanostructure samples. This typical surface plasma resonance absorption peak at 377.8nm by UV-visible spectrophotometer values reveal the incorporation of magnetite (Fe_3O_4) (Tang *et al.*, 2013; Mandić *et al.*, 2021), calcium oxide (CaO) (Sumathi V, 2017), Silica (Pham *et al.*, 2020) which is their wavelength peaks almost the same to this synthesized TMESP adsorbent. Even though, there is a reports that little deviate during the characterization process of the biosynthesized results using Ultraviolet-visible spectroscopy (UV-visible), as it had maximum absorbance wavelength at 450 nm, which was indicated by the presence of Ca-O bond in the biosynthesized sample (Ramli *et al.*, 2019). So, this investigation confirms that the synthesized of termite mound-chicken eggshell powder adsorbent that consists of magnetite, calcium oxide, and silica as explained in chapter two literature review section.

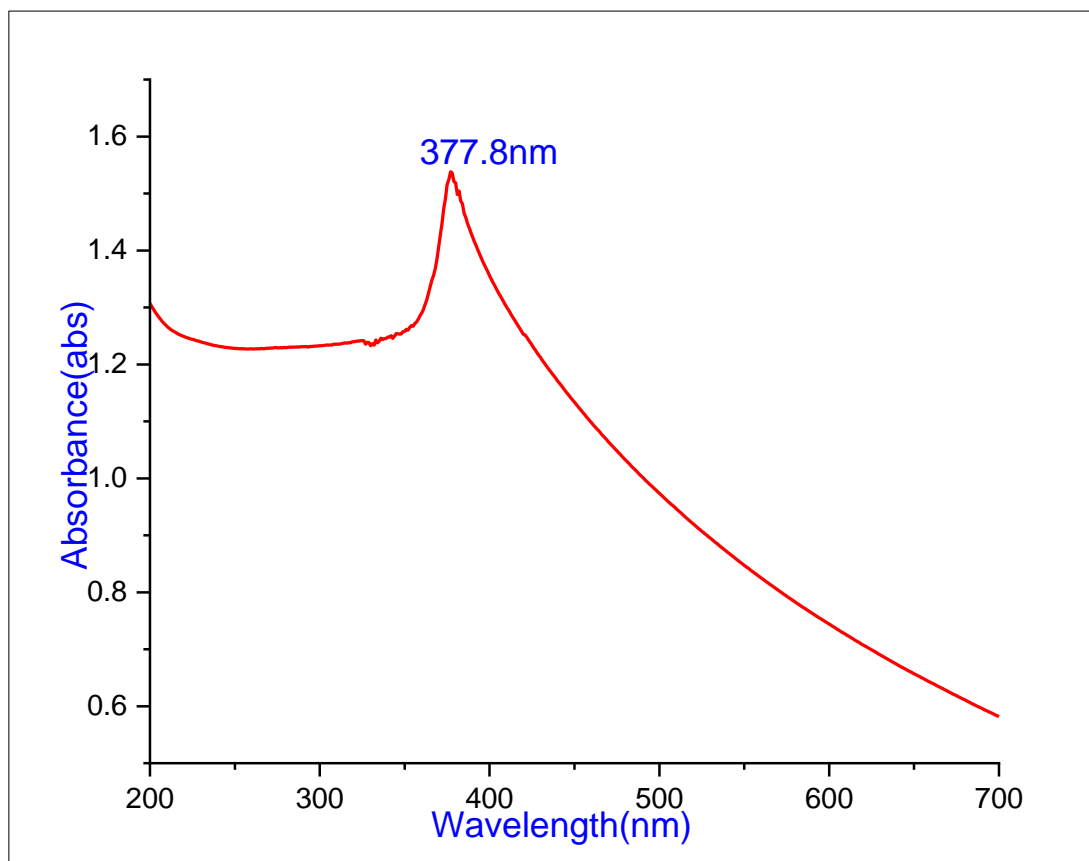


Figure 4. 1: Absorption spectra of synthesized TMESP adsorbent from UV– visible spectroscopy

4.3.2. Fourier Transform Infrared Spectroscopy

In this study the thermal calcination, the formation oxygen with functional groups are investigated for the surface of termite mound-chicken eggshell adsorbents that improve complexes with aqueous metal species and ion exchange with the displacement of protons consequently enhancing the adsorption process of aqueous metal cation. Because, the surface chemistry of adsorbent plays an important role in the adsorption process of aqueous heavy metal ions on the surface of calcined adsorbent that incorporates hydrophobic graphene layers and numerous hydrophilic functional groups (Xiao & Thomas, 2004). Based on this principle, organic compounds are adsorbed on the former, whereas polar species are adsorbed on the latter.

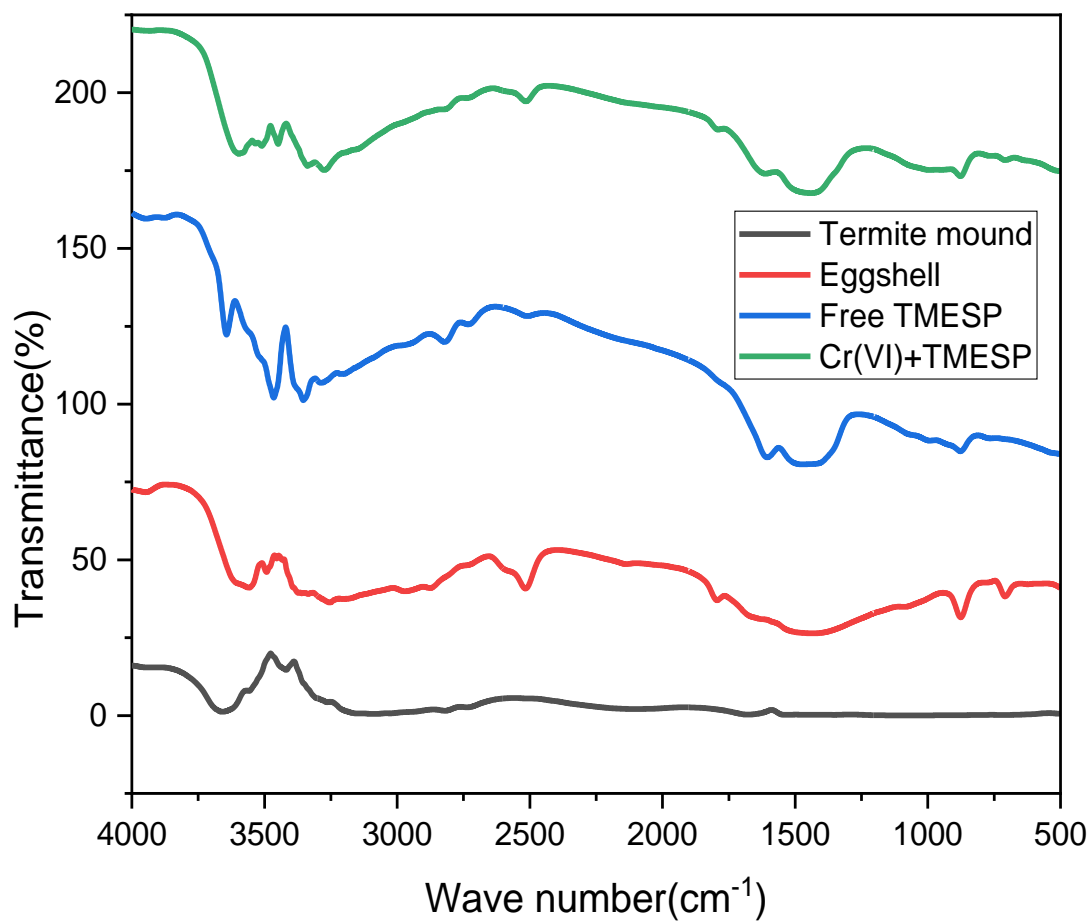


Figure 4. 2: Comparative FTIR image of TMESP adsorbent from raw material to its synthesized

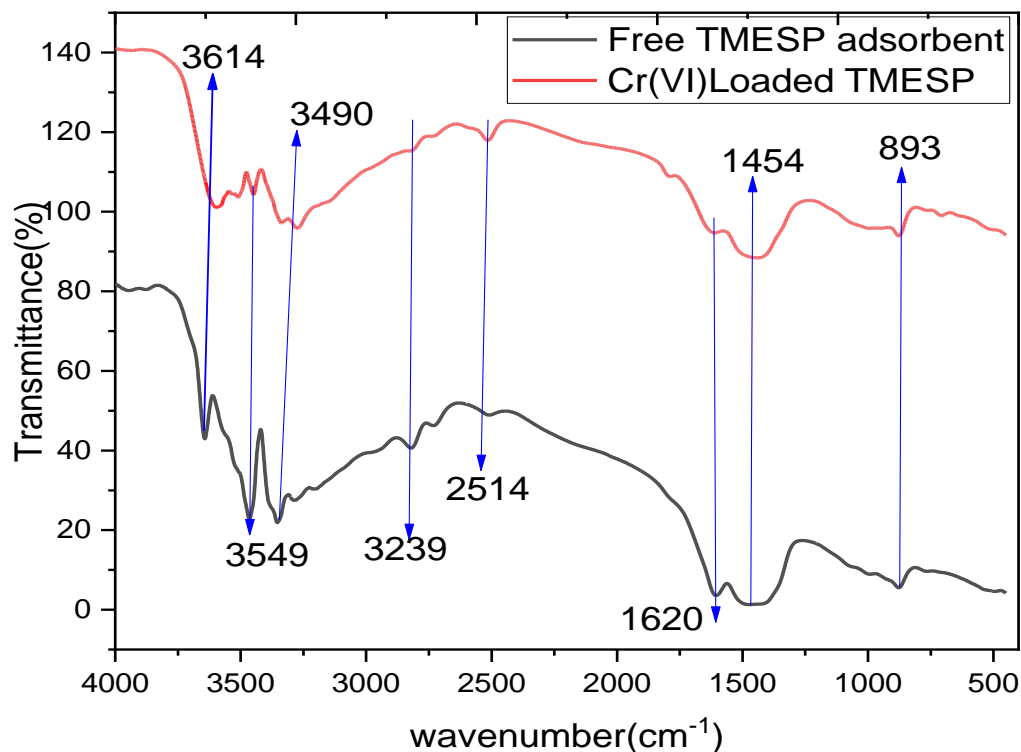


Figure 4. 3: FTIR result for TMESP-adsorbent before and after chromium adsorption

The highest peak shifts are observed as a result of the involvement of the major functional groups in the adsorption of Cr(VI) ions. The shift in a peak at 1454 cm^{-1} for carboxyl groups has occurred most likely due to the participation of Si-O-C and C-H groups in Cr(VI) adsorption. Some fingerprints are observed at 893 , 1620 , 2514 , 3239 , 3490 , 3549 , and 3614 cm^{-1} that indicate the presence of C-H, C=C, C-O, NH₄, N-H, O-H, and O-H with terms of aromatic, primary amine and amide groups, skeletal vibrations, alcohol respectively (Rai *et al.*, 2016). These the IR domain peaks almost the same value to Bhaumik *et al.* (2012) spectral analysis of chicken eggshell powder that displays peak at 712.86 , 875.56 , 2516 , 3431.25 cm^{-1} and explained to as the presence of alcohol hydroxyl group (-OH) and acidic hydrogen group (-OH) stretching respectively. Hence, the presence of these organic functional groups on the surface of calcined TMESP adsorbent enhances the capacity of heavy metals removal. Also, from the observation of PHpzc value the protonated oxygen-containing functional groups C-O and C=O present on the surface might be attributed to binding with hydrochromate (HCrO_4^-) in strong electrostatic

attraction between anion Yusuff (2019). In another way, the shift of the band in adsorption indicates the successful binding of Cr(VI) ions to the active sites of alkenes (C=C) and amine. This had happened because alkenes (C=C) have major active sites for the binding of metals/heavy metals (Nandiyanto *et al.*, 2019). Also according to Gucsik *et al.* (2014) reports Micro-IR reflectance spectra (650-1300 cm^{-1}) and powder absorption spectra (150-1500 cm^{-1}) of zircon were observed, this magnitude is found in the range of the above graph. The band of 893 cm^{-1} revealed as may correspond to SiO=H vibration for the termite mound-eggshell (Rotimi & Okeoghene, 2014). Also, as reported by Ipeaiyeda & Tesi (2014) out-of-plane bending for the aromatic hydrogen atom (C-H) and Al-Al-OH clay vibration gives a characteristic absorption band at 893 cm^{-1} . Similarly, the shift of the bands from before to after ranges revealed the involvement of C-O functional groups in the adsorption of Cr(VI) ions. This was because C-O functional groups have effective active sites that can be involved in the binding of heavy metals by ion exchange and/or ionic interactions. Also, as Sumathi (2017) reports in the study of CaO nanoparticles the peaks around 906 cm^{-1} and 871 cm^{-1} shows the existence of Ca-O stretching.

4.3.3. X-Ray Diffraction analysis of particle size

The XRD analysis as explained in the methodology section has the advantage of no damage to the information about crystal integrity (Joni.M, 2018). As Liu *et al.* (2016) state Kaolin adsorbent for the removal of chromium that composed aluminosilicate which is termed as crystalline materials. Similarly, the adsorbent crystallite size of TMESP-adsorbent was determined by Drawell XRD 7000, scanning range 5°-80°, scanning rate 0.0012-70°/min, that run by 25mA current and 30kV sources in the experimental study and the graph displayed in Figures (4.4 and 4.5) as follows. The average crystallite size 26.69nm of the synthesized TMESP-adsorbent was recorded and calculated by using Debye-Scherrer's formula Equation (3.9) with a help of origin software analysis which fulfills nano-particle character having an average crystallite size less than 30 nm that the nanoscale exist between 1-100nm (Ramli *et al.*, 2019) and nearly the same average size results found by Sumathi V. (2017) and Ramli *et al.* (2019) 25nm and 18.98 nm from CaO nanoparticles that reveal nanoscale particle size respectively. However, according to Reta *et al.* (2021) justification for uncalcined eggshell the average size become 79.4 μm of crystallite which indicate that the calcination process improves

the porosity of the adsorbent. Also, as Joni *et al.* (2018) explained the average crystallite size of silica was about 28 nm; So, this XRD analysis proves that as there is silica (SiO_2) that is relevant for adsorption. The value obtained is also nearly compatible with 13.57nm obtained from Yusuff (2019) investigation during the removal of Nickel(II) from an aqueous solution using TMESP-composite adsorbent.

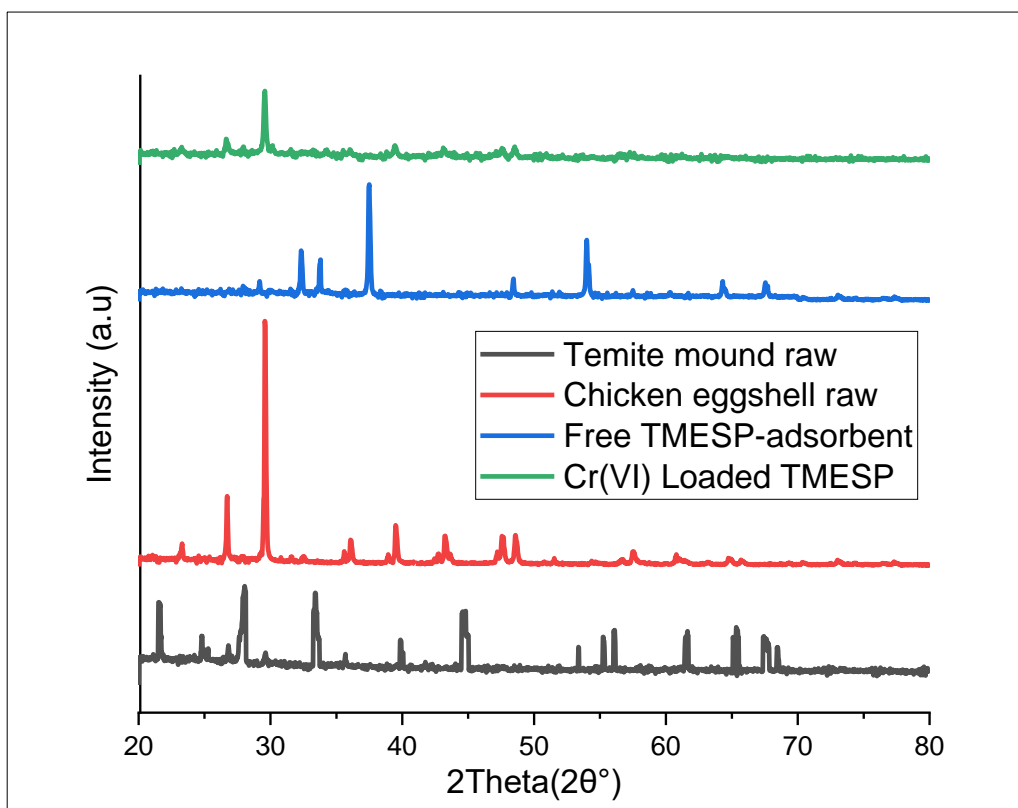


Figure 4. 4: Comparison of crystallinity peaks for TMESP adsorbent

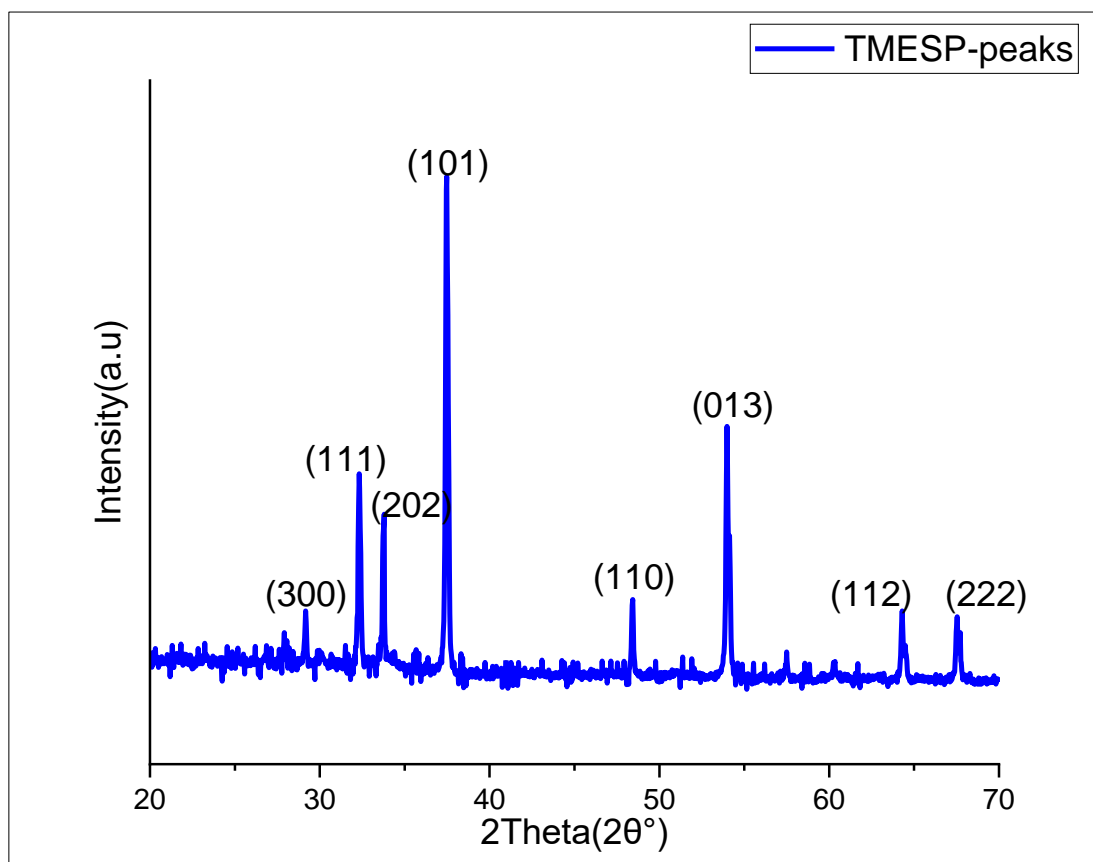


Figure 4. 5: Justification XRD crystallinity peaks for TMESP-adsorbent

In this XRD testing of TMESP adsorbent the 2theta ($2\theta^\circ$) domain peak appeared at 37.58° angle and the other no fingerprint crystalline peaks that characterize diffraction peaks at 2theta ($2\theta^\circ$) values of 29.13° , 32.27° , 33.3° , 48.42° , 53.38° , 64.3° , and 67.7° of diffraction angle indexed to their Miller indices of XRD peaks which depicted by using origin lab 2018b and x'pert high score plus software as follows in Table C4; where $d[A]$ is calculated using Bragg's law, which demonstrates the presence of silica, alumina, hematite, and calcite in the synthesized TMESP-adsorbent that displayed by using x'pert high score plus software. This result was evidenced by Yusuff (2019) the chemical compositions found in termite mound-eggshell were silica (SiO_2), alumina (Al_2O_3), iron oxide (Fe_3O_4), calcium oxide (CaO), and Zirconia (ZrO_2) using XRF analysis. Also, these values were nearly the same that proved to 26.64° and 59.24° that justifies the existence of silica (SiO_2) and 28.7° , 32.3° , 37.45° , 54.0° , 67.6° , 68.2° , and 34.3° and 47.3° are corroborated the existence of calcium oxide (CaO) and $\text{Ca}(\text{OH})_2$ respectively. In addition to that

according to Haddad *et al.* (2019) justification, the advantage of the existence of activated alumina in this adsorbent provides it as it has high porosity and surface area in excess of 200 m²/g. Also, the existence of Zirconia (ZrO₂) in termite mound-eggshell makes another future for this adsorbent like chemical stability, high thermal conductivity, relatively simple structure, and has a capacity to capture a number of dopant ions (Gucsik *et al.*, 2014). This ZrO₂ which is also known as zirconia in a ceramic nanoparticle that experienced in serving as an indispensable to in nano-filler processes. It can be incorporated in a variety of polymer and metal composites to improve the thermo-mechanical properties of the base material. Based on this the peaks above Figure 4.5 proves the crystallites of termite mound-chicken eggshell adsorbent.

4.3.4. Thermogravimetric analysis

This part of investigation mainly focuses to measure the thermal stability or sample degradation of synthesized termite mound–chicken eggshell powder adsorbent based on the principle. The result of mass loss as observed in the following Figure 4.6 curves 11.35% at temperature changes of 471 to 536°C and 2.03% 764 to 820°C respectively. According to Reta *et al.* (2021) explanation, this amount of weight loss was observed due to the loss of CO₂ during the carbonization of termite mound–chicken eggshell adsorbent that had high thermal stability and purity as shown in the curves revealed that the termite mound-chicken eggshell types of adsorbents have not significantly influenced at high thermal heating temperatures. So, this analysis confirms that the termite mound-chicken eggshell adsorbent is the best thermally adaptable and favorable for chromium adsorption.

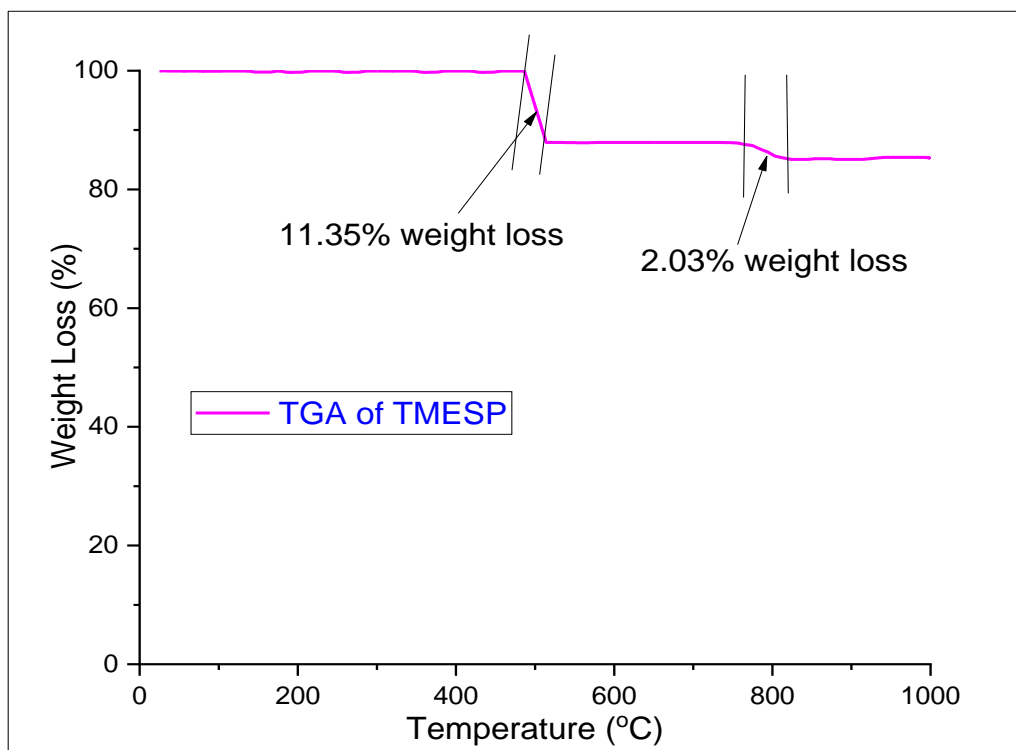


Figure 4. 6: TGA analysis for synthesized TMESP- adsorbent

4.3.5. Experimental design and statistical analysis of UV-Visible adsorption results

The UV-visible spectrum is used to determine the absorbance of synthesized TMESP adsorption and it displays the result in both absorbance (abs) and concentration (mg/L). Means, synthesized TMESP adsorption was accomplished by UV-visible spectral analysis using a range of standard solution graphs. A batch of adsorption experiments was performed in the laboratory and randomization was designed using Design-Expert software version 11 (Table 4.2), and the percentage removal of the adsorbate Cr(VI) was obtained from each adsorption experiment were used for further study after the supernatant solution filtered. Then the residual Cr(VI) concentration was measured by adjusting using sequential Cr(VI) concentration to a calibration graph in a UV-vis spectrophotometer. The obtained experimental results were calculated after the experimental works were accomplished and were recorded for the corresponding run order of parameters and analyzed by using the DOE software. Consequently, the well-fitted regression coefficient model of the adsorption process was determined from fit statistics analysis of RSM that incorporates CCD distribution.

Table 4. 2: Experimental result and predicted values for percentage removal of Cr(VI) ions

		Factor 1	Factor 2	Factor 3	Factor 4	Experimental	Predicted
Std	Run	A:Adsorbent	B:Conce	C:Contact	D:PH	Cr(VI) removal	Cr(VI) removal
			ntration	time		efficiency	efficiency
		g/L	mg/L	Min	PH	%	%
16	1	12	80	75	7	98.76	97.72
9	2	6	40	45	7	97.94	98.99
21	3	9	60	30	5	42.31	43.13
14	4	12	40	75	7	79.19	77.2
24	5	9	60	60	9	87	89.53
26	6	9	60	60	5	94.4	96.15
7	7	6	80	75	3	82.03	81.44
12	8	12	80	45	7	61.07	59.9
19	9	9	20	60	5	94.17	94.98
3	10	6	80	45	3	57.12	59.39
17	11	3	60	60	5	92.26	94.92
5	12	6	40	75	3	66.5	63.06
8	13	12	80	75	3	98.2	98.09
25	14	9	60	60	5	96	96.48
30	15	9	60	60	5	95.87	96.5
1	16	6	40	45	3	92.84	91.82
18	17	15	60	60	5	98.63	97.92
11	18	6	80	45	7	45.34	46.06
2	19	12	40	45	3	92.74	92.48
6	20	12	40	75	3	55.87	56.42
4	21	12	80	45	3	83.09	84.26
13	22	6	40	75	7	99.79	99.45
27	23	9	60	60	5	95.92	97.63
10	24	12	40	45	7	88.32	88.77

22	25	9	60	90	5	54.12	51.66
20	26	9	100	60	5	80.63	78.59
29	27	9	60	60	5	94.54	97.36
28	28	9	60	60	5	95.6	97.08
23	29	9	60	60	1	87.78	92.49
15	30	6	80	75	7	96.13	95.12

4.3.5.1. Model summary statistics for removal of Cr(VI) ions by synthesizing TMESP

In this analysis, the main purposes of the models were used to reveal the fitness of experimental output obtained from batch adsorption. As depicted in the following Table 4.3, the quadratic vs 2FI model was preferably selected and was suggested as the best fitting for Cr(VI) removal adsorption process. Under this justification, the highest order polynomial was selected where the additional terms are significant and the model is not aliased.

Table 4. 3: Fit summary of sequential model for TMESP adsorbent experimental result

Source	Sum of Squares	df	Mean Square	F-value	p-value	
Mean vs Total	2.110E+05	1	2.110E+05			
Linear vs Mean	727.99	4	182.00	0.5441	0.7049	
2FI vs Linear	4404.53	6	734.09	3.52	0.0163	
Quadratic vs 2FI	3944.96	4	986.24	1153.79	< 0.0001	Suggested
Cubic vs Quadratic	9.58	8	1.20	2.58	0.1144	Aliased
Residual	3.25	7	0.4636			
Total	2.201E+05	30	7335.85			

Table 4. 4: Fit Statistics of Cr(VI) removal efficiency using synthesized TMESP adsorbent

Std. Dev.	0.9245	R ²	0.9986
Mean	83.86	Adjusted R ²	0.9973
C.V. %	1.10	Predicted R ²	0.9931
		Adeq Precision	89.7612

Multiple regression coefficients R^2 is displayed from design expert specialist software program was 0.9986 indicates that the envisioned values are closer to experimental facts as shown in Table 4.4. Generally, the R^2 value always lies between 0 and 1; as more of the R^2 value is closer to one, the stronger the model and better fit (high correlation) between the experimental and predicted value that reveal the adequacy of the model (Bayuo *et al.*, 2020). Hence, for this investigation correlation coefficient R^2 value of 0.9986 indicates that experimental data was more compatible with the predicted model. The adjusted correlation coefficient (adjusted R^2) is a measure of goodness of fit, but it corrects the R^2 for the sample size and the number of terms in the model by using the degrees of freedom on its computations. If there are many terms in the model and the sample size is not very large, the adjusted R^2 may be noticeably smaller than the R^2 value. Here, the Predicted R^2 of 0.9931 is in reasonable agreement with the Adjusted R^2 of 0.9973 that very high to advocate for a high significance of the models, and the difference is 0.0042 less than 0.2., which ensures a satisfactory adjustment to the polynomial model to the experimental data. Adequacy precision measures the signal-to-noise ratio. A ratio greater than 4 is desirable; so, in this model design, the ratio value of 89.7612 indicates an adequate signal. This model can be used to navigate the design space.

4.3.5.2. Analysis of variance ANOVA for Quadratic model of Cr(VI) removal

Analysis of variance (ANOVA) is required to test the importance and adequacy of the model. The consequences of more than one linear regression carried out for the second-order response surface model by ANOVA are given in Table 4.5. The significance of the coefficient term is determined by the value of F and p, and the larger the value of F and the smaller the value of p, the more significant is the model.

Table 4. 5: Analysis of variance (ANOVA) response for Cr(VI) removal efficiency

Source	Sum of Squares	Df	Mean Square	F-value	p-value	
Model	9077.49	14	648.39	758.54	< 0.0001	Significant
A-Adsorbent	43.44	1	43.44	50.82	< 0.0001	
B-Concentration	256.96	1	256.96	300.61	< 0.0001	
C-Contact time	277.64	1	277.64	324.81	< 0.0001	

D-PH	149.95	1	149.95	175.42	< 0.0001	
AB	643.26	1	643.26	752.53	< 0.0001	
AC	123.27	1	123.27	144.21	< 0.0001	
AD	117.02	1	117.02	136.90	< 0.0001	
BC	2474.81	1	2474.81	2895.24	< 0.0001	
BD	365.10	1	365.10	427.12	< 0.0001	
CD	681.08	1	681.08	796.78	< 0.0001	
A ²	0.0025	1	0.0025	0.0029	0.9579	
B ²	112.00	1	112.00	131.03	< 0.0001	
C ²	3830.15	1	3830.15	4480.83	< 0.0001	
D ²	8.62	1	8.62	10.09	0.0063	
Residual	12.82	15	0.8548			
Lack of Fit	10.19	10	1.02	1.94	0.2411	not significant
Pure Error	2.63	5	0.5260			
Cor Total	9090.31	29				

Based on this statistical table the terms A, B, C, D, AB, AD, BC, BD, CD, B², C², and D² are significant for this model. However, the P-values greater than 0.1000 indicate the model terms are not significant; hence, the term insignificant for this model is only A². The Model F-value of 758.54 implies the model is significant. There is a large F-value that could only have a 0.01% chance to occur due to noise. Though, P-value for this model is very low (0.0001) proves the P-values terms less than 0.05 indicate the model is significant. If there are numerous insignificant model terms (not counting those required to support hierarchy), model reduction may enhance the model. Also, the Lack of Fit F-value of 1.94 implies that the Lack of Fit is not significant relative to the pure error that shows the model is compatible with the target and perfectness of the model. There is a 24.11% opportunity that a Lack of Fit F-value is this large could occur due to noise. Non-significant Lack of Fit is smoothly good in the general case; so, the model should be fit to the nearly actual circumstance of the design that displayed using stat-ease design of expert11.1.2.0 x64 software.

4.3.5.3. Diagnostic plot analysis of the model

From design expert of the diagnostic plot demonstrates a graphical representation of the model that helps the design to interpret the chance variation of the parameter's values. The normal plot of residuals as it was justified in Figure 4.7 from the normal probability plot, the residuals are following a normal distribution, and thus the residuals were approximated along a straight line confirming that the normality assumption was satisfied. Similarly, progress, for actual vs predicted diagnostic plot analysis. This indicates the selected quadratic polynomial model is good performance for the Cr(VI) adsorption examination (evaluation).

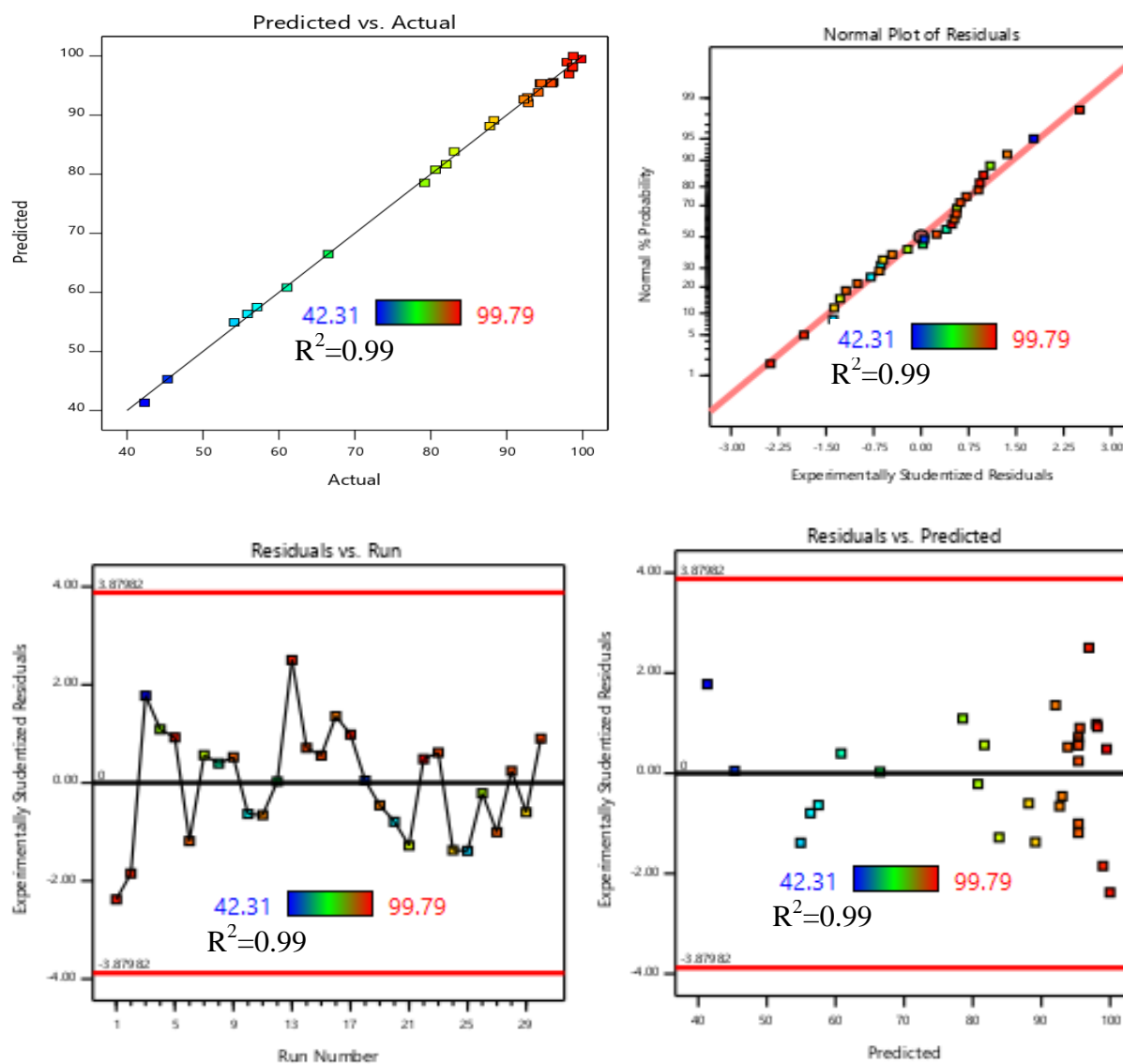


Figure 4. 7: Normal % probability versus residuals and predicted diagnostic plot analysis

These plots show that the close agreement between actual versus predicted and normal versus residual values are exhibited in Figure 4.7. Thus, the predicted values obtained by the model were very close to the experimental values and lie reasonably close to the calibrated curve of the model. Hence, the result outcomes indicate that the actual values were smoothly good agreement with the predicted values. Also, the other essential part of the diagnostic tool for confirming the adequacy of the fitted model for predicting the response is a residual versus predicted plot, which indicates the random scattering of the residuals. Here, in this assumption, residual means the difference between the value of actual results from experiments and the value of predicted results from the software. It checks for the assumption of constant variance that proves as there are no upward or downward pattern curves of the controlled bounded lines. Consequently, it also Figure 4.7 reveals that the residuals of the predicted values were randomly scattered on the plot, representing that the fitted values; therefore, it is an indication as there is no need for modification to minimize the personal error for the design model.

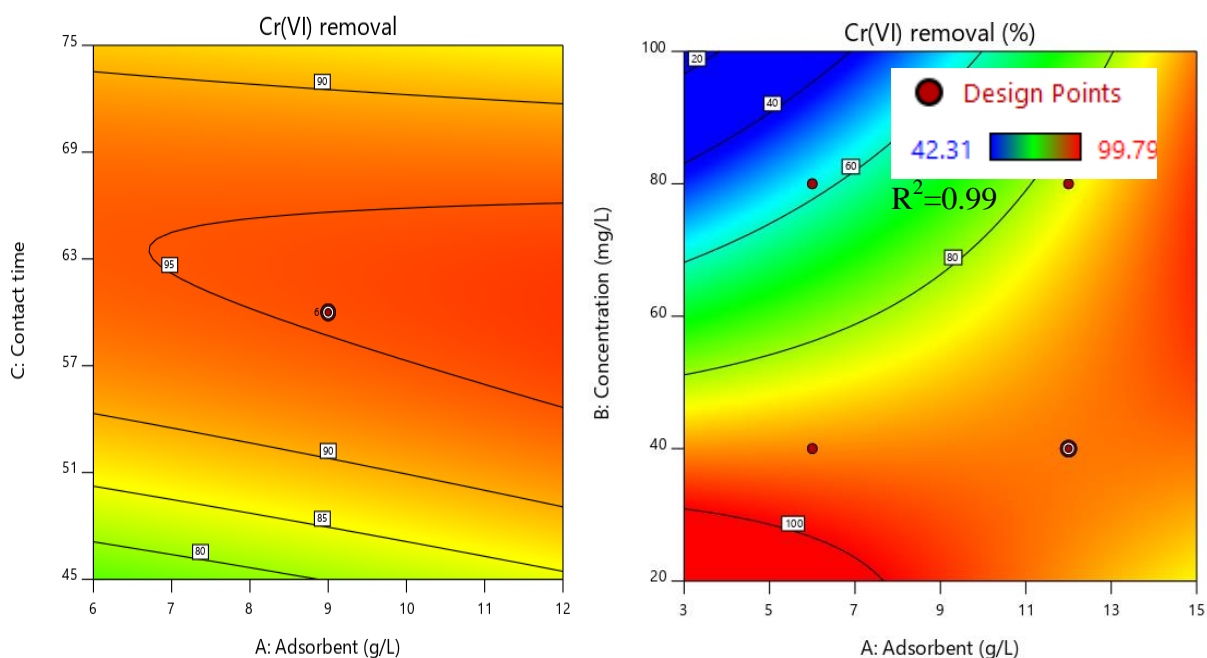
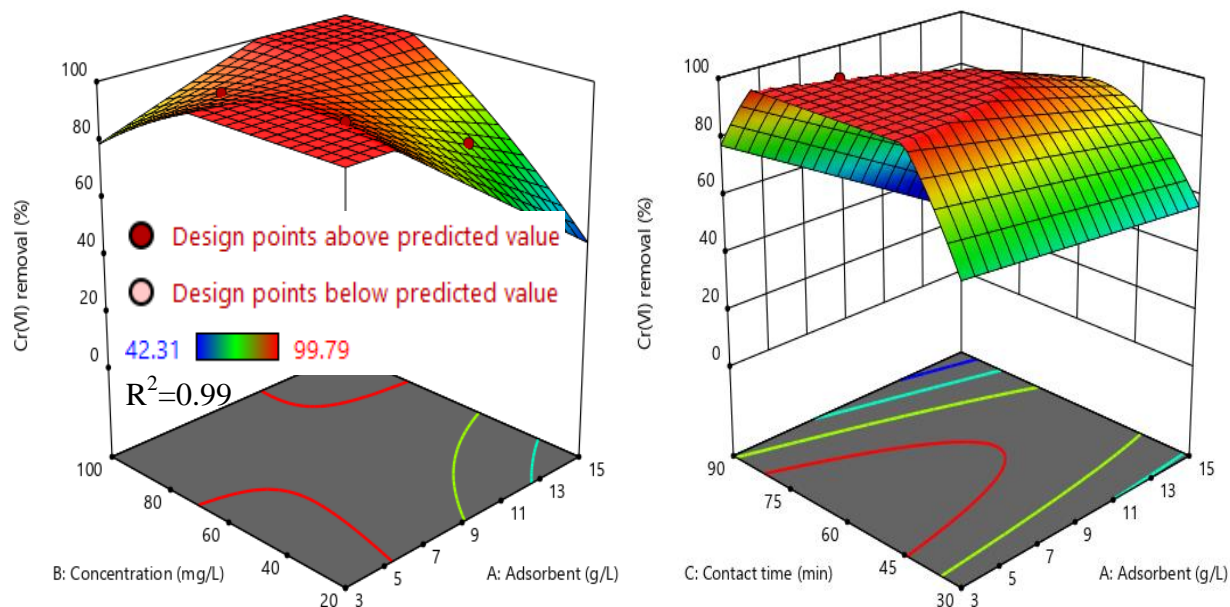


Figure 4. 8: Contour plot for the combined effect of adsorbent versus contact time, PH, and concentration of removal Cr(VI)

4.3.5.4. Interaction effect of process parameters for Cr(VI) removal

An interaction effect occurs if there is an interaction among the independent parameters that affect the dependent parameter target. In this study, it was found that the combined effect between initial Cr(VI) concentration and adsorbent dosage, adsorbent dosage and contact time, adsorbent dosage, and pH has a significant effect on the removal efficiency of Cr(VI) ions. Accordingly, the interaction effects between AB and AC have a significant effect on the Cr(VI) removal, followed by BC and then CD. Figure 4.9 Indicates the interaction effect of initial Cr(VI) concentration and contact time(C) to adsorbent dosage (A) on percentage removal of Cr(VI) ion. An increased residence time and adsorbent dosage resulted in increased percentage removal of Cr(VI) ions. Analogously, the increase in pH until the optimum conditions resulted in an increase in the removal efficiency of Cr(VI) ions. Conversely, an increased initial concentration of Cr(VI) retard the adsorption capacity or efficiency of the adsorption process.



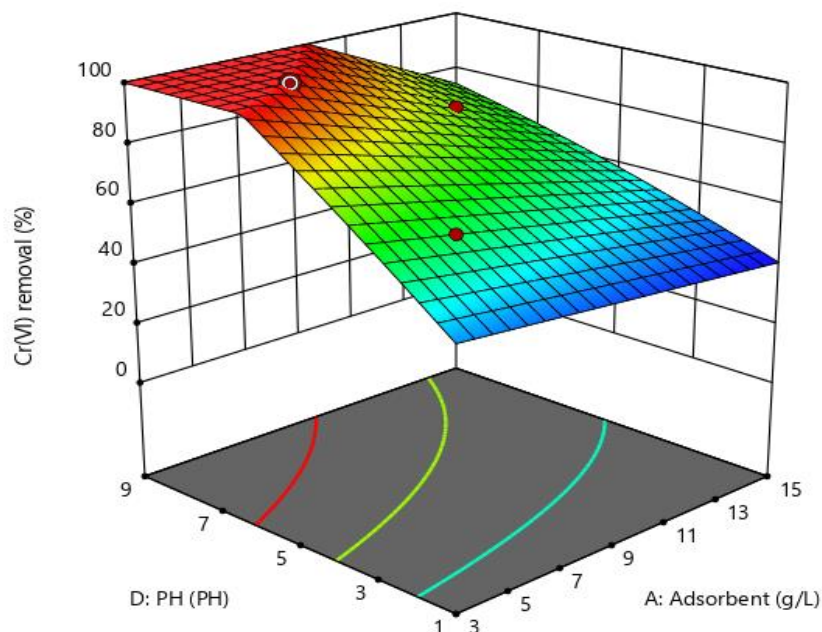


Figure 4. 9: Combined effect for a 3D plot of initial concentration, adsorbent dosage, PH, and contact time on Cr(VI) adsorption.

4.3.5.5. Generalized Final Model Equation in Terms of Coded Factors

The final model equation expressed in terms of coded factors can be used to make predictions about the response for manipulated levels of each factor. Arbitrarily, the high levels of the factors are coded as (+1) and the low levels are coded as (-1). The coded equation is purposeful for determining the relative influence of the parameters by balancing the factor coefficients as shown in the following Equation (4.1). Thus, the quadratic model that relates the removal efficiency of Cr(VI) with the independent process, parameters were described by the second-order polynomial equation and the percentage removal of chromium as a function of independent parameters (coded variables).

$$Z = +95.39 + 1.35A - 3.27B + 3.40C + 2.50D + 6.34AB - 2.78AC - 2.70AD + 12.44BC - 4.78BD + 6.52CD - 2.02B^2 - 11.82C^2 - 0.5607D^2 \quad (4.1)$$

Also, the equation in terms of actual factors can be used to make predictions about the response for given levels of each factor that are exhibited in the following Equation (4.2). Here, the levels should be specified in the original units for each factor. This equation should not be used to

determine the relative impact of each factor because the coefficients are scaled to accommodate the units of each factor and the intercept is not at the center of the design space.

$$Z = +72.6013 + 1.29A - 2.3987B + 3.5095C + 2.8247D + 6.1057AB - 1.0617AC - 1.4507AD + 5.0415BC - 1.1194BD + 2.175CD - 1.0051B^2 - 6.0523C^2 - 0.1402D^2 \quad (4.2)$$

Where Z is the response value of adsorption efficiency and A, B, C, D are the coded levels that represent adsorbent dosage, initial concentration Cr(VI), contact time, and pH that are used as independent input variables of the batch adsorption process respectively. The above equation describes the influence of each independent variable (linear and squared) and interactive effects on chromium adsorption onto the TMESP of adsorbent. As it is shown on the above equation the initial Cr(VI) concentration (B) reduces the response because it has negative relation whereas the quantity of adsorbent added to the solution (A) had a robust effect on the efficiency of response.

4.3.6. Optimization of efficient removal of hexavalent chromium ions

The main purpose of RSM is an effective statistical technique and also a critical tool that is used for modeling and analyzing the effects of multiple parameters on the process. The major advantages of this technique are to minimize the number of experimental trials, calculate the complex interaction between the independent parameters with analysis and optimization as well as increase the performance of the existing design. Also, this statistical approach is more practical compared to conventional experimental work as it arises from experimental techniques which include interactive effects among the variables, and finally, it shows the overall effects of the variables on the process. Also, the RSM technique is a popular tool in process optimization that determine the optimum settings of the control variables that result in a maximum (or a minimum) response over a certain region of interest. In the DOE numerical optimization, the possible goals are maximizing, minimizing, target, in range, and set to an exact value (factors only). Therefore, in the present study, the desired goal for each factor as well as for the response function was selected from the menu. Weight is usually assigned to each goal to adjust the shape of the specific desirability function. The goals are then combined to a total desirability function. Desirability is an objective function that could normally found between zero and one for all given response. A desirability value of one represents the ideal case while a zero indicates that one or more responses fall outside the desirable limits and the numerical optimization identifies a

point that was maximizing the desirability function to approach one magnitude as observed in Figure 4.10. The possibility of finding the best local maximum can generally be increased by starting from several points in the design space (Bayuo *et al.*, 2020).

Table 4. 6: Optimization solution after criteria is justified

Variables	Ultimate goal	Range of determined parameters		
		Lower limit	Upper limit	Importance
Adsorbent dose (g)	Is in range	6	12	3
Initial concentration Cr(VI) ion (ppm)	Is in range	40	80	3
Contact time (min)	Minimize	45	75	3
PH	Is in range	3	7	3
%Removal of chromium	Maximize	42.31	99.79	3

To verify the optimization results, an experiment was performed under predicted parameters conditions using the developed model. The model predicted 98.96% Cr (VI) removal of efficiency based on the allocated variables in Table 4.6. The experimental result value at these conditions was 95.15% and is nearly compatible with the result obtained from the DOE model output hence it indicating the high reliability of the model and proves validated the findings of the optimization. The absolute relative error of percentage from experimental and predicted values was nearly negligible (4%). Thus, this model has been confirmed as 96 percent confident.

Table 4. 7: Optimum conditions and model validation

Optimum Variables	Optimum results
Adsorbent dose (g)	6
Initial concentration Cr(VI) ion (mg/l)	40
Contact time (min)	45
PH	7
Predicted %removal of Cr(VI)	98.9642%
Experimental % removal of Cr(VI)	95.15%
Desirability	0.993

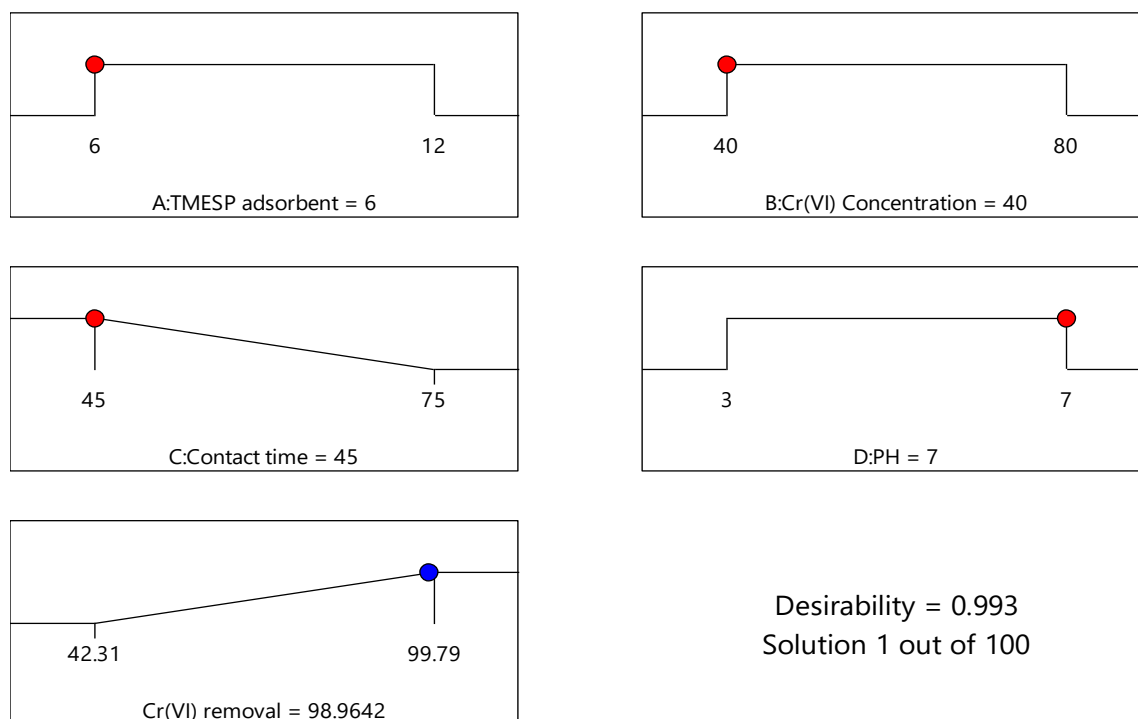


Figure 4. 10: Desirability ramp for the optimization of the parameters with its predicted response

4.4. Regeneration and reusability study for synthesized TMESP- adsorbents

Desorption process of hexavalent chromium adsorbate from a surface of AHESP adsorbent study was accomplished for investigation of adsorbents' reusability and regeneration is an important role to maintain the stability of the adsorbent as well as for environmental and economic purposes. Because, ones used adsorbent that filtered by using 55mm \emptyset and 11 μ m pore size (particle size) what man filter paper with a help of vacuum filtration were collected, and recovered after some treatment; hence, the regenerated adsorbent was determined in adsorption-desorption cycles to justify the reusability and facile of the synthesized termite mound-chicken eggshell adsorbent. In this investigation the results observed as it has good performance for removing hexavalent chromium regeneration and its final concentration (C_e) is not much significant different from cycle to cycle 1.49, 2.05, 2.38, 4.48, 5.92mg/L respectively within five cycles and demonstrated in Table C5 and Figure 4.11. The desorption was successfully accomplished with greater than 85% Cr(VI) ions removal efficiency after five cycles. This part of the investigation was justifies the attribute of adsorbent robustness, less sensitive to uncertainties process parameters like collision and rubbing within aqueous solution.

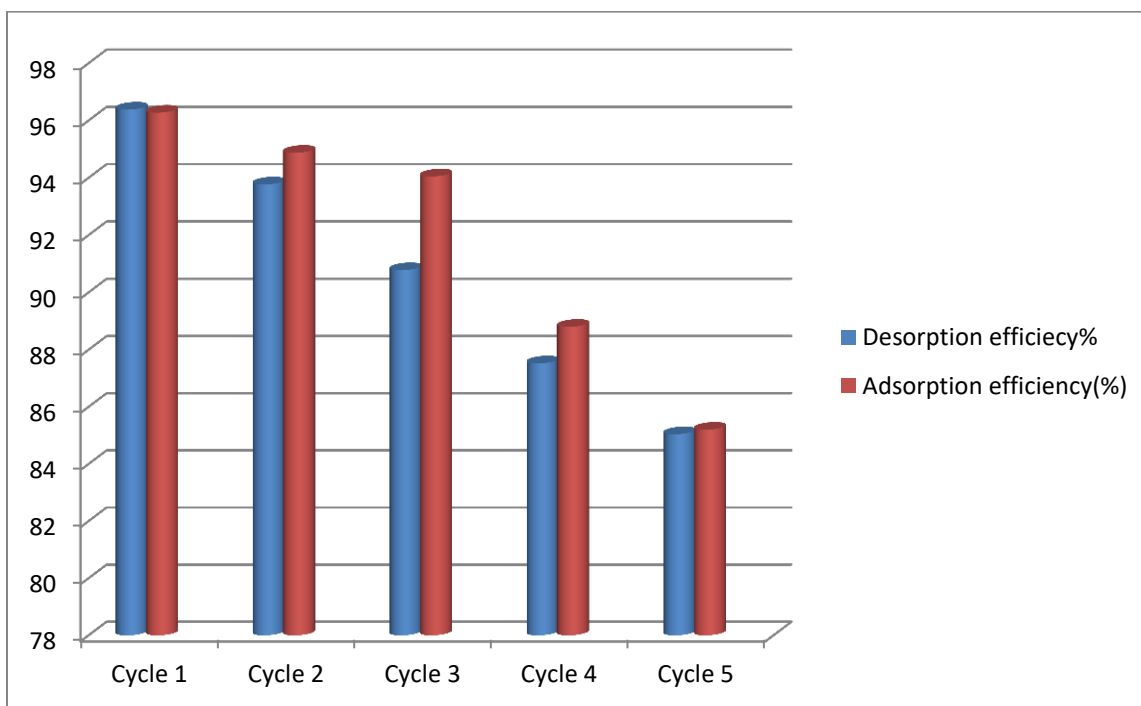


Figure 4. 11: Graphical expression of desorption versus adsorption efficiency comparative

4.5. Studies of removal efficiency based on pre-determined factors

4.3.5.1. Effect of the pH solution on Cr(VI) removal

The hexavalent chromium ions adsorption from an aqueous solution using synthesized TMESP accomplishment was dependent on the pH-value of the solution. The dependency of metal uptake on pH is related to both the ionization state of the functional groups on sorbent and the metal chemistry of the solution. In reverse to Kumar *et al.* (2017) investigation using rice straw, this study Figure 4.12 & Table B4 indicated that the removal percentage of Cr(VI) ions increased with increased pH ranges from 90 to 98.28% simultaneously the capacity load of Cr(VI) reveal the same trend. This was because the point of zero charges of the surface of TMESP adsorbent was at 7.6. The negatively ionic adsorption process is preferred at a pH less than the pH point of zero charges and vice versa. Similar to Ipeaiyeda & Tesi (2014) justification during the study of eggshells adsorbent to remove Pb, Ni, Mn, Zn, and Co metals the sorption was increased with an increase in pH from 4 to 7. The rate of sorption at pH 7 was extremely higher than at another pH

of standards. Beyond pH 7 there is not much significant increase in its removal capacity because of the repulsion of like charges principles (Ipeaiyeda & Tesi, 2014).

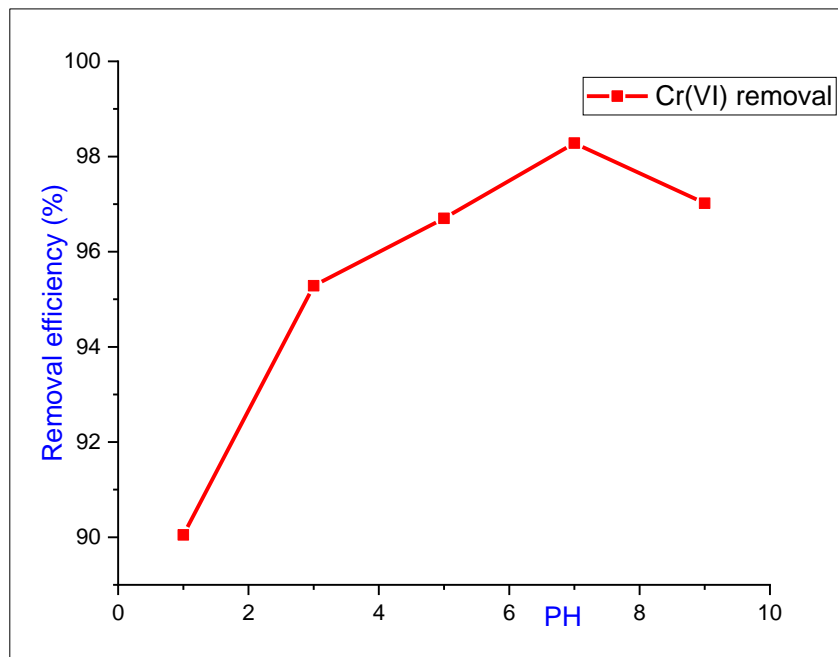


Figure 4. 12: Effects of PH on Cr(VI) removal efficiency for TMESP-adsorbent

4.5.2. Effect of adsorbent dosage on Cr(VI) removal

Adsorbent dosage influences were investigated using experimental values of captured chromium at ambient temperature quantifying amounts from 0.1 to 1.5gram ranges of synthesized termite mound-chicken eggshell powder sample, when the other adsorption parameters like contact time, pH, and initial concentration were fixed to the center point of adsorption that agitated with 150rpm speed. After batch adsorption was accomplished in a Jar test the homogenized solution was filtered by using 55mm diameter with $11\mu\text{m}$ pore size What man filter paper that supported by vacuum filtration and analyzed the residual Cr(VI) concentration within the solution using UV-spectrophotometer. As observed below the graph the efficiency of Cr(VI) ions adsorption versus adsorbent used increases from 76.8% to 98.92% against the adsorbent dosage employed 0.1 to 1.5g/100mL, The Figure 4.13 reveals that the amounts of metal ions removal increase with an increase in the quantity of with eggshell adsorbent at an initial metal ion concentration of 60 mg/L. Since the study of Yusuff (2017) proof or determine that the mixing proportion of termite

mound with eggshell mixture has no significant effect on adsorption capacity and morphological property of the mixture adsorbent one to one ratio is detailed scrutinized in this thesis.

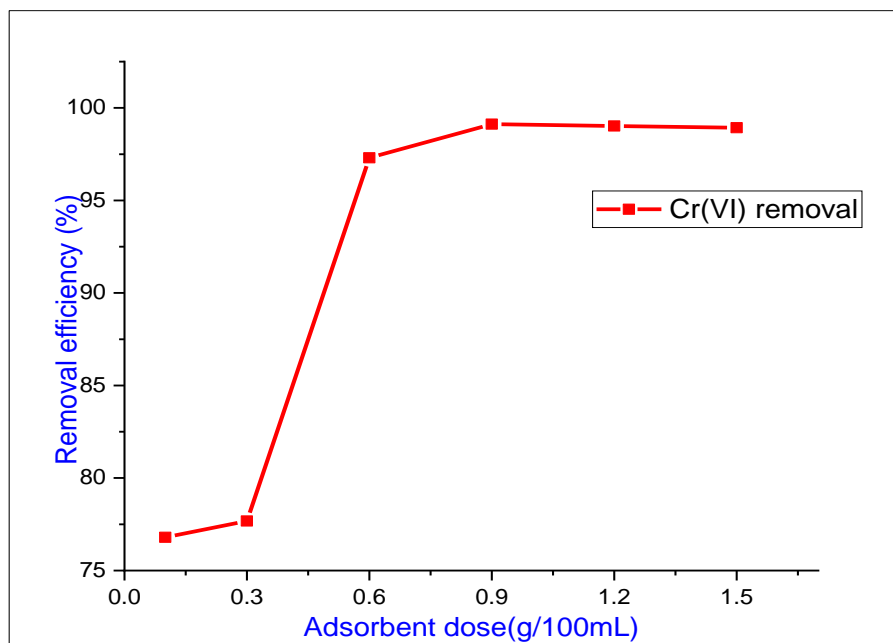


Figure 4. 13: Effects of adsorbent dose on chromium removal at center point condition

4.5.3. Effect of initial Cr(VI) ion concentration

The effect of initial Cr (VI) concentrations studied in this paper ranging from 10 to 100 mg/L on adsorption while keeping other parameters as constant like adsorbent dosage, pH of the solution, and contact time of, 6g/L, 7PH, and 45minute respectively. As Ipeaiyeda & Tesi (2014) states the initial concentration of metal ions provides an essential force to overcome all mass transfer resistances of the metal ions between the aqueous and solid phase. Based on this perspective at the initial stage, because of extreme dilution of chromium ion, it allows to freely moving within a medium of agent for binding to the active site of synthesized termite mound-chicken eggshell adsorbent hence its removal efficiency is not significantly influenced. However, logically as metal ions increase in the adsorption process binding to the fixed available active site of the adsorbent becomes occupied; so, it leads to adsorption loading capacity increase from 1.6 to 15.34mg/g and efficiency decrease from 98.6 to 92.05% that proves the negative effect of Cr(VI) concentration as stated in Equation (4.1). This concept illustrated in Figure 4.14 and Table B3

represents saturation of active sites found on TMESP adsorbent for interaction with contaminants favorable at low concentration of Cr(VI) that fit the abundant active sites and vice versa when the concentration of Cr(VI) is raised.

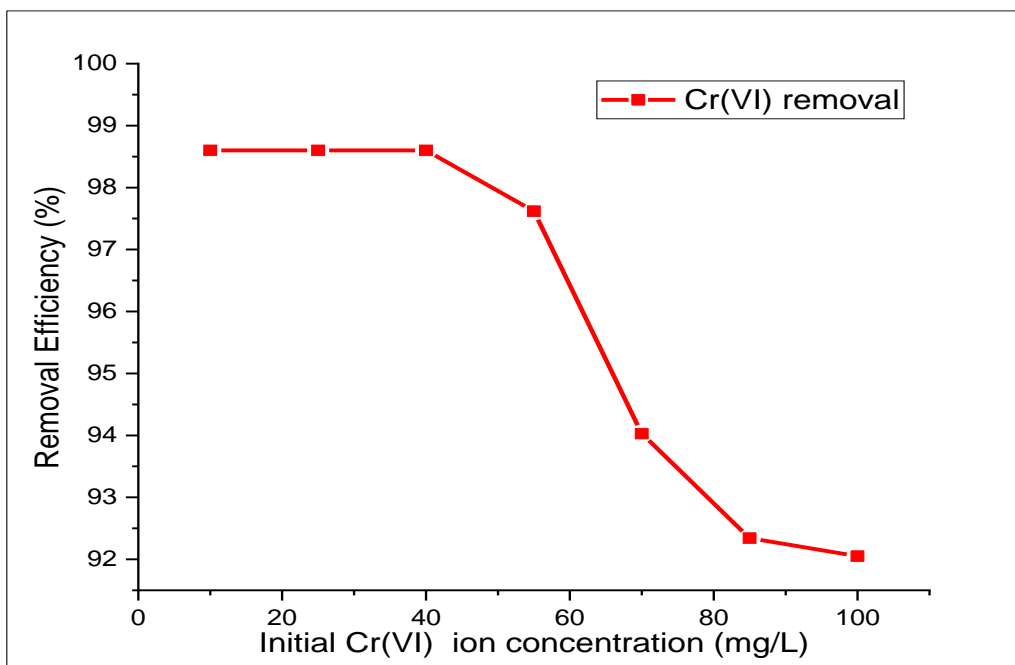


Figure 4. 14: Effect of Cr(VI) concentration at the optimum point of parameters

4.5.4. Effects of contact time

Time dependence batch adsorption process was examined by varying the contact time between the surface adsorbents and the adsorbates. These effects of contact time for adsorption investigated in this thesis ranges 10 to 90minutes at optimum PH, initial Cr(VI) concentration, adsorbent dosage, 7pH, 40mg/L, 0.6g respectively. In this study the influence of contact time on Cr(VI) removal using synthesized termite mound-chicken eggshell adsorbent sharply increase from 10 to 50minute as depicted graphically in the following Figure 4.15. However, this impact of contact time becomes stable from 60minutes to the maximum allocated time. This tipping point to become a stability of adsorption efficiency is termed as equilibrium time of adsorption.

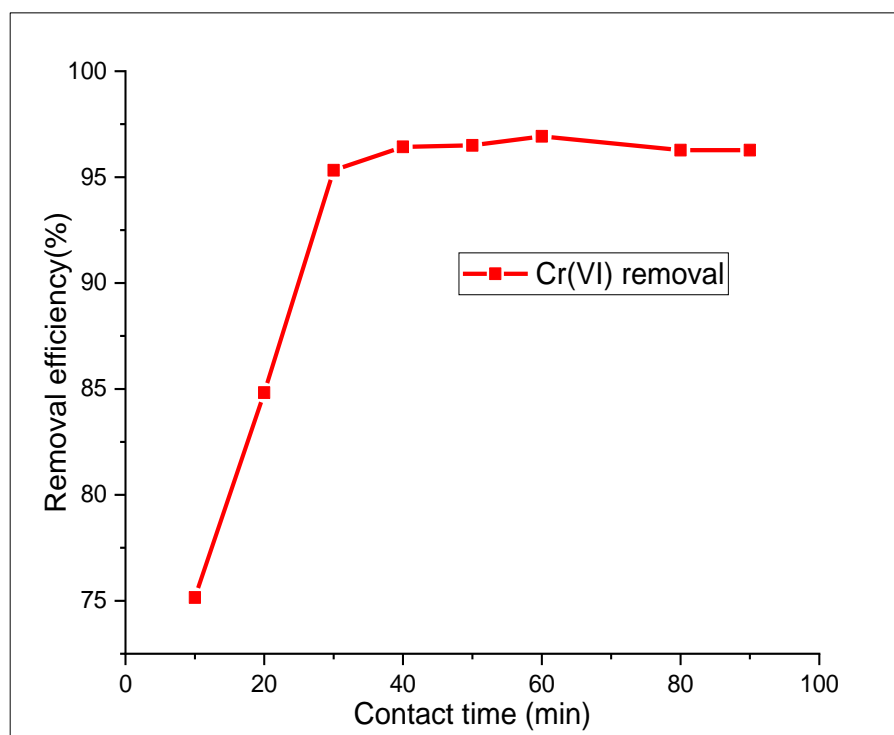


Figure 4. 15: Effects of contact time for Cr(VI) adsorption

4.5. Determination of point of zero charge

The point of zero charges of adsorbent has specified the area of detection for a particular adsorbent at a unique pH value, thus the charge on the surface of a specific adsorbent becomes zero. The graphs of change pH versus initial pH were drawn and used to determine the points at which the initial pH was equal to the final pH and that point was taken as the pH_{pzc} of the adsorbent (Xiao & Thomas, 2004). Figure 4.16 indicates the result of the pH of point of zero charges (PH_{pzc}) of TMESP-adsorbent was determined by a salt solution method. Accordingly, the PH_{pzc} of TMES adsorbent was measured after two days conducting at ambient temperature shaker the change of surface character of the synthesized adsorbent under varying pH values and was determined to be 7.6pH. This shows that the surface of TMESP is positively charged at solution pH < PH_{pzc}, however, at solution pH > PH_{pzc}, the surface of TMESP becomes negatively charged. Therefore, there is high adsorption of Cr(VI) when the pH of the solution is below PH_{pzc}. This indicates that Cr(VI) was found to negatively charge in an aqueous medium

termed as hydrochromate (HCrO_4^{-1}) (Tanhaei *et al.*, 2020). The idea also elaborated by Yosuff (2019) based on the capacity adsorption of Cr(VI) using *Leucaena leucocephala* seed pod activated carbon is favorable at pH value higher than PH_{pzc} , while anion (HCrO_4^{-1}) adsorption is favored at PH values lower than PH_{pzc} . Extensively, as Bahador *et al.* (2021) explanation at very low pHs, the value of positive (+) charges on the adsorbent surface is high and since chromium ion also has a negative charge, an electrostatic interaction occurs between the adsorbers and the metal ion, resulting in increased efficiency.

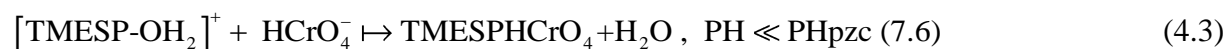


Table 4. 8: The point of zero charges of PH (PH_{pzc}) for TMESP adsorbent

PH_o	3	4	5	6	7	8	9	10	11	12
PH_f	5.587	6.042	6.498	6.625	7.204	7.911	8.892	9.784	10.394	10.957
ΔPH	-2.587	-2.042	-1.498	-0.625	-0.204	0.089	0.108	0.216	0.606	1.043

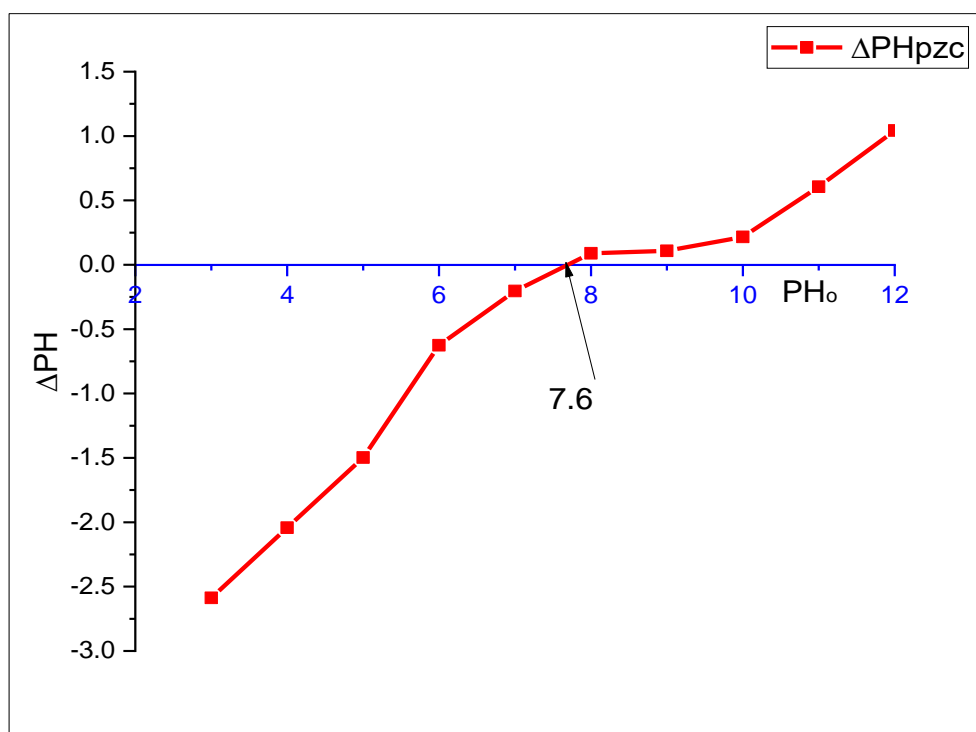


Figure 4. 16: Point of zero charges of PH for synthesized TMESP adsorbent

4.6. Adsorption isotherm studies

Adsorption isotherm was conducted experimental studies in the laboratory by varying initial Cr(VI) concentrations from 10-100 mg/L at room temperature using 100mL of distilled water with an adsorbent dose of 6g/L, shaking speed of 150rpm, the contact time of 45 minutes and pH of 7, and the experimental conduction results were depicted as follow allocated isotherm models equations. Also, this investigation demonstrates the relationship between the sorbate on the surface of the sorbents that is the number of species adsorbed per unit mass of sorbent, and the residual concentration of solute left within the solution. The adsorption behavior among the TMESP and Cr(VI) ions under different concentrations was interpreted by Langmuir, Freundlich, and Temkin isotherms model with their calibration graph respectively. The results given in Table C1 illustrate the experimental data that determine whether Langmuir, Freundlich, and Temkin model is the dominant adsorption isotherm model for TMESP adsorbent. Concerning this, as observed from Table 4.9 the best-fitted correlation data was obtained with the Freundlich isotherm model (0.99725) analysis than the Langmuir and Temkin adsorption isotherm model (0.99428) and (0.866) respectively. Thus, it was best depicted the equilibrium data of the sorption processes that indicate the adsorption of Cr(VI) ions on the surface of the TMESP effectively undergo the multilayer adsorption through heterogeneous condition can exist than monolayer and homogeneous adsorption process of Cr(VI) ions process.

Table 4. 9: Langmuir, Freundlich and Temkin model parameters for the removal of Cr(VI)

Adsorbent	Freundlich isotherm model				Langmuir isotherm model				Temkin isotherm		
	K_F	$\frac{1}{n}$	R^2	Q_e	q_e	K_L	R^2	R_L	R^2	B	A
Value	1.431	0.99	0.997	9.697	7.234	2.4	0.994	0.04	0.866	349	1.08

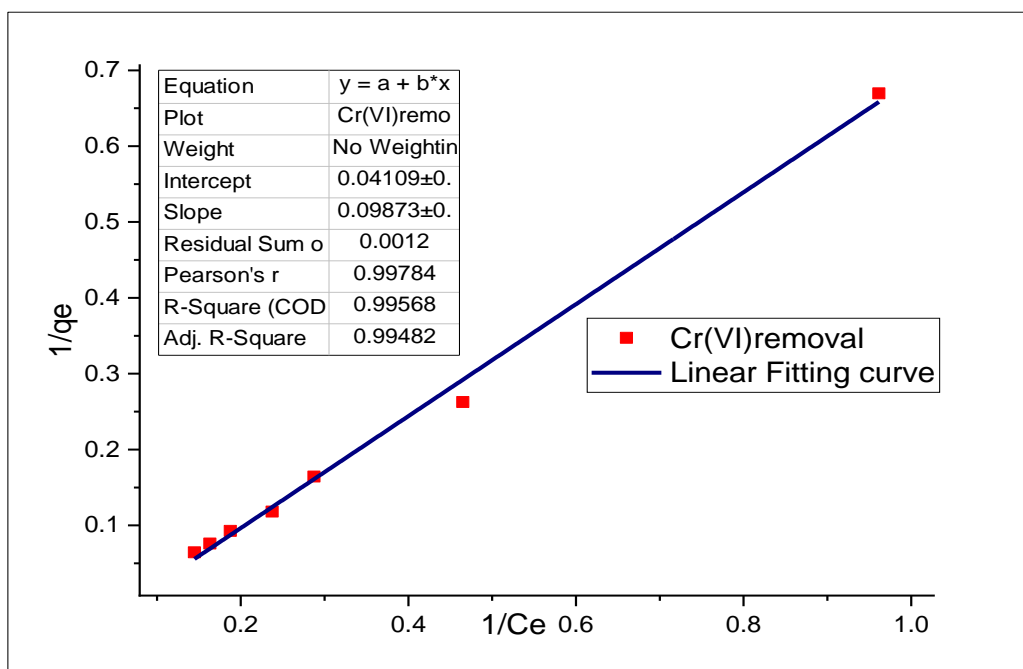


Figure 4. 17: Langmuir isotherm model at optimum parameters

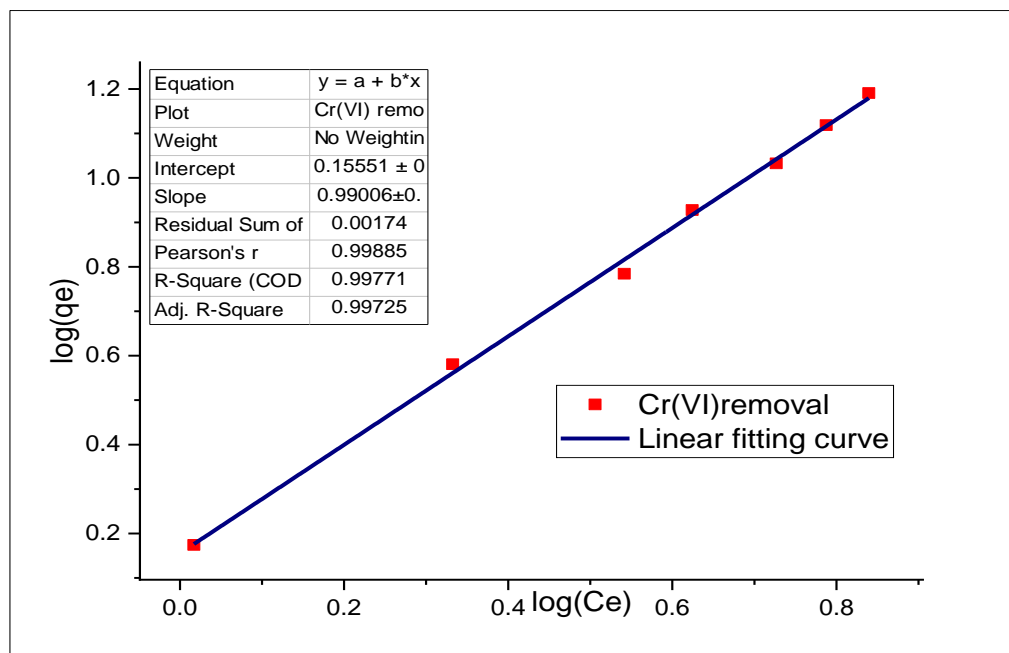


Figure 4. 18: Freundlich isotherm model at constant parameters used

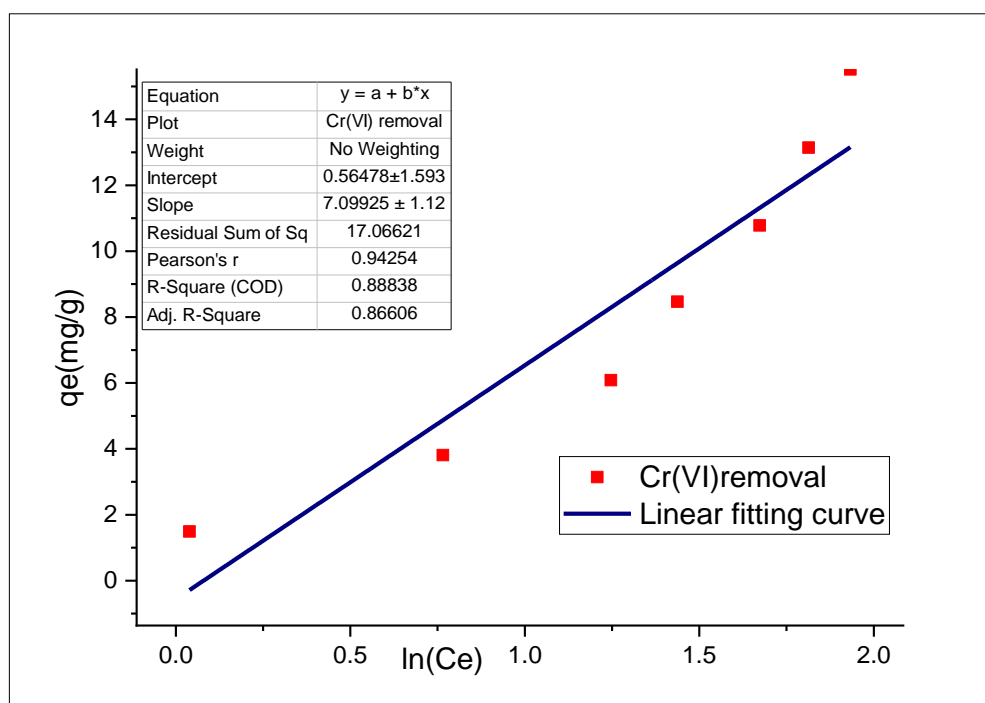


Figure 4. 19: Temkin isotherm model at constant parameters

Generally, these equilibrium graphs were obtained from experimental data that were accomplished at constant parameters like adsorbent dose, PH, contact time, the volume of dilution 6g/100mL, 7.0PH, 60minutes, and 100mL respectively. And based on their regression coefficient value obtained from the equilibrium curve that was generated from experimental investigation data, the Freundlich isotherm model best fits isotherm than Langmuir and Temkin isotherm model as summarized in Table 4.9 respectively. The favorability of Cr(VI) loading capacity of (R_L) for the adsorption process was also investigated in this portion of the study using Equation (3.16) obtained and calculated from the graph of the isotherms model. Hence, it was concluded that the more suitable one for the adsorption of Cr(VI) ions was the multilayer (Freundlich) isotherm model which is proved using a linear form of Equation(3.18) that indicates the distribution to active sites was heterogeneous on TMESP adsorbent surface. And based on the value of $1/n$ is less than one (0.99) that proves chemisorption's process (adsorption is a chemical process).

4.7. Adsorption kinetics studies

During experimental scrutinizing at laboratory conduction adsorption kinetics by changing contact time from 10-90minutes at room temperature using 100mL volume of dilution, 40 mg/L initial Cr(VI) solution with an adsorbent dose of 6g/L and PH 7, shaking speed of 150 rpm, and the experimental results were depicted based on adsorption kinetics models using pseudo-first-order, pseudo-second-order, and Intra particle diffusion models. Adsorption kinetics is important issue because it provides good information about the mechanism of the removal of adsorbate by the adsorbent, and more importantly, the kinetic study describes the influence of contact time on the purification of adsorbate as well as the rate of solute uptake at which adsorbate adsorbed from aqueous solution. Accordingly, as observed in Table B6 from the result of the adsorption rate of Cr(VI) on the surface of calcined TMESP-adsorbent was reached equilibrium at around 60 minutes with 96.93% of the Cr(VI) ions removed. The experimental data was demonstrated using pseudo-first-order, pseudo-second-order, intra-particle diffusion, and the experimental data fitted very well with pseudo-second-order than pseudo-first-order and intra-particle with a correlated coefficient of $R^2=0.9998$, $R^2=0.98982$ and $R^2= 0.5691$ respectively.

Table 4. 10: Data generated from the kinetics of adsorption TMESP-adsorbent models

Pseudo-first-order model			Pseudo-second-order model			Intra particle diffusion		
K_1 (min^{-1})	q_e	R^2	k_2 ($\text{g/mg}\cdot\text{min}$)	q_e	R^2	K_i	R^2	I
0.03449	1.1108	0.98982	0.14627	7.4733	0.9998	0.5757	0.5691	2.82885

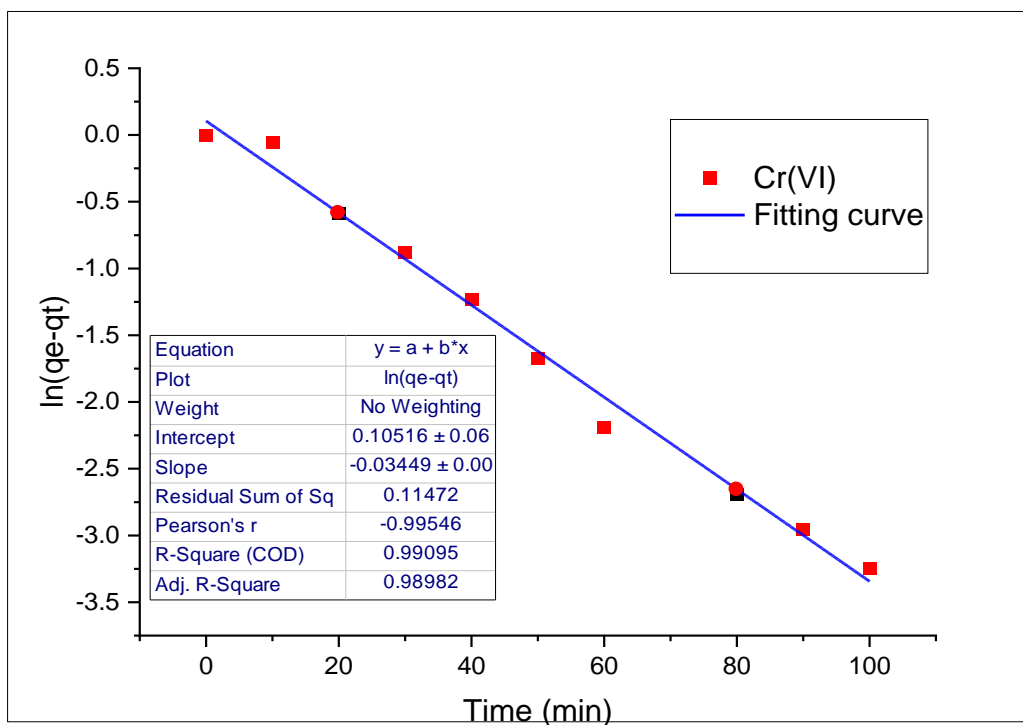


Figure 4. 20: Statistical analysis of pseudo-first-order kinetics model kinetic

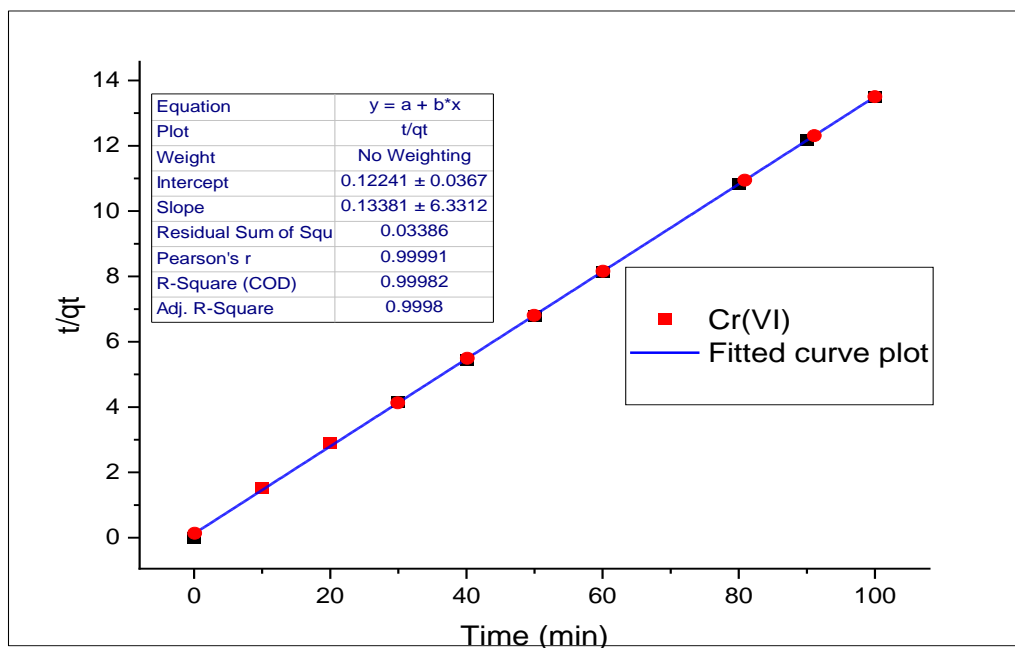


Figure 4. 21: Statistical analysis of pseudo-second-order kinetics model

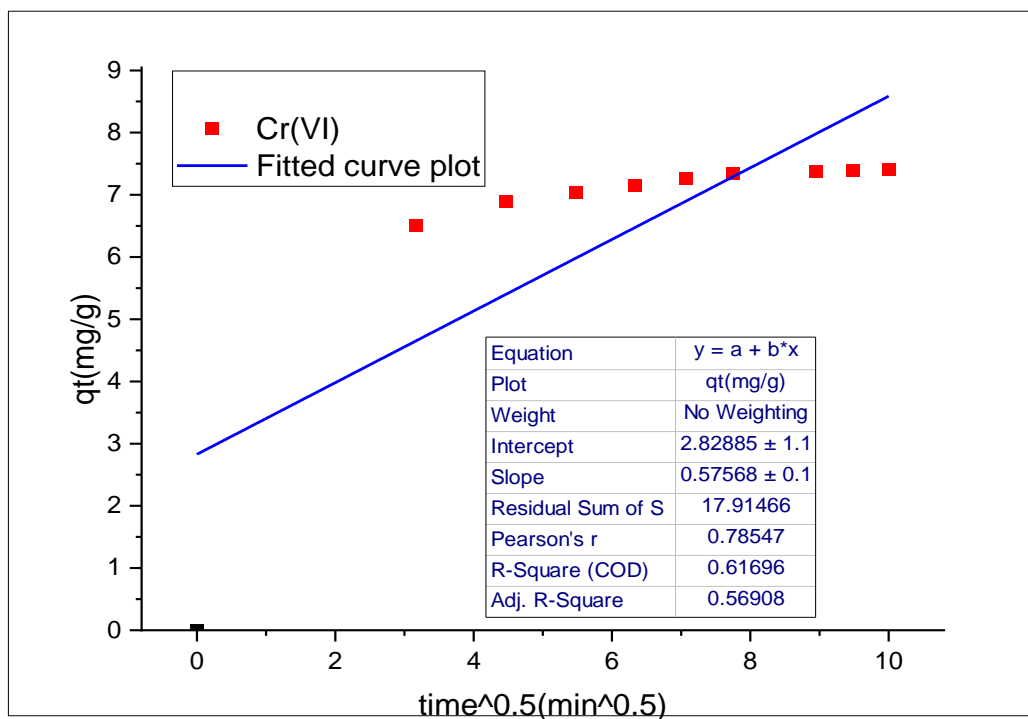


Figure 4. 22: Statistical analysis intraparticle diffusion kinetics model

These all adsorption kinetics models were determined the fitness based on their correlation coefficient (R^2 value) using experimental data generated from batch adsorption studies of TMESP adsorbent that sorb Cr(VI) ion adsorbate exist in liquid phase within pre-determined residence time. These correlation coefficients (R^2 value) and other parameters required using Equations (3.22 to 3.26) were calculated with a help of the respective above calibrated graphs and their value is referred to in Table 4.10. So, based on this correlation coefficient (R^2 value) the highest numerical value is the best fit model among others. That means, for this prediction model, the pseudo-second-order model is the best fit rather than the pseudo-first-order and intraparticle diffusion model for TMESP-adsorbent. And since the value of intercept (I) is different from zero in the intraparticle diffusion kinetics model that confirms as the boundary layer control.

4.8. Investigation of competitiveness of heavy metals to synthesized TMESP adsorbent

The adsorption of transitional metal ions from contaminated water solution as Xiao & Thomas (2004) justified also strongly influenced by competition of various aqueous metal ions to occupy the specified place of active sites of adsorbents, which decreases the removal efficiency of thermally activated materials for the metals of interest. The result of the presence of competitive ions (heavy metals) in an aqueous solution to the active site of the termite mound-chicken eggshell adsorbent as tabulated in Table 4.11 not much significantly affects the treatment efficiency of the targeted ion (hexavalent chromium). Their effect of affinity to adsorbent was ordered sequentially $Co > Pb > Ag > Zn > Ni > Cu$ based on quantitative value experimentally displayed from ultra-violet visible spectrophotometry for both their capacity and efficiency. Among these, copper, nickel, and chromium are proved by Matouq *et al.* (2015) during an investigation of trace metal ion removal from polluted water using Moringa pods and had almost the same optimum contact time 40 min, 30 min, and 40 min respectively that did not enhance the bio-sorption removal beyond these optimum value. Based on this, the optimum point is decided as appropriate parameters for this competitive investigation in this thesis paper. In another way according to Ipeaiyeda & Tesi (2014) explanation during the study of eggshells adsorbent to adsorb Pb, Ni, Mn, Zn, and Co metals, the sorption was increased with an increase in pH from 4 to 7. The rate of sorption at pH 7 was extremely higher than at another pH of standards. Beyond pH 7 there is not much significant increase in its removal capacity. However, for this termite mound- chicken eggshell adsorbent competitive metal ions study, the PH was fixed to the optimum value of PH even if its value is not contradicted to above stated by Ipeaiyeda & Tesi (2014) as the extreme value of a parameter.

Table 4. 11: Competitiveness of heavy metals to synthesized TMESP active site of adsorbent

Heavy metals	Absorbance (abs)	C_f (mg/L)	Efficiency (%)	Capacity (mg/g)
Cu(II) vs Cr (VI)	0.3854	5.46	86.35	5.7567
Ag (II) vs Cr (VI)	0.3510	4.89	87.78	5.8517
Pb (II) vs Cr (VI)	0.3488	4.86	87.85	5.8567
Ni (II) vs Cr (VI)	0.3818	5.40	86.50	5.7667

Zn (II) vs Cr (VI)	0.3702	5.21	86.98	5.7983
Co (II) vs Cr (VI)	0.3414	4.74	88.15	5.8767
Cr (VI) alone	0.2088	1.94	95.15	6.3433

At the center point of design (adsorbent dosage=0.6g/100mL, $C_i=40\text{mg/L}$, contact time=45minutes, and PH=7)

Also, as observed in the above Table 4.11 experimentally generated value recorded and calculated by using Equation (3.10) and (3.11) accordingly the presence of some heavy metals ion that fit for TMESP during Cr(VI) adsorption process has no significant influence on its capacity as well as its removal efficiency. Especially, its removal efficiency of adsorption was found almost the same in the range value of Table 4.2. To do this, the final concentration value of the same heavy metals found in a different form of a compound was taken their average and considered as single competitive heavy metal ion values.

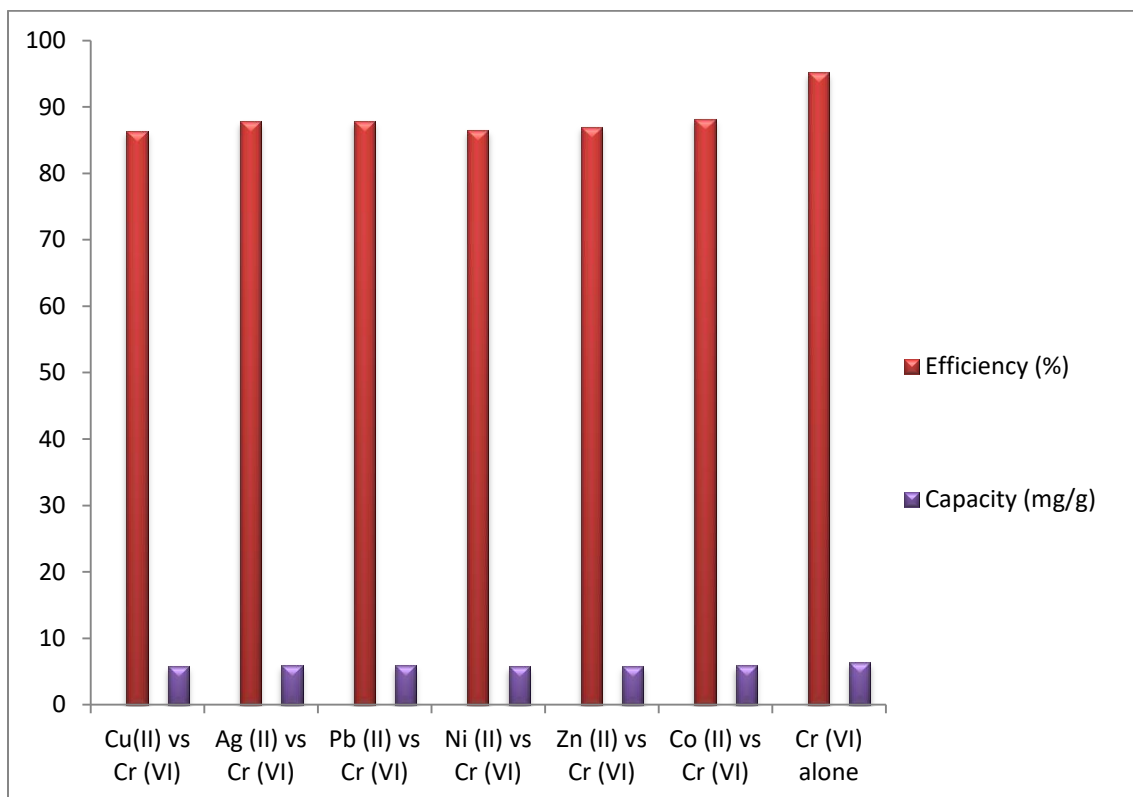


Figure 4. 23: Graphical demonstration of competitiveness heavy metals to TMESP-adsorbent

5. CONCLUSIONS AND RECOMMENDATION

5.1. Conclusion

In this thesis, the significant and adsorption behavior of synthesized TMESP adsorbent was successfully accomplished to remove Cr(VI) from an aqueous solution. The impact of adsorption parameters like adsorbent dose, contact time, PH, and initial concentration of Cr(VI) on efficiency and capacity to remove from aqueous solution using batch mode of experiments was worthily investigated. The characterization of the calcined TMESP adsorbent was performed using XRD, FT-IR, TGA, and UV-vis analysis technique in addition to those proximate analyses. From XRD determination the average crystallite size value was obtained to 26.69nm using origin software analysis; while the residual Cr (VI) ion concentration within the solution after adsorption was recorded from UV-visible spectrophotometry reading. Effects of different parameters such as contact time, pH, amount of adsorbents, and initial Cr (VI) concentration were depicted using RSM design techniques. Also, in this investigation, the adsorption process of Cr (VI) from an aqueous solution using TMESP adsorbent was optimized with the help of design expert CCD method. Based on this technique, the optimum adsorption independent factors of analysis: were displayed to 6g/L, 40 mg/L, 7.0PH, and 45minutes for adsorbent dose, Cr(VI)ion concentration, pH, and contact time respectively from the suggested quadratic model. At these optimum process parameters, the average experimental removal efficiency of Cr(VI) was obtained 95.15% which significantly confirmed to the suggested model. In this process, the adsorption isotherm and kinetics data were well predicted to Freundlich isotherm and pseudo-second-order model respectively that had the highest correlated coefficient. During reusability of TMESP adsorbent studying in experiment desorption by using 1.0MNaOH treatment of adsorbent become above 85% of Cr(VI) removal efficient after five times repetition. In this paper also the competitiveness of Cr>Co>Pb>Ag>Zn>Ni>Cu of heavy metal ions to the active site of synthesized termite mound-chicken eggshell powder adsorbent was compared at optimum point parameters. Generally, this thesis reveals that TMESP adsorbent is good promising for Cr(VI) removal efficient, and environmentally friendly.

5.2. Recommendation

- Morphology as well as its crystallite and particle size distributions of termite mound-chicken eggshell-adsorbent should be investigated by using Scanning Electron Microscope (SEM) and Transmissions Electron Microscopy (TEM) analysis respectively.
- These embedded compositions of materials should be investigated for the purification of TSS, BOD, and COD for those familiar with different industrial applications polluted water concerning to their removal efficiency and capacity. In addition to these, it is also preferable if it will be tested for real industrial wastewaters to prove its industrial application.
- Their competitiveness to the active site of termite mound- chicken eggshell mixture adsorbent of different ions should be scrutinized by extending to other metal ions and also for non-metals in addition to heavy metals studied in this thesis.
- During batch adsorption variation of experimental parameters like thermodynamic properties of adsorption which incorporate temperature and agitation speed should be investigated to improve the adsorption efficiency and capacity.
- Also, to assure adsorption of TMESP adsorbent effectiveness for competitive ions of batch adsorption should be carried out at different experimental factors rather than only confined to the optimum point of PH, contact time and adsorbent dosage.

REFERENCES

- Abbas, B. F., Al-jubori, W. M. K., Abdullah, A. M., Sha, H., & Mohammed, M. T. (2018). *Environmental Pollution with the Heavy Metal Compound*. May 2019, 11(9),1-8. <https://doi.org/10.5958/0974-360X.2018.00743.6>
- Abraha, Gebrekidan, and M. (2009). No Title: Environmental impacts of Sheba tannery (Ethiopia) effluents on the surrounding water bodies. *short communication*, 23(2), 269–274.
- Acharyya, K., Schulte, S. W., & Herbst, E. (2020). The Effect of Chemisorption on the Chemical Evolution of Star-forming Regions. *The Astrophysical Journal Supplement Series*, 247(1), 4. <https://doi.org/10.3847/1538-4365/ab6599>
- Aigbe, U. O., & Osibote, O. A. (2020). A review of hexavalent chromium removal from aqueous solutions by sorption technique using nanomaterials. *Journal of Environmental Chemical Engineering*, 8(6), 104503. <https://doi.org/10.1016/j.jece.2020.104503>
- Ajala, E.O., Eletta, O.A.A. , Ajala1, M.A. and Oyeniyi, S. K. (2018). www.azojete.com.ng. *characterization and evaluation of chicken eggshell for use as a bio-resource*, 14(1), 26–40.
- Alghamdi, A. A., Al-Odayni, A. B., Saeed, W. S., Al-Kahtani, A., Alharthi, F. A., & Aouak, T. (2019). Efficient adsorption of lead (II) from aqueous phase solutions using polypyrrole-based activated carbon. *Materials*, 12(12). <https://doi.org/10.3390/ma12122020>
- Ali, A., Saeed, K., & Mabood, F. (2016). Removal of chromium (VI) from aqueous medium using chemically modified banana peels as efficient low-cost adsorbent. *Alexandria Engineering Journal*, 55(3), 2933–2942. <https://doi.org/10.1016/j.aej.2016.05.011>
- Ali, H., Kim, K., Kumar, V., Kim, S., & Park, J. (2019). Nanomaterials-based treatment options for chromium in aqueous environments. *Environment International*, 130(April), 104748. <https://doi.org/10.1016/j.envint.2019.04.020>
- Azis, M. Y., Amedyan, N. N., Hanefiatni, & Suprabawati, A. (2021). Study of reducing Chromium (VI) to Chromium (III) ion using reduction and coagulation methods for electroplating industrial waste. *Journal of Physics: Conference Series*, 1763(1). <https://doi.org/10.1088/1742-6596/1763/1/012042>
- Badessa, T. S., Wakuma, E., & Yimer, A. M. (2020). Bio - sorption for effective removal of chromium (VI) from wastewater using Moringa stenopetala seed powder (MSSP) and

banana peel powder (BPP). *BMC Chemistry*, 1–12.

<https://doi.org/10.1186/s13065-020-00724-z>

Badrealam, S., Roslan, F. S., Dollah, Z., Bakar, A. A. A., & Handan, R. (2020). *Exploring the Eggshell from Household Waste as Alternative Adsorbent for Heavy Metal Removal from Wastewater*. 020077(October 2018).

Bahador, F., Foroutan, R., Esmaeili, H., & Ramavandi, B. (2021). Enhancement of the chromium removal behavior of Moringa oleifera activated carbon by chitosan and iron oxide nanoparticles from water. *Carbohydrate Polymers*, 251(August 2020), 117085.

<https://doi.org/10.1016/j.carbpol.2020.117085>

Bain, R., Johnston, R., Mitis, F., Chatterley, C., & Slaymaker, T. (2018). Establishing sustainable development goal baselines for household drinking water, sanitation and hygiene services. *Water (Switzerland)*, 10(12). <https://doi.org/10.3390/w10121711>

Bayuo, J., Abdullai, M., Kenneth, A., & Pelig, B. (2020). Desorption of chromium (VI) and lead (II) ions and regeneration of the exhausted adsorbent. *Applied Water Science*, 10(7), 1–6. <https://doi.org/10.1007/s13201-020-01250-y>

Bayuo, J., Abukari, M. A., & Pelig-Ba, K. B. (2020). Optimization using central composite design (CCD) of response surface methodology (RSM) for biosorption of hexavalent chromium from aqueous media. *Applied Water Science*, 10(6), 1–12.

<https://doi.org/10.1007/s13201-020-01213-3>

Beatriz, H., Peixoto, T., Araújo, D., Tait, D., Angélica, M., Dornellas, S., Barros, D., Guttierrez, R., & Bergamasco, R. (2020). Chitosan , alginate and other macromolecules as activated carbon immobilizing agents : A review on composite adsorbents for the removal of water contaminants. *International Journal of Biological Macromolecules*, 164, 2535–2549.

<https://doi.org/10.1016/j.ijbiomac.2020.08.118>

Berihun, D. (2017). Removal of Chromium from Industrial Wastewater by Adsorption Using Coffee Husk. *Journal of Material Science & Engineering*, 06(02), 6–11.

<https://doi.org/10.4172/2169-0022.1000331>

Bhaumik, R., Mondal, N. K., Das, B., Roy, P., Pal, K. C., Das, C., Banerjee, A., & Datta, J. K. (2012). Eggshell powder as an adsorbent for removal of fluoride from aqueous solution: Equilibrium, kinetic and thermodynamic studies. *E-Journal of Chemistry*, 9(3), 1457–1480.

<https://doi.org/10.1155/2012/790401>

- Billah, R. E. K., Haddaji, Y., Goudali, O., Agunaou, M., & Soufiane, A. (2021). Removal and regeneration of iron (Iii) from water using new treated fluorapatite extracted from natural phosphate as adsorbent. *Biointerface Research in Applied Chemistry*, *11*(5), 13130–13140. <https://doi.org/10.33263/BRIAC115.1313013140>
- Bisht, R., Agarwal, M., & Singh, K. (2015). *Removal of Chromium from Waste Water using Agricultural Waste : a Review. January.* <https://doi.org/10.1002/adsu.201934078>.
- Brema, S., & Selvarani, J. (2017). *Microfiltration Technology in Waste Water Treatment*. *9*(03), 47310–47312. <https://doi.org/10.1719/j.cej.2019.126359> .
- Chen, J., Hong, X., Zhao, Y., & Zhang, Q. (2014). Removal of hexavalent chromium from aqueous solution using exfoliated polyaniline/montmorillonite composite. *Water Science and Technology*, *70*(4), 678–684. <https://doi.org/10.2166/wst.2014.277>
- Chisanga, K., Ndakidemi, P. A., Mbega, E., & Komakech, H. (2017). The potential of anthill soils in agriculture production in Africa: A review. *International Journal of Biosciences (IJB)*, *11*(5), 357–377. <https://doi.org/10.12692/ijb/11.5.357-377>
- Dereje, T. M., Alemayehu, E., & Lennartz, B. (2021). Adsorptive removal of phosphate from aqueous solutions using low-cost volcanic rocks: Kinetics and equilibrium approaches. *Materials*, *14*(5). <https://doi.org/10.3390/ma14051312>
- Ekpete, O. A., Marcus, A. C., & Osi, V. (2017). Preparation and Characterization of Activated Carbon Obtained from Plantain (*Musa paradisiaca*) Fruit Stem. *Journal of Chemistry*, *2017*. <https://doi.org/10.1155/2017/8635615>
- Engelhardt, T. L. (2010). *Coagulation , Flocculation and Clarification of Drinking Water*. 1–57.
- Evbuomwan, B. O., & Sodje, J. O. (2020). *Characterization and Adsorptive Performance of Hen Feather and Eggshell as Non-Convectional Low-Cost Sorbents*. *4*, 232–238.
- Fufa, F., Alemayehu, E., & Lennartz, B. (2014). Sorptive removal of arsenate using termite mound. *Journal of Environmental Management*, *132*(5), 188–196. <https://doi.org/10.1016/j.jenvman.2013.10.018>
- Gangaraju, G., Uma, R., & Shah, K. J. (2021). *Chapter 1 Introduction to Conventional Wastewater Treatment Technologies : Limitations and Recent Advances* (Issue February).

<https://doi.org/10.21741/9781644901144-1>

- Garcia, F. H., Wiesel, E., & Fischer, G. (2013). The Ants of Kenya (Hymenoptera: Formicidae)—Faunal Overview, First Species Checklist, Bibliography, Accounts for All Genera, and Discussion on Taxonomy and Zoogeography. *Journal of East African Natural History*, 101(2), 127–222. <https://doi.org/10.2982/028.101.0201>
- Garud, R. M., Kore, S. V, Kore, V. S., & Kulkarni, G. S. (2011). A Short Review on Process and Applications of Reverse Osmosis. *Universal Journal of Environmental Research and Technology*, 1(3), 233–238.
- Genawi, N. M., Ibrahim, M. H., El-naas, M. H., & E. Alshaik, A. (2020). Chromium Removal from Tannery Wastewater by Electrocoagulation : Optimization and Sludge Characterization. *Water*, 12, 1–12. <https://doi.org/10.3390/w12051374>
- Ghorbani-Khosrowshahi, S., & Behnajady, M. A. (2016). Cr(VI) adsorption from aqueous solution by prepared biochar from Onopordom Heteracanthom. *International Journal*, 13(7), 1803–1814. <https://doi.org/10.1007/s13762-016-0978-3>
- Gucsik, A., Zhang, M., Koeberl, C., Salje, E. K. H., Redfern, S. A. T., & Pruneda, J. M. (2014). Infrared and Raman spectra of ZrSiO₄ experimentally shocked at high pressures. *Mineralogical Magazine*, 68(5), 801–811. <https://doi.org/10.1180/0026461046850220>
- Habib, G. (2018). *Application of Electrodialysis in Waste Water Treatment and Impact of Application of Electrodialysis in Waste Water Treatment and Impact of Fouling on Process Performance*. January. <https://doi.org/10.4172/2155-9589.1000182>
- Haddad, A. Z., Pilgrim, C. D., Sawvel, A. M., Hohman, J. N., & Gadgil, A. J. (2019). On the Conversion of Bauxite Ores to Highly Activated Alumina Media for Water Remediation. *Advanced Sustainable Systems*, 3(7), 1–12. <https://doi.org/10.1002/adsu.201900005>
- Hossain, M. N., Hossain, M. N., Rahaman, A., Hena, M. A., Khatun, A. A., & Matin, M. A. (2019). *Removal of chromium from tannery effluents using egg and snail shells*. February. <https://www.researchgate.net/publication/331011086>
- Ipeaiyeda, A. R., & Tesi, G. O. (2014). Sorption and Desorption Studies on Toxic Metals From Brewery Effluent Using Eggshell as Adsorbent. *Advances in Natural Science*, 7(2), 15. <https://doi.org/10.3968/5394>
- Islam, A., Angove, M. J., & Morton, D. W. (2019). Environmental Nanotechnology , Monitoring

- & Management Recent innovative research on chromium (VI) adsorption mechanism, 12(August), 100267. <https://doi.org/10.1016/j.enmm.2019.100267>
- Jafar, A., Wang, L., Waseem, H., Djellabi, R., Oladoja, N. A., & Pan, G. (2020). FeS @ rGO nanocomposites as electrocatalysts for enhanced chromium removal and clean energy generation by microbial fuel cell. *Chemical Engineering Journal*, 384(August 2019), 123335. <https://doi.org/10.1016/j.cej.2019.123335>
- Jain, D. S. M. C. K., & Yadav, A. K. (2016). *Removal of heavy metals from emerging cellulosic low-cost adsorbents : a review*. <https://doi.org/10.1007/s13201-016-0401-8>
- Joni.M. (2018). Characteristics of crystalline silica (SiO₂) particles prepared by simple solution method using sodium silicate (Na₂SiO₃) precursor, 5(3), 1–7. <https://doi.org/10.1088/1742-6596/1080/1/012006>
- Kale, A. V. B. A. S. (2017). Calcined eggshell as a cost effective material for removal of dyes from aqueous solution. *Applied Water Science*, 7(8), 4255–4268. <https://doi.org/10.1007/s13201-017-0558-9>
- Kannan A., & Thambidurai*S. (2008). removal of hexavalent chromium from aqueous solution using activated carbon derived from palmyra palm fruit seed. *Water Science and Technology*, 22(2), 183-196. <https://doi.org/10.2166/wst.2014.277>
- Kasozi, K. I., Namubiru, S., Kamugisha, R., Eze, E. D., Tayebwa, D. S., Ssempijja, F., Okpanachi, A. O., Kinyi, H. W., Atusiimirwe, J. K., Suubo, J., Fernandez, E. M., Nshakira, N., & Tamale, A. (2019). Safety of Drinking Water from Primary Water Sources and Implications for the General Public in Uganda. *Journal of Environmental and Public Health*, 2019, 12. <https://doi.org/10.1155/2019/7813962>
- Kassahun, S. K., Kiflie, Z., Shin, D. W., & Park, S. S. (2017). Photocatalytic Decolorization of Methylene Blue by N-doped TiO₂ Nanoparticles Prepared Under Different Synthesis Parameters. *Nanotechnol. J. Water Environ. Nanotechnol. J. Water Environ. Nanotechnol.*, 2(23), 136–144. <https://doi.org/10.22090/jwent.2017.03.001>
- Kavitha, B., & Thambavani, D. D. S. (2014). Physico-Chemical Characterization of Riverbed Sand from Mullai Periyar, Tamilnadu. *IPhysico-Chemical Characterization of Riverbed Sand from Mullai Periyar, Tamilnadu*, 7(9), 54–56. <https://doi.org/10.9790/5736-7915456>
- Khalifa, E. Ben, Rzig, B., Chakroun, R., Nouagui, H., & Hamrouni, B. (2019). Chemometrics

- and Intelligent Laboratory Systems Application of response surface methodology for chromium removal by adsorption on low-cost biosorbent. *Chemometrics and Intelligent Laboratory Systems*, 189(January), 18–26. <https://doi.org/10.1016/j.chemolab.2019.03.014>
- Khalil, U., Shakoor, M. B., Ali, S., Ahmad, S. R., Rizwan, M., Alsahli, A. A., & Alyemeni, M. N. (2021). Selective Removal of Hexavalent Chromium from Wastewater by Rice Husk: Kinetic, Isotherm and Spectroscopic Investigation. *Water*, 13(3), 263. <https://doi.org/10.3390/w13030263>
- Khan, T. A., Nazir, M., Ali, I., & Kumar, A. (2017). Removal of Chromium (VI) from aqueous solution using guar gum – nano zinc oxide biocomposite adsorbent. *Arabian Journal of Chemistry*, 10, S2388–S2398. <https://doi.org/10.1016/j.arabjc.2013.08.019>
- Kipsanai, J. J., Namango, S. S., & Muumbo, A. M. (2017). *A Study of Selected Kenyan Anthill Clays for Production of Refractory Materials*. 7(9), 169–179.
- Kristiansen, S. M., & Amelung, W. (2001). Abandoned anthills of *Formica polyctena* and soil heterogeneity in a temperate deciduous forest: Morphology and organic matter composition. *European Journal of Soil Science*, 52(3), 355–363. <https://doi.org/10.1046/j.1365-2389.2001.00390.x>
- Kuang, Y., Zhang, X., & Zhou, S. (2020). Adsorption of methylene blue in water onto activated carbon by surfactant modification. *Water (Switzerland)*, 12(2), 1–19. <https://doi.org/10.3390/w12020587>
- Kulkarni, S., & Kaware, J. (2014). Regeneration and Recovery in Adsorption- a Review. *International Journal of Innovative Science, Engineering & Technology*, 1(8), 61–64.
- Kumar, R., Arya, D. K., Singh, N., & Vats, H. K. (2017). Removal of Cr (VI) Using Low Cost Activated Carbon Developed By Agricultural Waste. *IOSR Journal of Applied Chemistry*, 10(01), 76–79. <https://doi.org/10.9790/5736-1001017679>
- Kunal, Rajput, S., & Yadav, S. (2019). Advanced Techniques for Wastewater Treatment : A Review. *Open Access Journal of Waste Management & Xenobiotics*, 2(3), 1–11.
- Kunowsky, M., Suárez-García, F., & Linares-Solano, Á. (2013). Adsorbent density impact on gas storage capacities. *Microporous and Mesoporous Materials*, 173, 47–52. <https://doi.org/10.1016/j.micromeso.2013.02.010>
- Labied, R., Benturki, O., Eddine Hamitouche, A. Y., & Donnot, A. (2018). Adsorption of

- hexavalent chromium by activated carbon obtained from a waste lignocellulosic material (Ziziphus jujuba cores): Kinetic, equilibrium, and thermodynamic study. *Adsorption Science and Technology*, 36(3–4), 1066–1099. <https://doi.org/10.1177/0263617417750739>
- Lee, Y., Ali, H., Kim, K., Kwon, E. E., Lee, M., Kim, J., Song, H., & Szulejko, J. E. (2019). Utilization of activated carbon as an effective replacement for a commercialized three-bed sorbent (Carbopack) to quantitate aromatic hydrocarbons in ambient air. *Environmental Research*, 179(October), 108802. <https://doi.org/10.1016/j.envres.2019.108802>
- Li, B., Huang, M., Fu, T., Pan, L., Yao, W., & Guo, L. (2012). Microfiltration process by inorganic membranes for clarification of TongBi liquor. *Molecules*, 17(2), 1319–1334. <https://doi.org/10.3390/molecules17021319>
- Linlin, D., Gao, P., Meng, Y., Liu, Y., Le, S., & Yu, C. (2020). Highly Efficient Removal of Cr(VI) from Aqueous Solutions by Polypyrrole / Monodisperse Latex Spheres. 5(Vi), 6651–6660. <https://doi.org/10.1021/acsomega.9b04438>
- Liu, J., Wu, X., Hu, Y., Dai, C., Peng, Q., & Liang, D. (2016). Effects of Cu(II) on the Adsorption Behaviors of Cr(III) and Cr(VI) onto Kaolin. *Journal of Chemistry*, 2016(Vi), 1–12. <https://doi.org/10.1155/2016/3069754>
- Liu, Q., Yang, B., Zhang, L., & Huang, R. (2015). Adsorptive removal of Cr(VI) from aqueous solutions by cross-linked chitosan/bentonite composite. *Korean Journal of Chemical Engineering*, 32(7), 1314–1322. <https://doi.org/10.1007/s11814-014-0339-1>
- Llitan, P. (2010). coagulation and flocculation treatment of wastewater in textile industry by using chitosan. *mohd ariffin abu hassan1, tan pei lil, zainura zainon noor1*, 4(1), 43–53.
- Lubello, C., Gori, R., Bernardinis, A. M. De, & Simonelli, G. (1998). *Ultrafiltration as tertiary treatment for industrial reuse*. 161–168.
- Maheshwari, U., & Gupta, S. (2015). Removal of Cr(VI) from wastewater using a natural nanoporous adsorbent: Experimental, kinetic and optimization studies. *Adsorption Science and Technology*, 33(1), 71–88. <https://doi.org/10.1260/0263-6174.33.1.71>
- Makuchowska, et al. (2019). Use of The Eggshells in Removing Heavy Metals from Waste Water - The Process Kinetics and Efficiency. *Ecological Chemistry and Engineering S*, 26(1), 165–174. <https://doi.org/10.1515/eces-2019-0012>
- Mandić, L., Sadžak, A., Erceg, I., Baranović, G., & Šegota, S. (2021). The fine-tuned release of

- antioxidant from superparamagnetic nanocarriers under the combination of stationary and alternating magnetic fields. *Antioxidants*, 10(8), 1–14.
<https://doi.org/10.3390/antiox10081212>
- Matouq, M., Jildeh, N., Qtaishat, M., Hindiye, M., & Al Syouf, M. Q. (2015). The adsorption kinetics and modeling for heavy metals removal from wastewater by Moringa pods. *Journal of Environmental Chemical Engineering*, 3(2), 775–784.
<https://doi.org/10.1016/j.jece.2015.03.027>
- McNeill, L., & Mclean, J. (2012). State of the Science of Hexavalent Chromium in Drinking Water. *Water Research Foundation*, May, 1-37,
<https://www.researchgate.net/publication/267845110>.
- Mhemed, A. H. (2018). A General Overview on the Adsorption. *Indian Journal of Natural Science*, 9(51), 16127–16131.
- Moradi, M., Fazlzadehdavil, M., Pirsahab, M., Mansouri, Y., Khosravi, T., & Sharafi, K. (2016). Response surface methodology (RSM) and its application for optimization of ammonium ions removal from aqueous solutions by pumice as a natural and low cost adsorbent. *Archives of Environmental Protection*, 42(2), 33–43. <https://doi.org/10.1515/aep-2016-0018>
- Nandiyanto, A. B. D., Oktiani, R., & Ragadhita, R. (2019). How to read and interpret ftir spectroscopy of organic material. *Indonesian Journal of Science and Technology*, 4(1), 97–118. <https://doi.org/10.17509/ijost.v4i1.15806>
- Nogueira, H. P., Toma, S. H., Silveira, A. T., Carvalho, A. A. C., Fioroto, A. M., & Araki, K. (2019). Efficient Cr (VI) removal from wastewater by activated carbon superparamagnetic composites. *Microchemical Journal*, 149(June), 104025.
<https://doi.org/10.1016/j.microc.2019.104025>
- Nur-E-Alam, M., Mia, M. A. S., Ahmad, F., & Rahman, M. M. (2020). An overview of chromium removal techniques from tannery effluent. *Applied Water Science*, 10(9), 1–22.
<https://doi.org/10.1007/s13201-020-01286-0>
- Ouyang, D., Zhuo, Y., Hu, L., Zeng, Q., Hu, Y., & He, Z. (2019). Research on the adsorption behavior of heavy metal ions by porous material prepared with silicate tailings. *Minerals*, 9(5), 1–16. <https://doi.org/10.3390/min9050291>
- Owalude, S. O., & Tella, A. C. (2016). Removal of hexavalent chromium from aqueous solutions

- by adsorption on modified groundnut hull. *Beni-Suef University Journal of Basic and Applied Sciences*, 5(4), 377–388. <https://doi.org/10.1016/j.bjbas.2016.11.005>
- Padmavathy, K. S., Madhu, G., & Haseena, P. V. (2016). A study on effects of pH , adsorbent dosage , time , initial concentration and adsorption isotherm study for the removal of hexavalent chromium (Cr (VI)) from wastewater by magnetite nanoparticles. *Procedia Technology*, 24(5), 585–594. <https://doi.org/10.1016/j.protcy.2016.05.127>
- Pham, X. H., Hahm, E., Kim, H. M., Son, B. S., Jo, A., An, J., Thi, T. A. T., Nguyen, D. Q., & Jun, B. H. (2020). Silica-coated magnetic iron oxide nanoparticles grafted onto graphene oxide for protein isolation. *Nanomaterials*, 10(1), 1–14. <https://doi.org/10.3390/nano10010117>
- Rai, M. K., Shahi, G., Meena, V., Meena, R., Chakraborty, S., Singh, R. S., & Rai, B. N. (2016). Removal of hexavalent chromium Cr (VI) using activated carbon prepared from mango kernel activated with H₃PO₄. *Resource-Efficient Technologies*, 2(3), S63–S70. <https://doi.org/10.1016/j.reffit.2016.11.011>
- Rajapaksha, A. U., Alam, M. S., Chen, N., Alessi, D. S., Igalavithana, A. D., Tsang, D. C. W., & Ok, Y. S. (2018). Removal of hexavalent chromium in aqueous solutions using biochar: Chemical and spectroscopic investigations. *Science of the Total Environment*, 625, 1567–1573. <https://doi.org/10.1016/j.scitotenv.2017.12.195>
- Rajendran, A. (2011). Extraction of Chromium from Tannery Effluents Using Waste Egg Shell Material as an Adsorbent. *British Journal of Environment and Climate Change*, 1(2), 443–452. <https://doi.org/10.9734/bjcecc/2011/262>
- Ramli, M., Rossani, R. B., Nadia, Y., Banta Darmawan, T., Febriani, Saiful, & Ismail, Y. S. (2019). Nanoparticle fabrication of calcium oxide (CaO) mediated by the extract of red dragon fruit peels and its application as inorganic-anti-microorganism materials. *IOP Conference Series: Materials Science and Engineering*, 509(1), 1–6. <https://doi.org/10.1088/1757-899X/509/1/012090>
- Raouf MS, A., & Raheim ARM, A. (2016). Removal of Heavy Metals from Industrial Waste Water by Biomass-Based Materials: A Review. *Journal of Pollution Effects & Control*, 05(01), 1–13. <https://doi.org/10.4172/2375-4397.1000180>
- Reta, J. G., Chamada, T. A., & Kasirajan, D. R. (2021). Calcium oxide nanoparticles synthesis

- from hen eggshells for removal of lead (Pb(II)) from aqueous solution. *Environmental Challenges*, 4(June), 100193. <https://doi.org/10.1016/j.envc.2021.100193>
- Rotimi, A., & Okeoghene, G. (2014). *Sorption and Desorption Studies on Toxic Metals From Brewery Effluent Using Eggshell as Adsorbent*. 7(2), 15–24. <https://doi.org/10.3968/5394>
- Saravanakumar, K., Karthik, R., Chen, S. M., Vinoth Kumar, J., Prakash, K., & Muthuraj, V. (2017). Construction of novel Pd/CeO₂/g-C₃N₄ nanocomposites as efficient visible-light photocatalysts for hexavalent chromium detoxification. *Journal of Colloid and Interface Science*, 504(June), 514–526. <https://doi.org/10.1016/j.jcis.2017.06.003>
- Sen, M., & Dastidar, M. G. (2010). *Review CHROMIUM REMOVAL USING VARIOUS BIOSORBENTS*. 7(3), 182–190. <https://doi.org/10.1815/j.scitotenv.2019.12.236>
- Shahmansouri, A., & Bellona, C. (2015). Nanofiltration technology in water treatment and reuse: Applications and costs. *Water Science and Technology*, 71(3), 309–319. <https://doi.org/10.2166/wst.2015.015>
- Silva, A., Yogafanny, E., & Fuchs, S. (2015). *Intermittent Slow Sand Filtration for Drinking Water Treatment in Developing Intermittent Slow Sand Filtration for Drinking Water Treatment in Developing Countries*. September. <https://doi.org/10.13140/RG.2.1.1828.1449>
- Silva, B., Neves, I. C., & Tavares, T. (2016). *A sustained approach to environmental catalysis : Reutilization of chromium from wastewater*. 46, 1622–1657.
- Simina, D., & Meghea, I. (2014). Comptes Rendus Chimie Mechanism of simultaneous removal of Ca²⁺, Ni²⁺, Pb²⁺ and Al³⁺ ions from aqueous solutions using Purolite 1 S930 ion exchange resin. *Comptes Rendus - Chimie*, 17(5), 496–502. <https://doi.org/10.1016/j.crci.2013.09.010>
- Singha, B., & Das, S. K. (2011). Biosorption of Cr(VI) ions from aqueous solutions: Kinetics, equilibrium, thermodynamics and desorption studies. *Colloids and Surfaces B: Biointerfaces*, 84(1), 221–232. <https://doi.org/10.1016/j.colsurfb.2011.01.004>
- Slopiecka, K., Bartocci, P., & Fantozzi, F. (2012). Thermogravimetric analysis and kinetic study of poplar wood pyrolysis. *Applied Energy*, 97(May), 491–497. <https://doi.org/10.1016/j.apenergy.2011.12.056>
- Sreedharan, S. (2018). *solvent extraction and adsorption*. june 2016. <https://doi.org/10.5121/civej.2016.3214>

- Stephen, N., Edmore, S., Netai, M.-M., & Munyaradzi, S. (2017). Comparative biosorption of Pb²⁺ ions from aqueous solution using *Moringa oleifera* plant parts: Equilibrium, kinetics and thermodynamic studies. *African Journal of Biotechnology*, 16(48), 2215–2231. <https://doi.org/10.5897/ajb2017.16066>
- Sumathi V. (2017). Optical Characterization of Calcium Oxide Nanoparticles. *International Journal of Advanced Technology in Engineering and Science*, 5(2), 63–67.
- Suresh, G., & Babu, B. V. (n.d.). Removal of Cr (VI) from Wastewater using Fly ash as an Adsorbent. *Chemical Engineering Birla Institute of Technology and Science (BITS), Pilani, Rajasthan, India*, 6(3), 1–10. <https://www.researchgate.net/publication/237426144>
- Tang, J., Myers, M., Bosnick, K. A., & Brus, L. E. (2013). Magnetite Fe₃O₄ nanocrystals: Spectroscopic observation of aqueous oxidation kinetics. *Journal of Physical Chemistry B*, 107(30), 7501–7506. <https://doi.org/10.1021/jp027048e>
- Tangahu, B. V., Sheikh Abdullah, S. R., Basri, H., Idris, M., Anuar, N., & Mukhlisin, M. (2011). A review on heavy metals (As, Pb, and Hg) uptake by plants through phytoremediation. *International Journal of Chemical Engineering*, 4(5), 31. <https://doi.org/10.1155/2011/939161>
- Tanhaei, B., Karimi, F., & Alizadeh, M. (2020). *Jo ur* (Issue Vi). <https://doi.org/10.1016/j.molliq.2020.115062>
- Tao, H., Hua, J., Sun, X., Hong, Y., Bo, Z., Rong, S., Weng, W., Xing, S., Xu, H., Bing, W., Shan, Y., Ming, F., & Huang, Y. (2015). NH₂-rich polymer / graphene oxide use as a novel adsorbent for removal of Cu (II) from aqueous solution. *chemical engineering journal*, 263, 280–289. <https://doi.org/10.1016/j.cej.2014.10.111>
- Teklay, A., Gebeyehu, G., Getachew, T., Yayneshet, T., & Sastry, P. (2018). Quantification of Solid Waste Leather Generation Rate from the Ethiopian Leather Sector - A Contributing Perspective to Waste Management Approach. *Innovative Energy & Research*, 07(02). <https://doi.org/10.4172/2576-1463.1000208>
- Thallapalli, B., & Prasad, S. (2016). *removal of chromium from wastewater using low cost removal of chromium from wastewater using low. September 2015.*
- Uwizeyimana, H., Wang, M., Chen, W., & Khan, K. (2017). The eco-toxic effects of pesticide and heavy metal mixtures towards earthworms in soil. *Environmental Toxicology and*

- Pharmacology*, 55(August), 20–29. <https://doi.org/10.1016/j.etap.2017.08.001>
- Wiesman, J. (2012). Stratified Sand Filter Treatment Systems Stratified Sand Filter Treatment Systems. *Stratified Sand Filter Treatment Systems*, 9(3), 1–30.
- Xiao, B., & Thomas, K. M. (2004). Competitive adsorption of aqueous metal ions on an oxidized nanoporous activated carbon. *Langmuir*, 20(11), 4566–4578. <https://doi.org/10.1021/la049712j>
- Yousef, R., Qiblawey, H., & El-Naas, M. H. (2020). Adsorption as a process for produced water treatment: A review. *Processes*, 8(12), 1–22. <https://doi.org/10.3390/pr8121657>
- Yusuff, Adeyinka S. (2019). Adsorption of hexavalent chromium from aqueous solution by *Leucaena leucocephala* seed pod activated carbon: equilibrium, kinetic and thermodynamic studies. *Arab Journal of Basic and Applied Sciences*, 26(1), 89–102. <https://doi.org/10.1080/25765299.2019.1567656>
- Yusuff, Adeyinka Sikiru. (2017). Research Article Preparation and Characterization of Composite Anthill-Chicken Eggshell Adsorbent: *Optimization Study on Heavy Metals adsorption using Response Surface Methodology*, 10(3), 12. <https://doi.org/10.3923/jest.2017.120.130>
- Yusuff, Adeyinka Sikiru. (2019). *optimization of the preparation conditions of an eggshell / anthill composite adsorbent using a central composite design*. 54(6), 1202–1214.
- Zeng, Y. (2016). *Fundamental Study of Adsorption and Desorption Process in Porous Materials with Functional Groups*. 10(3), 122. <https://doi.org/10.1019/i.srs.2013.09.00>.

APPENDIXES

Appendix A: Laboratory experimental setup

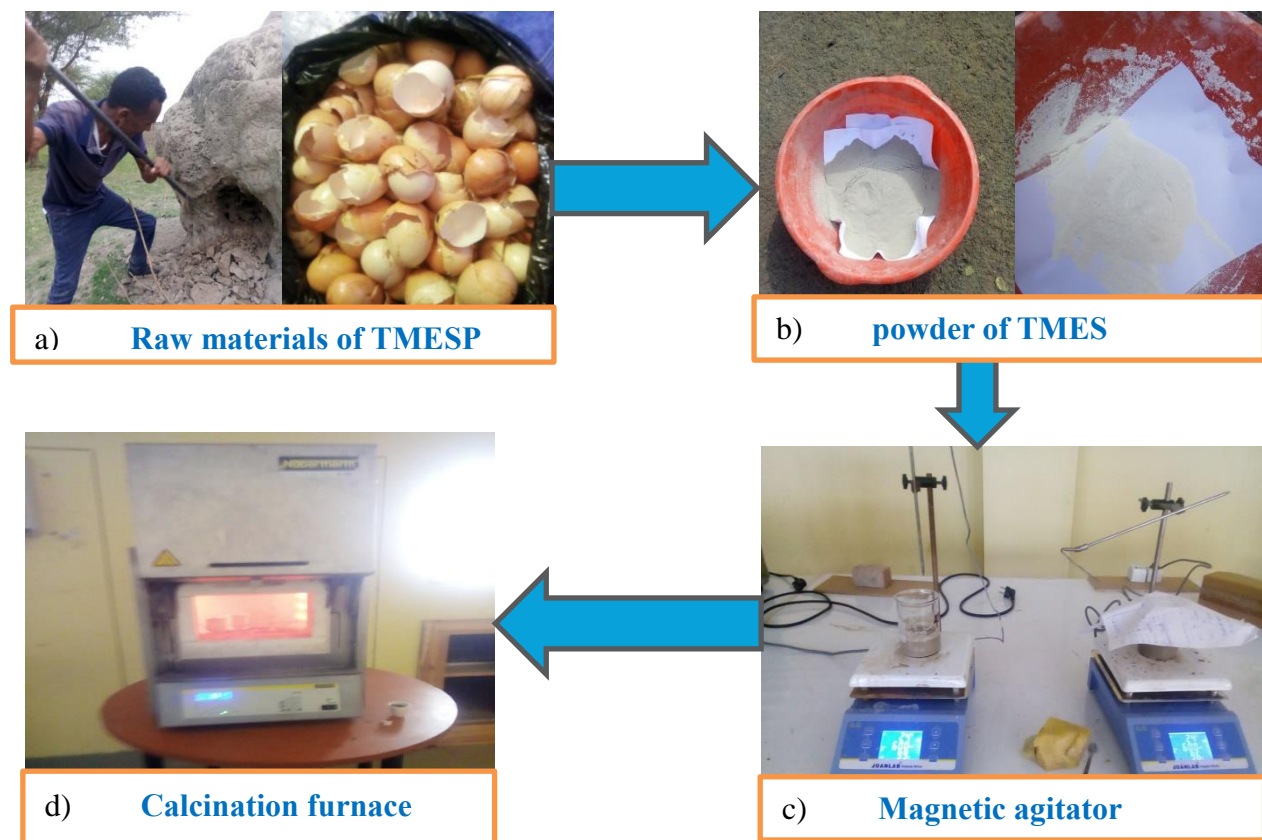


Figure A 1: Raw material collection and synthesizing of TMESP adsorbent



Figure A 2: Proximate analysis of ash for TM-ES raw materials before and after mixing



Figure A 3: Particle density for TMESP adsorbent using a pycnometer

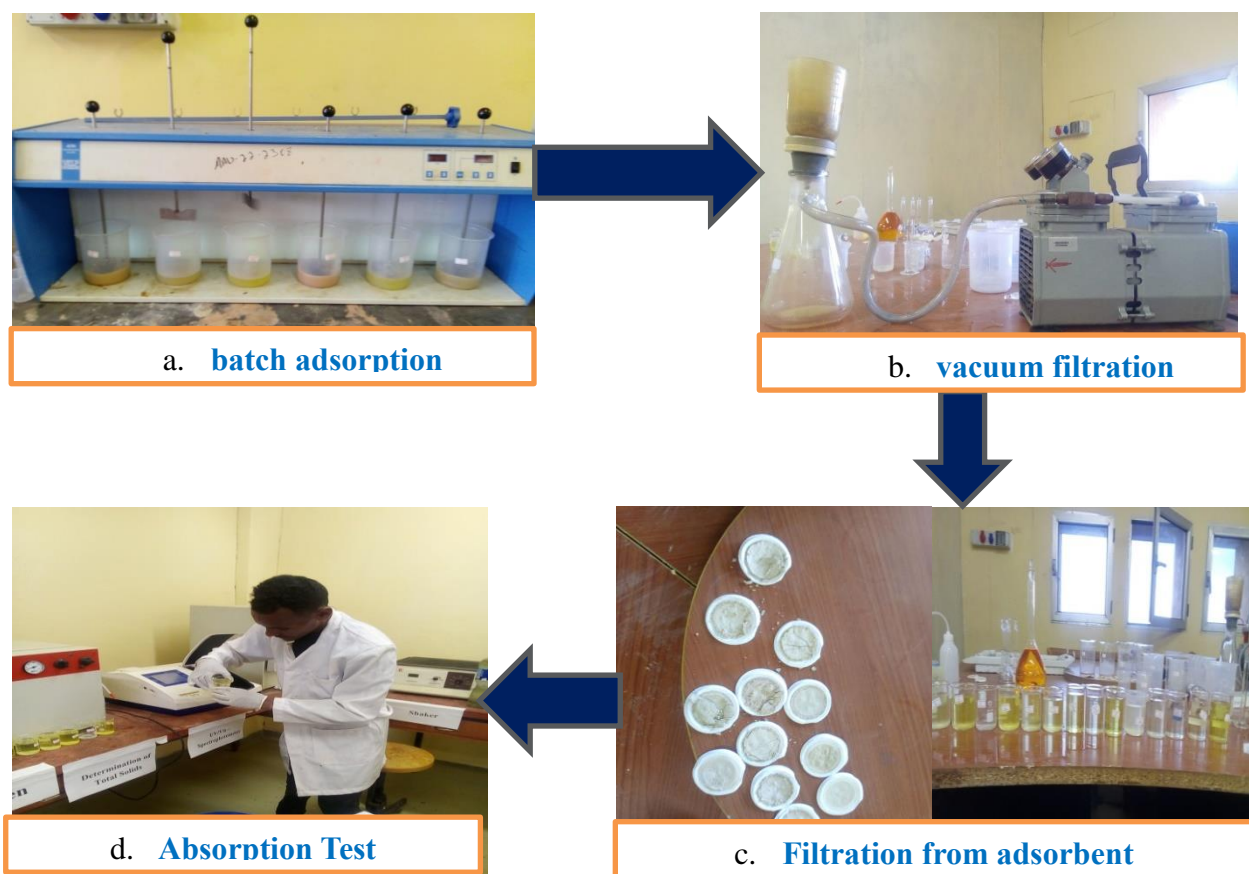


Figure A 4: Batch adsorption process for removal of Cr(VI) ions

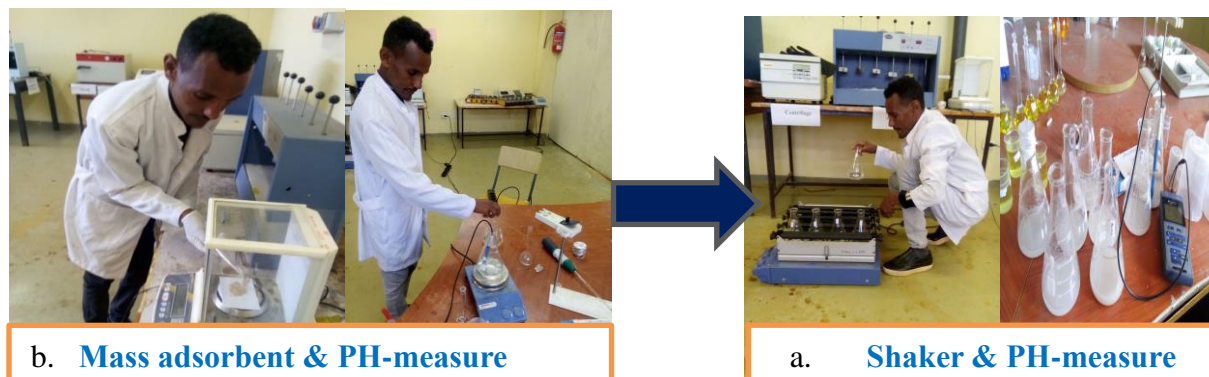


Figure A 5: Point zero charge of (PH_{pzc}) determination

Appendix B: Laboratory experimental generated data

Table B 1: standard concentration for UV-vis spectrophotometer calibration graph

Initial concentration(mg/L)	Absorbance (Abs)		
	A1	A2	AV
10	0.024	0.120	0.072
20	0.039	0.306	0.173
40	0.118	0.549	0.334
60	0.266	0.655	0.461
80	0.353	0.706	0.5295
100	0.522	0.752	0.637

Table B 2: Evaluation of point of zero charge (PH_{pzc}) for TMESP-adsorbent surface

PH_o	3	4	5	6	7	8	9	10	11	12
PH_f	5.587	6.042	6.498	6.625	7.204	7.911	8.892	9.784	10.394	10.957
ΔPH	-2.587	-2.042	-1.498	-0.625	-0.204	0.089	0.108	0.216	0.606	1.043

Table B 3: Effect of initial concentration on Cr(VI) removal

Initial Concentration(mg/L)	Cr(VI)	Absorbance (Abs)			Ce (mg/l)	Adsorption capacity (qe)(mg/g)	Efficiency %
		A1	A2	AV			
10		0.086	0.032	0.059	0.14	1.6433	98.6
25		0.075	0.071	0.073	0.35	4.1083	98.6
40		0.108	0.064	0.086	0.56	6.5733	98.6
55		0.198	0.066	0.132	1.31	8.9483	97.62
70		0.217	0.397	0.307	4.18	10.5817	94.03
85		0.479	0.421	0.450	6.51	13.0817	92.34
100		0.603	0.473	0.538	7.95	15.3417	92.05

Constant parameters used: adsorbent dose = 0.6g/100mL, PH=7, Contact time= 45minutes

Table B 4: Effect of pH on Cr(VI) removal using TMESP-adsorbent

PH	Absorbance (abs)			Ce (mg/L)	Adsorption capacity (qe)(mg/g)	Efficiency %
	A1	A2	AV			
1	0.551	0.282	0.4167	5.97	6.0033	90.05
3	0.141	0.308	0.2245	2.83	6.3522	95.28
5	0.189	0.156	0.1725	1.98	6.4467	96.70
7	0.096	0.133	0.1144	1.03	6.5522	98.28
9	0.175	0.147	0.1609	1.79	6.4678	97.02

Constant parameters used: adsorbent dose = 0.9g, Initial concentration = 60mg/L, contact time=60minute, volume of dilution=100mL

Table B 5: Effect of adsorbent dose on Cr(VI) removal

Adsorbent dose(g/100mL)	Absorbance (abs)			Ce (mg/L)	Adsorption capacity (qe)(mg/g)	Efficiency %
	A1	A2	AV			
0.1	0.587	0.651	0.619	9.28	30.72	76.8
0.3	0.599	0.597	0.598	8.93	10.3567	77.68
0.6	0.150	0.084	0.117	1.08	6.4867	97.3
0.9	0.075	0.071	0.073	0.35	4.4056	99.13
1.2	0.097	0.053	0.075	0.39	3.3008	99.03
1.5	0.081	0.075	0.078	0.43	2.638	98.93

Constant parameters used: Initial concentration = 60 mg/L, PH=7, contact time=60minute

Table B 6: Effect of contact time on Cr(VI) removal

Time (min)	Absorbance (abs)			Ce (mg/L)	Adsorption capacity(mg/g)	Efficiency %
	A1	A2	AV			
10	0.690	0.630	0.660	9.94	5.01	75.15
20	0.356	0.490	0.423	6.07	5.655	84.83
30	0.135	0.135	0.135	1.37	6.4383	95.58
40	0.130	0.148	0.139	1.43	6.4283	96.43
50	0.129	0.145	0.137	1.40	6.4333	96.5
60	0.128	0.126	0.127	1.23	6.5	96.93
70	0.128	0.144	0.136	1.38	6.4367	96.55
80	0.157	0.131	0.144	1.49	6.4183	96.28
90	0.157	0.131	0.144	1.49	6.4183	96.28

Constant parameters used: adsorbent dose =0. 6g/100mL, Initial concentration = 40mg/L, PH=7

Appendix C: Characterization of adsorption models

Table C 1: Parameters values for Langmuir and Freundlich isotherm models

Run No.	C _i (mg/L)	C _e (mg/L)	1/C _e	log(C _e)	ln(C _e)	q _e (mg/g)	1/q _e	log(q _e)
1	10	1.04	0.9615	0.0170	0.0392	1.4933	0.6696	0.1742
2	25	2.15	0.4651	0.3324	0.7655	3.8083	0.2626	0.5807
3	40	3.48	0.2874	0.5416	1.2470	6.0867	0.1643	0.7844
4	55	4.21	0.2375	0.6243	1.4375	8.465	0.1181	0.9276
5	70	5.33	0.1876	0.7267	1.6734	10.7783	0.0928	1.0326
6	85	6.13	0.1631	0.7875	1.8132	13.145	0.0761	1.1188
7	100	6.91	0.1447	0.8395	1.9329	15.515	0.0644	1.1908

Constant parameters used: adsorbent dose = 0.6g, PH=7, Contact time= 60min

Table C 2: Parameters values for pseudo-first-order & pseudo-second-order kinetics model

Run No.	Time (min)	C _e (mg/L)	q _t (mg/g)	ln(q _e -q _t)	t/q _t	time ^{0.5} (min)
0	0	0	0	0	0	0
1	10	9.94	5.01	0.3987	1.9960	3.1623
2	20	6.07	5.655	-0.1684	3.5367	4.4721
3	30	4.67	5.8883	-0.4594	5.0948	5.4772
4	40	3.43	6.095	-0.8557	6.5627	6.3246
5	50	2.39	6.2683	-1.3797	7.9766	7.0711
6	60	1.63	6.395	-2.0794	9.3823	7.7459
8	70	1.19	6.4217	-2.3194	10.9006	8.3666
9	80	1.03	6.4683	-2.9629	12.3679	8.9443
10	90	0.9	6.495	-5.2983	13.8568	9.4868

Constant parameters used: adsorbent dose =0. 6g/100mL, PH=7 and C_i=40mg/L

Table C 3: TMESP mixture ratio using design expert software synthesizing adsorbent

Std	Run	Component 1	Component 2	Experimental	Predicted
		A: Termite mound (g)	B: Eggshell (g)	Cr(VI) removal efficiency (%)	Cr(VI) removal Efficiency (%)
5	1	0.375	0.625	97.06	88.68
3	2	0.5	0.5	97.71	97.6
8	3	0.5	0.5	97.64	97.85
7	4	0.25	0.75	97.3	96.7
1	5	0.75	0.25	83.07	83.8
6	6	0.75	0.25	87.34	87.65
4	7	0.625	0.375	73.42	73.49
2	8	0.25	0.75	97.19	97.22

Table C 4: Crystalline size derived from XRD data analysis of the synthesized TMESP adsorbent

h	k	l	d [Å] calculated	d [Å]	2Theta (2θ°)	FWHM (β)	D (nm) (Crystalline size)	D=average(nm)
3	0	0	3.0631	3.0454	29.13	0.0713	20.9853	= 26.69nm
1	1	1	2.7718	2.5190	32.27	0.0571	26.4019	
2	0	2	2.6498	2.7000	33.8	0.0527	28.7197	
1	0	1	2.3915	2.3790	37.58	0.0371	41.2315	
1	1	0	1.8784	1.8750	48.42	0.0813	19.5303	
0	1	3	1.7149	1.7400	53.38	0.0517	31.3514	
1	1	2	1.4476	1.4536	64.3	0.0713	23.9894	
2	2	2	1.3829	1.3820	67.7	0.0819	21.2909	

Table C 5: Regeneration removal efficiency recorded and calculated from UV-vis output

Cycle	C _{ad} (mg/L)	C _e (mg/L)	Abs (y)	Slope (m)	Intercept (b)	C _{de} = $\left(\frac{y-b}{m}\right)$	De = $\left(\frac{C_{de}}{C_{ad}}\right)$	De%	Eff (%)
1	38.51	1.49	0.399	0.01045	0.01113	37.1168	0.9638	96.3821	96.275
2	37.95	2.05	0.383	0.01045	0.01113	35.5857	0.9377	93.7698	94.875
3	37.62	2.38	0.368	0.01045	0.01113	34.1502	0.9078	90.7768	94.05
4	35.52	4.48	0.336	0.01045	0.01113	31.0880	0.8752	87.5226	88.8
5	34.08	5.92	0.314	0.01045	0.01113	28.9828	0.8504	85.0434	85.2

At optimum condition (Initial Cr(VI) concentration=40mg/L, Contact time=45minute, Adsorbent dosage=0.6g/100mL, PH=7)

Table C 6: Calcination temperature and time determination for TMESP-adsorbent

		Factor 1	Factor 2	Experimental	Predicted
Std	Run	A:Temperature	B:Time	Cr(VI) removal efficiency	Cr(VI) removal Efficiency
		Celsius	Hour	(%)	(%)
13	1	850	2.5	81.13	82.56
1	2	700	1	74.05	69.72
11	3	850	2.5	81.11	89.73
5	4	637.868	2.5	78.04	94.48
9	5	850	2.5	83.09	85.86
8	6	850	4	98.38	97.03
3	7	700	4	96	96.08
7	8	850	3	88.52	72.55
10	9	850	2.5	80.25	82.58
2	10	1000	1	71.88	75.04
12	11	850	2.5	80.11	87.15
6	12	1062.13	2.5	85	83.8
4	13	1000	4	83.89	85.4

Table C 7: Functional groups found on the surface of TMESP-adsorbent using FTIR analysis

Wave number (cm ⁻¹)	Function groups	Justification
893	C-H	Vinylidene bend and Si ₂ O stretch
1454	C-H	Methylene C-H bend/Carbonate ion
1620	C=C	skeletal vibrations stretch
2514	C-O	Stretching and bending
3239	NH ₄	Ammonium ion
3490	N-H	Aromatic primary amine
3549	O-H	Internally bonded OH stretch
3614	O-H	Tertiary alcohol, OH stretch

Appendix D: Pre-determined parameters output for Cr(VI) removal

Table D 1: Predetermined factors to run batch adsorption process including a fit summary

NO.		Factor 1	Factor 2	Factor 3	Factor 4	Response 1
Std	Run	A:Adsorbent	B:Concentration	C:Contact time	D:PH	Cr(VI) removal
		g/L	mg/L	Min	PH	%
16	1	12	80	75	7	
9	2	6	40	45	7	
21	3	9	60	30	5	
14	4	12	40	75	7	
24	5	9	60	60	9	
26	6	9	60	60	5	
7	7	6	80	75	3	
12	8	12	80	45	7	
19	9	9	20	60	5	
3	10	6	80	45	3	
17	11	3	60	60	5	
5	12	6	40	75	3	
8	13	12	80	75	3	
25	14	9	60	60	5	
30	15	9	60	60	5	
1	16	6	40	45	3	
18	17	15	60	60	5	
11	18	6	80	45	7	
2	19	12	40	45	3	
6	20	12	40	75	3	
4	21	12	80	45	3	
13	22	6	40	75	7	
27	23	9	60	60	5	
10	24	12	40	45	7	
22	25	9	60	90	5	
20	26	9	100	60	5	
29	27	9	60	60	5	
28	28	9	60	60	5	
23	29	9	60	60	1	
15	30	6	80	75	7	
Source	Sequential p-value	Lack of Fit p-value	Adjusted R ²	Predicted R ²		
Linear	0.7049	< 0.0001	-0.0671	-0.3941		
2FI	0.0163	< 0.0001	0.3355	0.2998		
Quadratic	< 0.0001	0.2411	0.9973	0.9931	Suggested	
Cubic	0.1144	0.5914	0.9985	0.9898	Aliased	

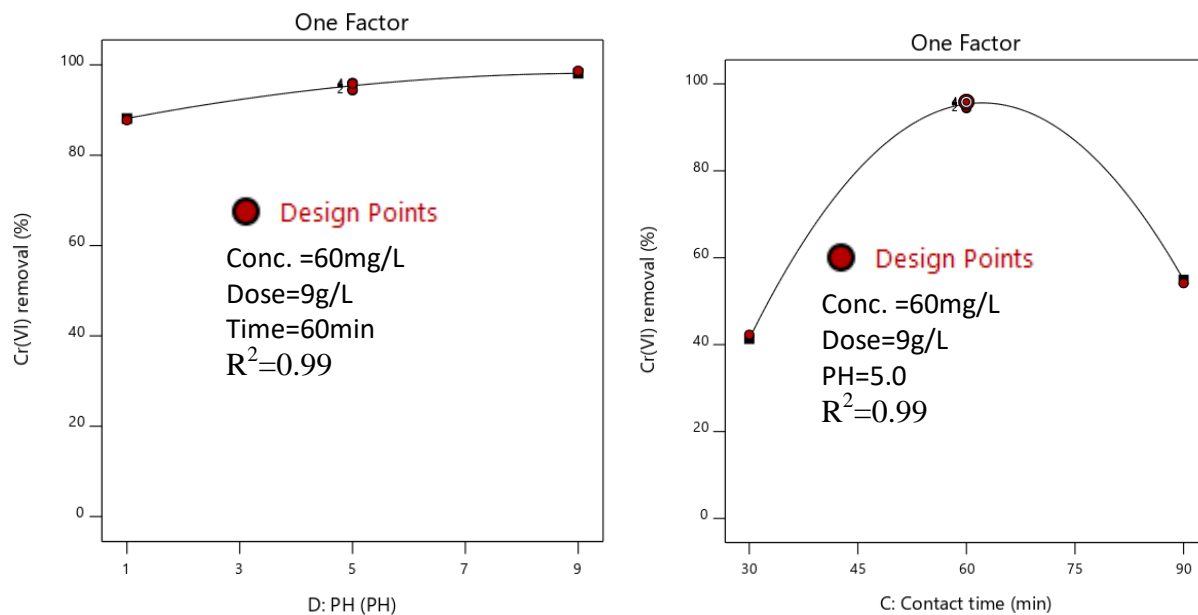
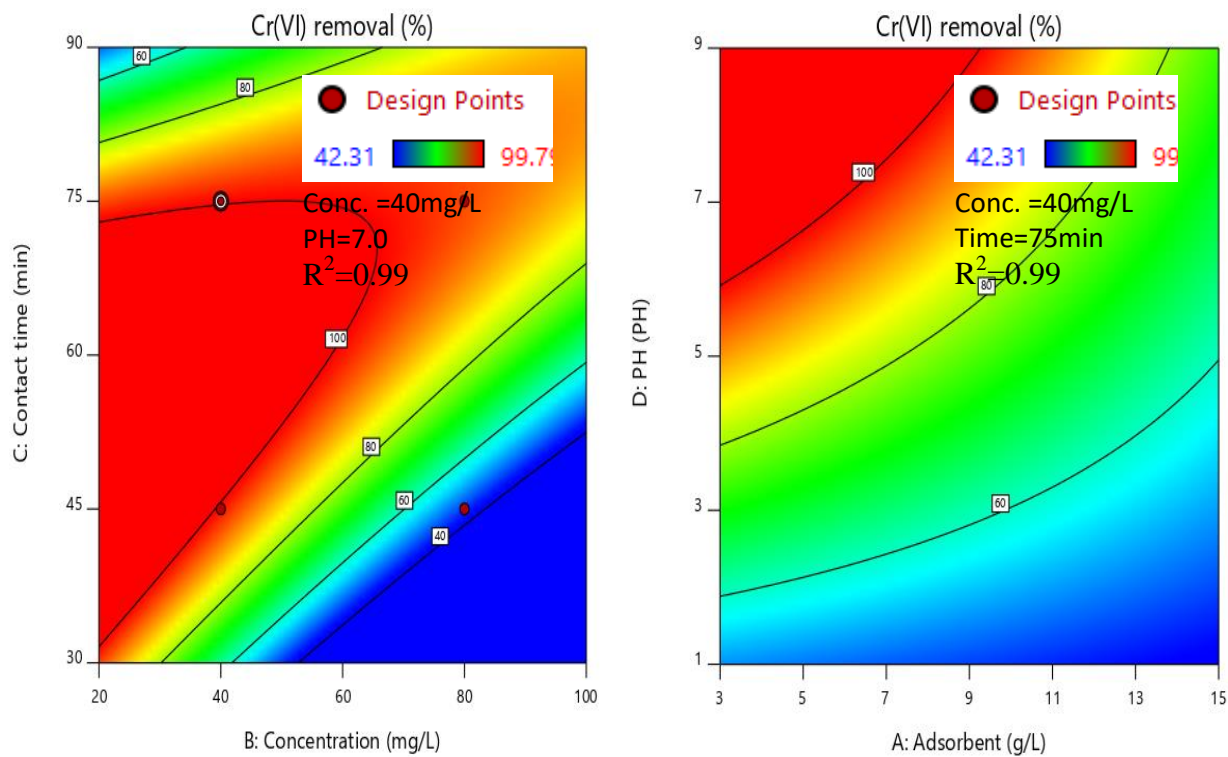


Figure D 1: Proportionality of parameters as one factor effect for Cr(V) adsorption



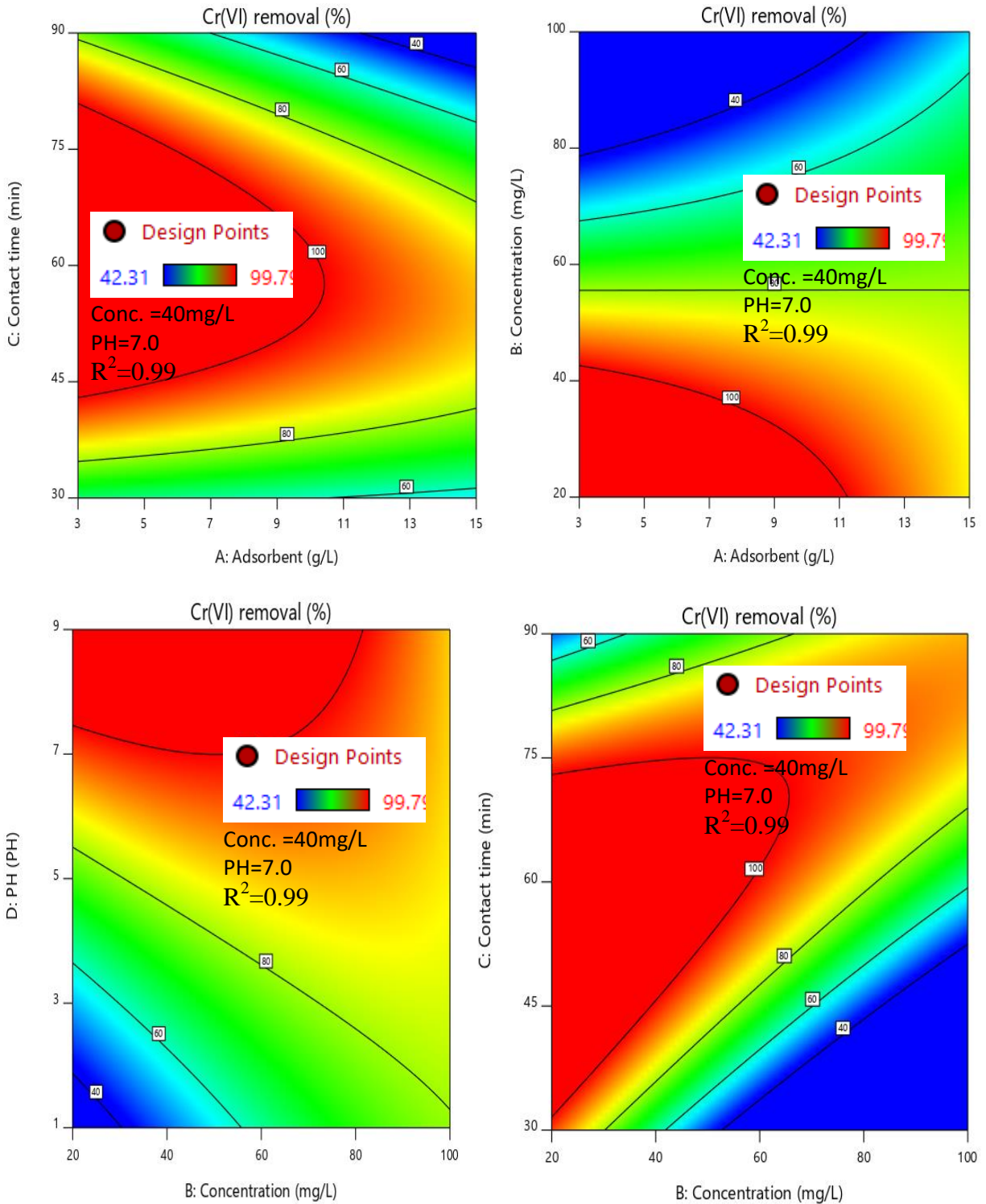


Figure D 2: Contour plot for the combined effect of adsorption parameters for Cr(VI) removal

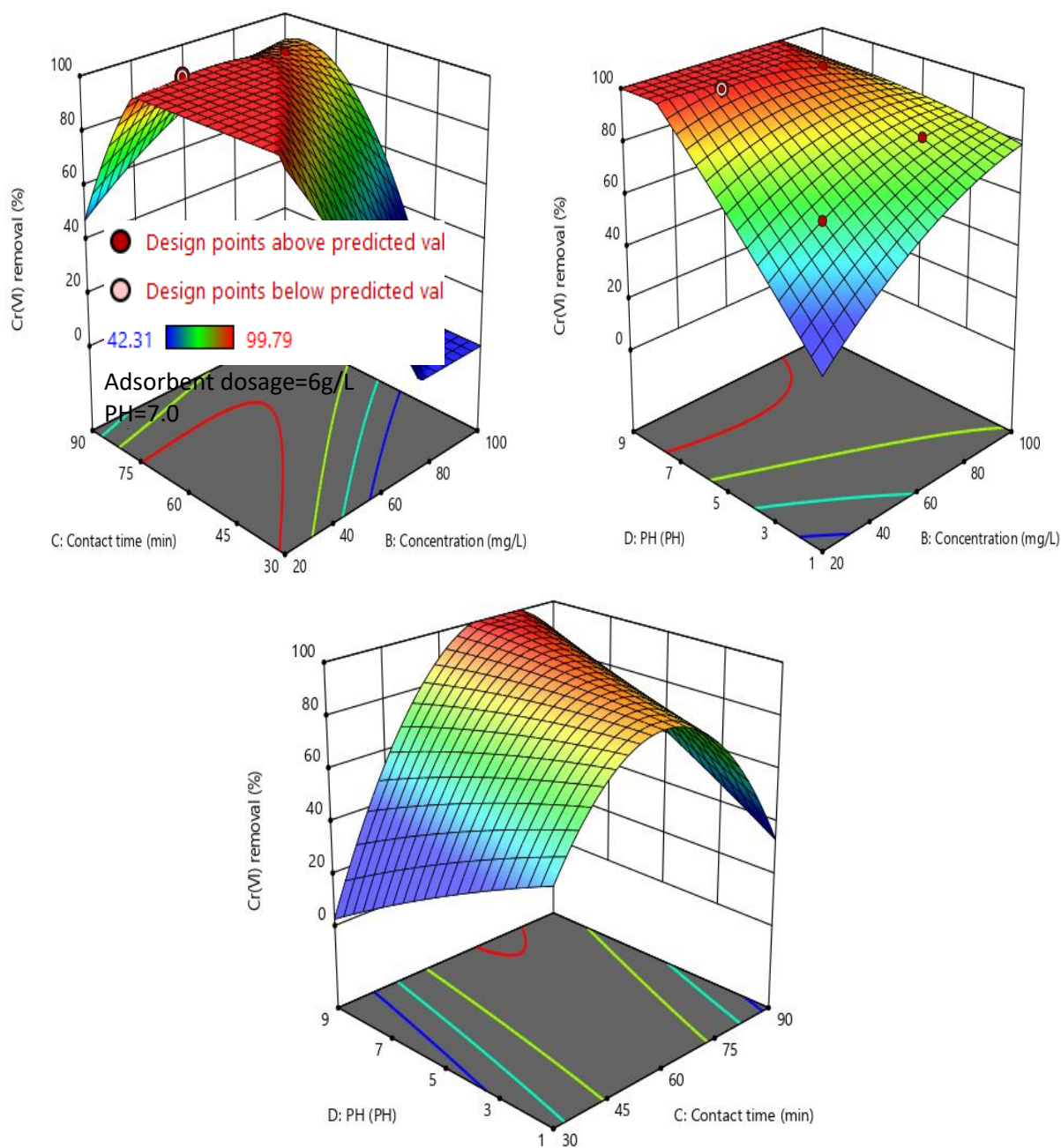


Figure D 3: Combined effect for a 3D plot for Cr(VI), adsorbent dosage, PH, and contact time.

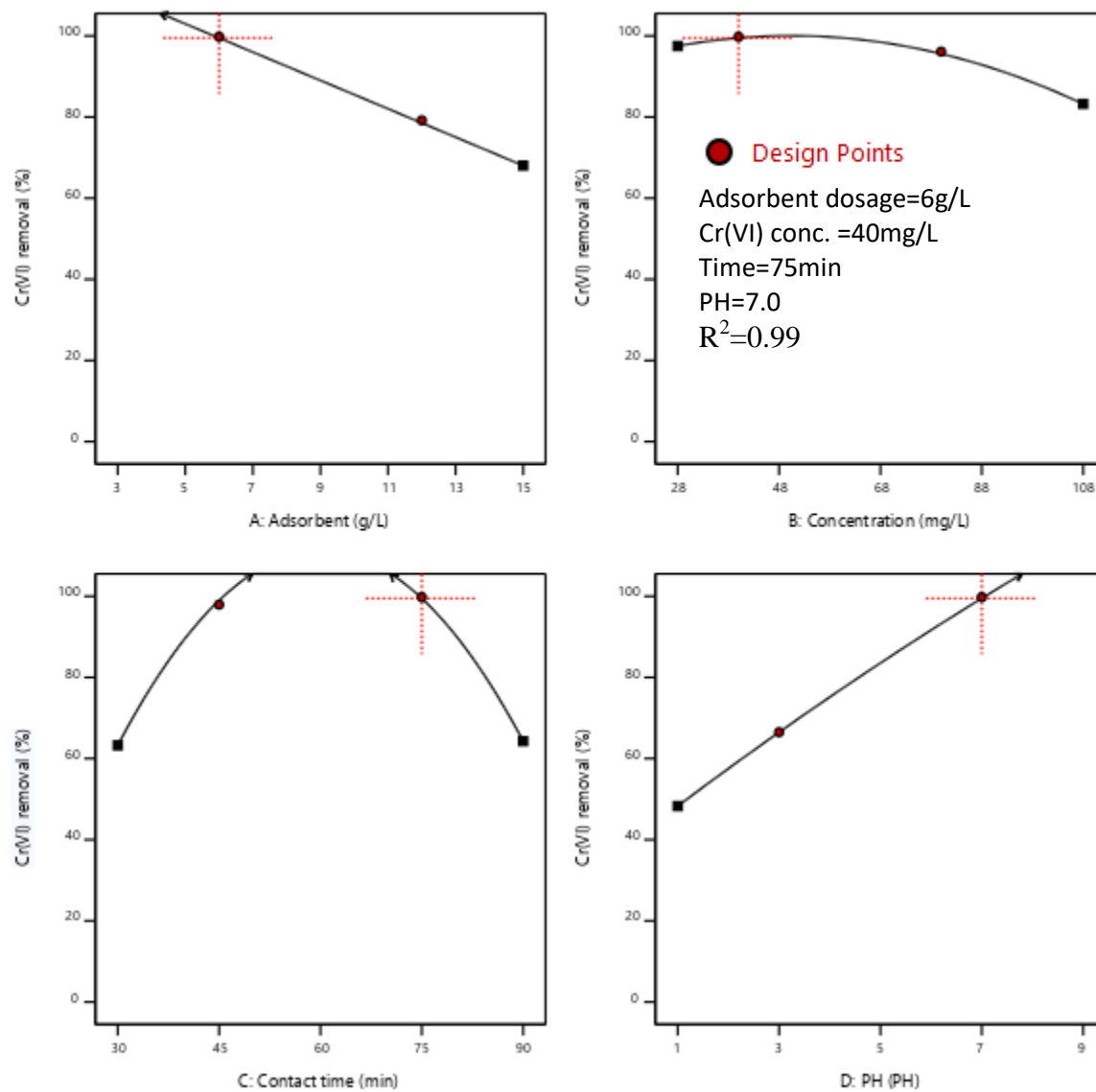


Figure D 4: Proportionality of parameters as all factors effect for Cr(V) adsorption

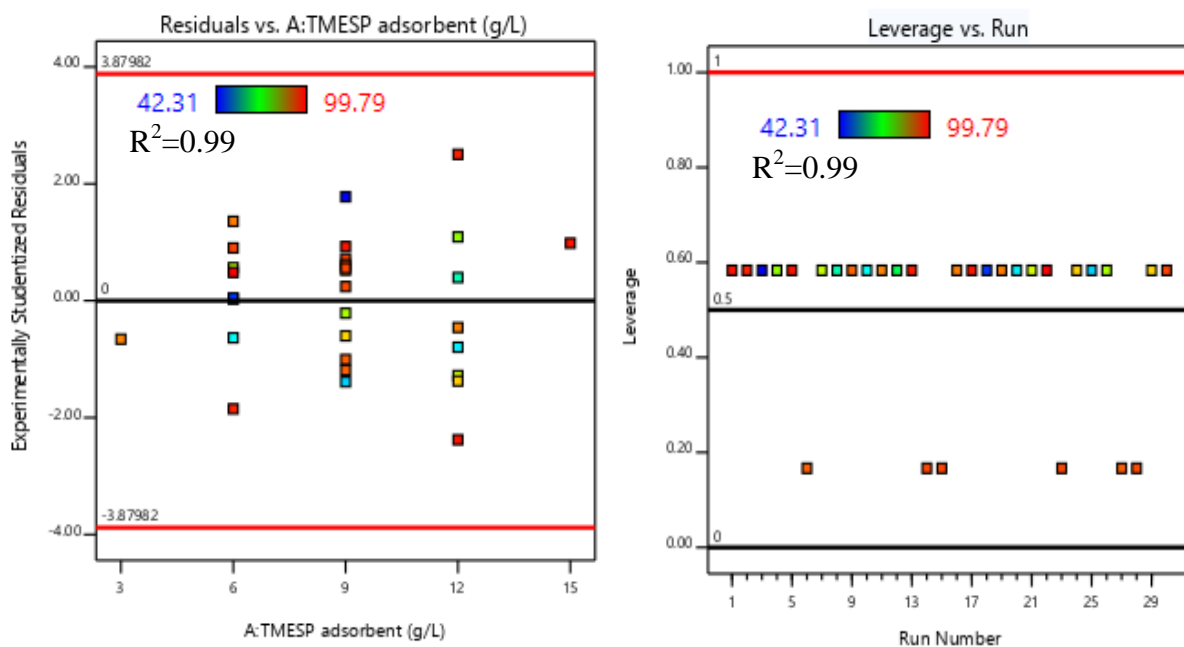


Figure D 5: Residual versus TMESP- adsorbent and run experiment

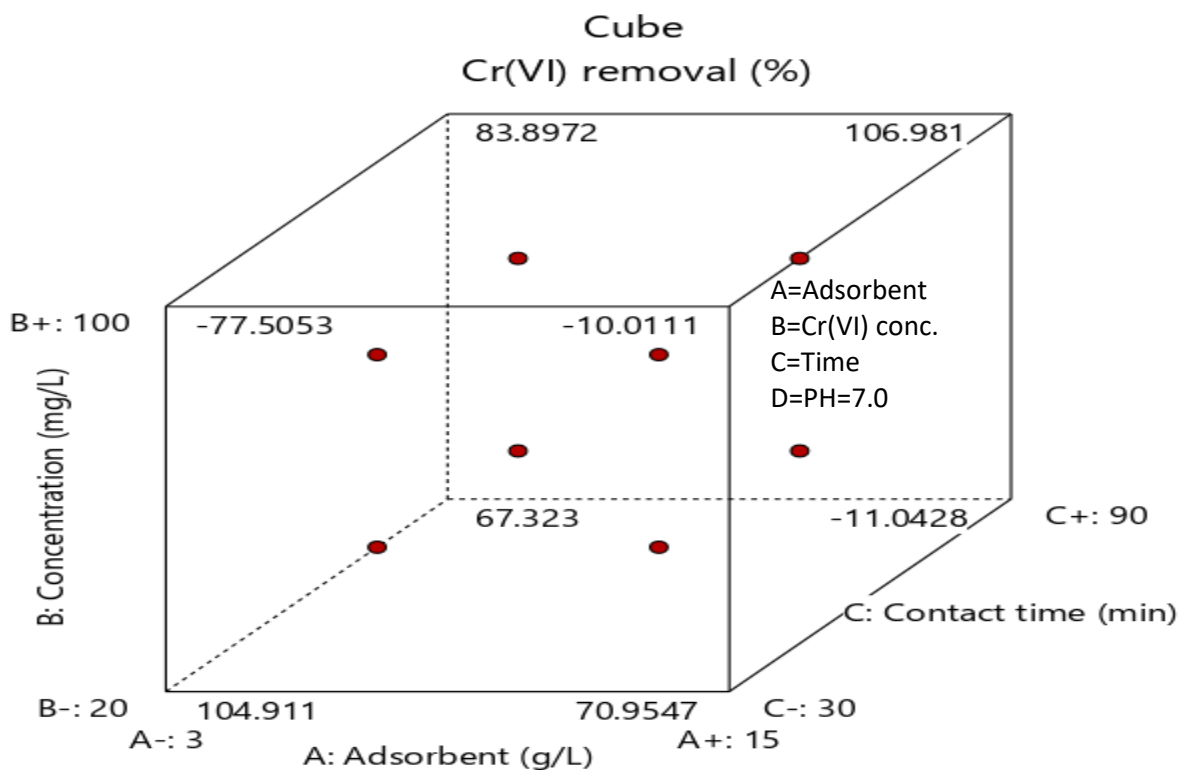


Figure D 6: Cubic interaction of parameters for Chromium removal efficiency

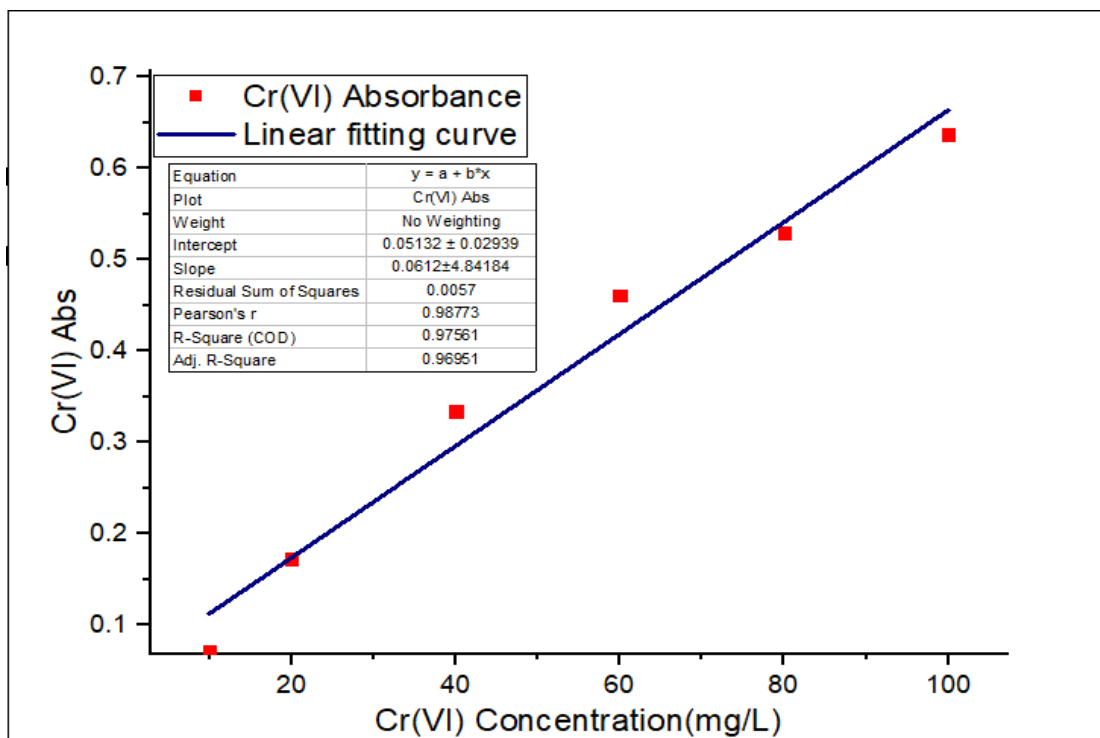


Figure D 7: Standard concentration for UV-vis spectrophotometer calibration graph

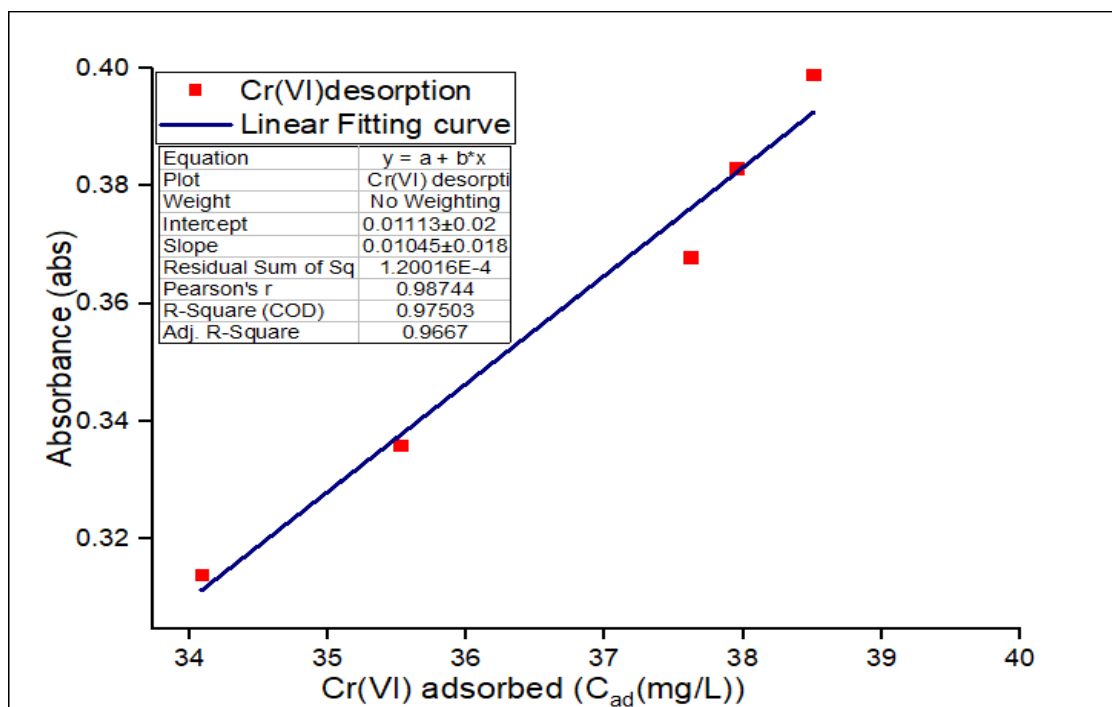


Figure D 8: Regeneration efficiency recorded and calculated using UV-vis generated data